

Effect of Akt (PKB) on the activity of mammalian target of rapamycin (mTOR)

**vorgelegt von
Diplom-Ingenieurin
Annett Hahn-Windgassen
aus Chicago**

von der Fakultät III -Prozesswissenschaften
-Biotechnologie-
der Technischen Universität Berlin

zur Erlangung des akademischen Grades Doktor der Naturwissenschaften
-Dr.rer.nat.-

genehmigte Dissertation

Promotionsausschuss:

Vorsitzender: Prof. Dr. R. Lauster

1.Berichter: Prof. Dr. rer. nat. Dipl.-Ing. U. Stahl

2.Berichter: Prof. Dr. N. Hay

Tag der wissenschaftlichen Aussprache: 18. November 2004

Berlin 2004

D83

This thesis is dedicated to the loving memories
of my grandmother Elli Schumann “Oma Elli”
and Dirk’s mother Edith Windgassen.

Acknowledgments

This thesis is dedicated to the loving memories of my grandmother Elli Schumann “Oma Elli” and Dirk’s mother Edith Windgassen. Both, very important women in our lives, died at young ages from breast cancer.

I am very grateful for the tremendous scientific direction and environment provided to me by my thesis advisor Prof. Dr. Nissim Hay. He allows all students to grow as scientists, and as people, in their own unique way. Working under his direction has been an honor and a privilege, one that I am very thankful for.

I would like to thank Prof. Dr Ulf Stahl, who supported my thesis in Germany at the University of Technology in Berlin. He is a very inspiring teacher and scientist in my first years of study in genetics and biology.

I am certainly appreciative of my fellow graduate students and colleagues for their support and friendship: from those who left: Nate and Kathrin, to those who are still there: Vero, Prashanth, Deepa, Chia-Chen, Joel, Jen, Pei Zhang, William, Xiao-ding, Yongmei and Ivana.

A special thanks to two of my colleagues who were with me for almost the entire journey, Veronique and Nate. Vero and Nate have been extraordinary labmates, always willing to go the extra mile to help.

A very special thanks to my family and friends for their support and encouragement over the last three years. Thanks to you, I am ending my graduation with my spirit intact.

At the heart of my support system were my parents Dieter and Renate Hahn, my loving son Sebastian, my sisters Kerstin and Ines, who lend me unending support in everything I do, whether they agree or not.

The greatest support and belief has been undoubtedly the love of my life, Dirk. His unconditionally support and belief in me lifted me from darkest times that inevitably present themselves along the road to the PhD (Dr.). “It doesn’t matter it’s dark out there if you are the light.”

A very special thanks to my beloved son Sebastian, who has taught me in our journey as mother and son to focus on the outcome not on the problem. I am certainly very proud of him and he is attending college specialized in Biology, Chemistry and Physics, sciences that we both love.

TABLE OF CONTENTS

TABLE OF CONTENTS	I
TABLE OF FIGURES	IV
ABBREVIATIONS	V
I. THEORETICAL- THE ROLE OF AKT (PKB) IN CELL GROWTH (SIZE) AND CELL PROLIFERATION.....	1
1. Introduction.....	1
2. Akt or protein kinase B (PKB).....	2
2.1 Upstream of Akt.....	4
2.1.1 PI3-Kinase and PTEN.....	4
2.1.2 PDK1, Akt activating kinase.....	6
3. Physiological roles of Akt (PKB).....	6
3.1 Metabolism	6
3.2 Apoptosis.....	8
3.3 Proliferation	9
4. Akt activity on mTOR controlled by growth factors.....	10
4.1 TSC1-TSC2 tumor suppressor	10
4.2 Rheb, a small G protein, activates mTOR	11
4.3 TOR- target of rapamycin	12
4.4 Downstream targets of mTOR.....	14
5. Control of mTOR by nutrients and energy metabolism.....	15
5.1 Protein-protein interaction with mTOR senses nutrient availability?	15
5.2 Energy sensor mTOR, regulation through AMPK?	16
5.3 LKB1 potentiates the effect on AMPK.....	17
5.4 Amino acid sensor mTOR, AMPK-sensing mechanism?.....	18
6. Conclusion	19
II. PRACTICAL- EFFECT OF AKT (PKB) ON THE ACTIVITY OF MAMMALIAN TARGET OF RAPAMYCIN (MTOR)	21
1. Introduction.....	21
1.1 Objective.....	22
2. Network.....	24
3. Materials and Methods	25
3.1 Materials.....	25
Chemicals.....	25
3.1.2 Enzymes and kits.....	27

3.1.3	Equipment.....	27
3.1.4	Plasmids and constructs	28
3.1.5	Enzymes and Antibodies.....	29
3.1.6	Bacteria and Cell lines	30
3.1.7	Media, agarose plates, antibiotica and materials	31
3.1.8	Buffers and solutions.....	32
3.2	Cell culture methods	33
3.2.1	Culture conditions, stimulations and Inhibitions	33
3.2.2	Maintenance of cell lines.....	34
3.2.3	Storage of cells	34
3.3	Mouse embryo fibroblast (MEF) isolation	35
3.4	Transfection of adherent mammalian cells for recombinant expression 36	
3.4.1	Calcium phosphate method	36
3.4.2	Lipofectamine 2000 method.....	36
3.4.3	DEAE-Dextran-Chloroquine method	37
3.5	Retrovirus production and infection	38
3.6	Modification and amplification of DNA	38
3.6.1	Methods of <i>in vitro</i> modification of DNA	38
3.6.2	Preparation of vector-DNA.....	39
3.6.3	Gel electrophoresis	40
3.6.4	Isolation of restriction fragments from gel slices	40
3.6.5	Phenol extraction and ethanol precipitation of DNA.....	40
3.6.6	Quantitative determination of DNA concentration	41
3.6.7	Production of competent bacteria cells for transformation	41
3.6.8	Transformation of vector or plasmid DNA in competent bacteria	42
3.6.9	Mini-preparation	42
3.6.10	Maxi-preparation.....	43
3.7	Protein Methods	44
3.7.1	Whole-Cell Lysate Preparation	44
3.7.2	Quantification of proteins	45
3.7.3	SDS-PAGE	45
3.7.4	Protein transfer	47
3.7.5	Immunoblotting and Development	48
3.7.6	Immunoprecipitation.....	49
3.8	Adenine nucleotide analysis	51
4.	Results.....	52
4.1	Cellular atrophy of skeletal muscle and impaired mTOR activity in Akt1/Akt2 DKO cells	52
4.1.1	Cellular atrophy of skeletal muscle in Akt1/Akt2 DKO cells	52
4.1.2	Status of mTOR-activity in AKT1/AKT2 DKO cells.....	52
4.1.3	Status of TSC2 phosphorylation by Akt in Akt1/Akt2 DKO MEFs	56
4.2	Akt maintains the intracellular level of ATP and regulates AMPK activity 59	
4.2.1	Akt deficiency significantly reduce intracellular ATP level and increases AMP/ATP ratio.....	59
4.2.2	Akt deficiency markedly increases AMPK activity	62
4.2.3	Expression of activated Akt increases intracellular ATP level, reduces AMP/ATP ratio and affects AMPK activity.....	63

III

4.3	ATP depletion and activation of AMPK attenuates Akts ability to activate mTOR	66
4.3.1	ATP depletion in Rat1a cells expressing activated Akt	66
4.3.2	ATP depletion of insulin-stimulated Rat1a cells	68
4.3.3	Activation of AMPK by AICAR in Rat1a cells expressing activated Akt	69
4.3.4	Co-expression experiment with constitutively activated AMPK and 4EBP1	71
4.4	Reduced AMPK activity by over expression of dominant negative AMPK restores mTOR activity in Akt1/Akt2 DKO MEFs	72
4.4.1	Stable Akt1/Akt2 DKO MEF cell line expressing dominant negative AMPK restores mTOR activity	72
4.4.2	Increasing expression of dominant negative AMPK in Akt1/Akt2 DKO MEFs restores mTOR activity	75
4.5	Akt's ability to activate mTOR by inhibiting AMPK is dependent on TSC2	76
4.5.1	TSC2 deficiency renders cells almost resistant to ATP depletion	76
4.5.2	TSC2 KO cells exert a high AMP/ATP ratio and the expression of activated Akt is able to decrease this ratio	79
4.5.3	Inhibition of AMPK by Akt despite TSC2 phosphorylation is also required for mTOR activity	81
5.	Discussion	85
5.1	Akt can determine the cell mass and is required for mTOR activity	85
5.2	Akt is a key regulator for energy metabolism and regulates indirectly AMPK activity	86
5.3	Akt-mediated phosphorylation of TSC2 is not sufficient to fully activate mTOR	89
5.4	New mechanism by which growth factors activate mTOR	91
5.5	Concluding Remarks	92
6.	Summary	94
7.	Zusammenfassung	96
III.	REFERENCES	98

TABLE OF FIGURES

Figure 1: Structure of serine/threonine kinase Akt (PKB).....	3
Figure 2: Activation of the serine/threonine kinase Akt (PKB).	5
Figure 3: Structure of mammalian target of rapamycin (mTOR).....	13
Figure 4: Scheme of the Akt-TSC2-mTOR pathway summarizing current literature.	19
Figure 5: Hypothetical scheme for the regulation of the AKT-TSC2-mTOR pathway.	23
Figure 6: Skeletal muscle atrophy in Akt1/Akt2 DKO mice.	53
Figure 7: mTOR activity in WT and Akt1/Akt2 DKO MEFs.....	55
Figure 8: TSC2 phosphorylation in WT and Akt1/Akt2 DKO cells, immunoblotting.....	57
Figure 9: TSC2 phosphorylation in WT and Akt1/Akt2 DKO cells, immunoprecipitation.	57
Figure 10: ATP level is reduced in Akt1/Akt2 DKO cells vs. WT.....	59
Figure 11: ATP level in cells expressing activated Akt vs. control cells.	60
Figure 12: AMP/ATP ratio in Akt1/Akt2 DKO cells vs. WT.....	61
Figure 13: AMPK activity in Akt1/Akt2 DKO cells vs. WT.....	63
Figure 14: AMP/ATP ratio in cells expressing activated Akt vs. control cells.	64
Figure 15: AMPK activity in cells expressing activated Akt vs. control cells and correlation with mTOR activity.....	65
Figure 16: ATP depletion attenuates the ability of activated Akt to activate mTOR.....	67
Figure 17: ATP depletion of insulin-stimulated Rat1a cells, and its inhibition of the growth-factors-dependent activation of mTOR.....	68
Figure 18: Dose-dependent activation of AMPK by AICAR.....	70
Figure 19: Co-expression of activated AMPK and 4EBP1 in HEK293 and HEK293MAkt cells.....	72
Figure 20: Expression of dominant-negative AMPK in Akt1/Akt2 DKO cells vs. WT.	74
Figure 21: Dose-dependent co-expression of dominant-negative AMPK and 4EBP1 in Akt1/Akt2 DKO MEFs.	76
Figure 22: mTOR activity in TSC2 ^{-/-} vs. control cells following ATP depletion	78
Figure 23: AMP/ATP ratio in TSC2 ^{-/-} , mAkt-TSC2 ^{-/-} and TSC2 ^{-/+} cells.....	79
Figure 24: Akt and AMPK activity in TSC2 ^{-/-} , mAkt-TSC2 ^{-/-} and TSC2 ^{-/+} cells.....	80
Figure 25: Expression of Akt-phosphomimetic mutant of TSC2 in TSC2 ^{-/-} cells.....	82
Figure 26: Expression of Akt-phosphomimetic mutant of TSC2 in TSC2 ^{-/-} cells sensitizes mTOR activity to ATP depletion, which is restored by activated Akt.....	83
Figure 27: Proposed model for the regulation of mTOR activity by Akt.	91

ABBREVIATIONS

A ₂₆₀	absorbance at 260 nm
Aa	amino acids
Amp ^r	ampicillin resistance
AMP	adenosine 5' monophosphate
ADP	adenosine 5' diphosphate
ATP	adenosine 5' triphosphate
AICAR	5-aminoimidazole-4-carboxamide-ribose
bp	base pairs
BSA	bovine serum albumin
cDNA	complementary deoxyribonucleic acid
d	day
Da	Dalton
GTP	guanosine triphosphate
DNA	deoxyribonucleic acid
DNAse	deoxyribonuclease
DTT	dithiothreitol
EB	ethidium bromide
EDTA	ethylene diaminetetraacetic acid
EtOH	ethanol
g	gram
g	gravity
h	hour
HEPES	N-2-hydroxyethylpiperazine-N'-2-ethansulfonic acid
kb	kilo base pairs
M	molar
mcs	multiple cloning site
min	minute
MOPS	3-(N-morpholino) propane sulfonic acid
MRNA	messenger ribonucleic acid
MW	molecular weight
NADH	nicotinamide adenine dinucleotide (reduced form)
nt	nucleotides
OD ₂₆₀	optical density at 260 nm
oligo	oligonucleotide
ORF	open reading frame
PAA	polyacrylamide

PAGE	polyacrylamide gel electrophoresis
PCR	polymerase chain reaction
PEG	polyethylene glycol
RNA	ribonucleic acid
RNase	ribonuclease
rpm	rounds per minute
rRNA	ribosomal ribonucleic acid
RT	room temperature
RT-PCR	reverse transcriptase PCR
s	second
SD	standard deviation
SDS	sodium dodecyl sulfate
ss	single stranded
TEMED	N, N, N', N'-tetramethyl-ethylenediamine
Tris	trihydroxymethylaminomethane
tRNA	transfer ribonucleic acid
U	unit
UV	ultraviolet light
V	volt
WT	wild type

PREFIXES FOR MULTIPLES AND SUBMULTIPLES

G	giga	10^9
M	mega	10^6
k	kilo	10^3
c	centi	10^{-2}
m	milli	10^{-3}
μ	micro	10^{-6}
n	nano	10^{-9}

I. THEORETICAL- The role of Akt (PKB) in cell growth (size) and cell proliferation

1. Introduction

Why are mice smaller than men? Why are pea pods smaller than pumpkins? What controls the progression of growth, and when the proper size is attained, what tells organs and organisms to stop growing? These are fundamental questions of cell biology. The first evidence that animals can monitor dimension came from haploids and polyploids in amphibian.

Cell size of a given cell type is usually proportional to ploidy in amphibians. It was shown that haploid cells are about half the volume of diploids cells, diploids cells are about half the volume of tetraploid cells and so on (Day and Lawrence 2000). For example in plants and flies, endoreduplicating nuclei can contain over a thousand copies of their chromosomes, and these cells have a corresponding enlargement in total cell size. However, different cell types within a multicellular organism often vary in size, despite containing identical genomes of the same ploidy. The ratio of DNA:cytoplasm indicates that the amount of DNA is not necessary determining the cell size (Saucedo and Edgar 2002).

Another way to look at the restriction on cell size is the ratio of cell volume to surface area. Volume expands more quickly than surface area, and as a consequence cell membrane associated reactions, such as import and export, may set constraints on cell size (Saucedo and Edgar 2002).

Insulin signaling was first observed to affect organism size in mammals in the early 1990s (Efstratiadis 1998). Shioi et al. have demonstrated that either an increase or decrease in PI3K (phosphatidylinositol-3-kinase) activity, which activates serine/threonine protein kinase Akt (PKB), led to a larger or smaller organ size by directing expression specifically to the heart (Shioi et al. 2002). Strong loss-of-function mutations in the insulin receptor gene are lethal, but flies with some loss of function survive and show a growth pattern similar to that induced by starvation: delayed development, smaller overall size and a reduction in both cell number and cell size (Chen et al. 1996).

The maintenance of cell size requires homeostasis between macromolecule synthesis and degradation and, in multicellular systems, is intimately linked to nutrient and growth factor availability. As environmental conditions change, cells can reduce and restore their size. When nutrients and growth factors are saturated, however, there appears to be a limit to the maximum size a given cell type can reach (Saucedo and Edgar 2002).

2. Akt or protein kinase B (PKB)

In 1991 three research groups discovered the cDNA of Akt (PKB), a novel serine/threonine kinase. Two research groups identified it by homology cloning, searching for novel members of protein kinase A (PKA) and protein kinase (PKC). It was termed by one group RAC-PK (Related to A and C-Protein Kinase) (Coffer and Woodgett 1991; Jones et al. 1991).

At the same time, another research group identified it as the cellular homologue of the murine oncogene v-akt, from a transforming retrovirus (AKT8) in spontaneous thymoma of the AKR mouse and therefore, it was termed c-Akt (Bellacosa et al. 1991). PKB β and PKB γ or Akt2 and Akt3, two additional PKB or Akt isoforms have been identified as well (Cheng et al. 1992; Brodbeck et al. 1999).

Akt (PKB) kinases are evolutionarily conserved in eukaryotes ranging from *C.elegans* to human. The amino acid identity between mouse, rat and human is more than 95%, whereas between *C.elegans* and human, it is only 60% (Hanada et al. 2004).

Three isoforms of Akt encoded by three separate genes have been found in mammalian cells. Akt1 is ubiquitously expressed in mammalian cells and tissues. Akt2 is expressed at lower level than Akt1, except in insulin-responsive tissues: skeletal muscle, heart, liver and kidney (Altomare et al. 1995; Altomare et al. 1998). Akt 3 is expressed at the lowest level in most tissues, except for testes and brain (Brodbeck et al. 1999). Akt1 is the predominant isoform in most tissues and mouse embryo fibroblasts (Chen et al. 2001).

The expression pattern of three isoforms may not always reflect their activities. Different levels of kinase activities of the different Akt isoforms have been observed in certain tissues and during differentiation, which is not

necessarily correlated with their level of expression (Walker et al. 1998; Fujio et al. 1999).

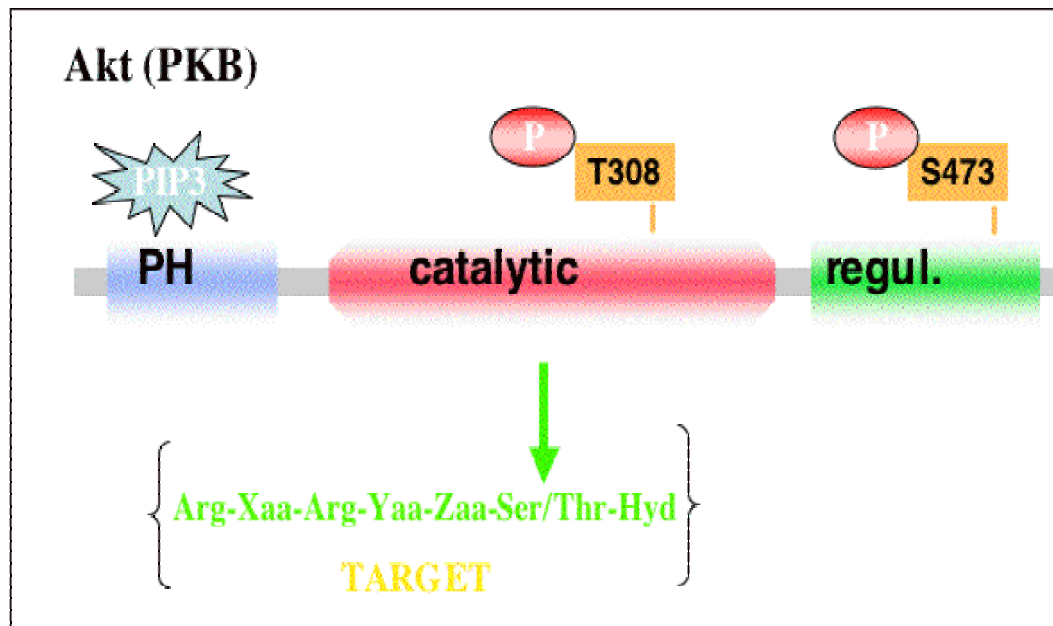


Figure 1: Structure of serine/threonine kinase Akt (PKB).

Scheme demonstrates the structure of Akt, with PH-domain, catalytic-domain and regulatory domain.

The amino acid identity between Akt1, Akt2 and Akt3 isoforms is >80%. All three Akt-isoforms share a similar protein structure that contains a pleckstrin homology (PH) domain that binds phospholipids (Figure 1), a short glycine-rich region that bridges to the catalytic domain, and the regulatory domain (Walker et al. 1998).

The catalytic domain of all Akt isoforms share similarity with a group of kinases from the AGC family [cAMP-dependent protein kinase (PKA)/protein kinase G/protein kinase C (PKC)]. The AGC family consists of more than 80 kinases, most of them are protein kinases and are regulated by second messenger, for example CA^{2+} , cyclic mononucleotides and phosphoinositides. The carboxyl-terminal regulatory domain that contains the hydrophobic motif is characteristic for AGC-kinases (Hanada et al. 2004).

The PH domain interacts with membrane lipid products, such as phosphatidylinositol-(3,4,5)triphosphat (PIP3/ PtdIns (3,4,5), Figure 1) produced by PI-3-kinase (phosphatidylinositol-3-kinase). Biochemical analysis revealed that the PH

domain of Akt binds to both PtdIns (3,4,5) P3 [PIP3] and PtdIns (3,4) P2 [PIP2] with similar affinity (James et al. 1996; Frech et al. 1997). The kinase domain/catalytic domain is located in the central region of the molecule and shares a high similarity with other AGC-kinases such as PKA, PKC, p70S6K and p90RSK (Peterson and Schreiber 1999).

All three Akt-isoforms have a carboxyl terminal extension of around 40 Aa, this region possesses the F-X-XF/Y-S/T-YF hydrophobic motif (where X is any amino acid), and is characteristic for AGC-family kinases (Peterson and Schreiber 1999). The phosphorylation on the Serine or Threonine residue within this hydrophobic motif is necessary for full activation of all AGC-family kinases. Akt's motif is F-P-Q-F-S-Y, point mutation of this motif completely abolished enzymatic activity (Andjelkovic et al. 1997).

All three Akt-isoforms have a conserved threonine and serine residue (Threonine 308 and Serine 473, in Akt1) and the phosphorylation of those sites is critical for full activation of Akt. Those serine and threonine residues are also present in p70S6K and all PKC isoforms in a similar Aa context. The distance between the two phosphorylation sites/residues is around 160-170 Aa and is also conserved in AGC-Kinases (Kandel and Hay 1999).

2.1 Upstream of Akt

The activation of Akt has been shown to be a multi- step process and several proteins responsible for each step were identified. The first rate-limiting step for Akt activation is the binding of PIP3 (phosphatidylinositol-(3,4,5)triphosphate) or PtdIns (3,4,5) P3) to the pleckstrin homology (PH) domain of Akt and the translocation of Akt to the plasma membrane (Brazil et al. 2002) (Hanada et al. 2004) (Kandel and Hay 1999).

2.1.1 PI3-Kinase and PTEN

Akt activity is dependent on PI3-kinase, this finding was the most significant finding in regards to Akt regulation (Figure 2). Activation of receptor tyrosine kinases through a number of stimuli activates Akt. Stimuli, by which Akt is activated, are platelet derived growth factor (PDGF-R), insulin, epidermal growth factor (EGF), basic fibroblast growth factor (bFGF) and insulin like growth factor

(IGF-1) (Burgering and Coffey 1995; Cross et al. 1995; Franke et al. 1995; Kohn et al. 1995). PI3-kinase is activated by growth factor receptors through binding of growth factor, its regulatory subunit p85 is activated by phosphotyrosin residue in the receptor.

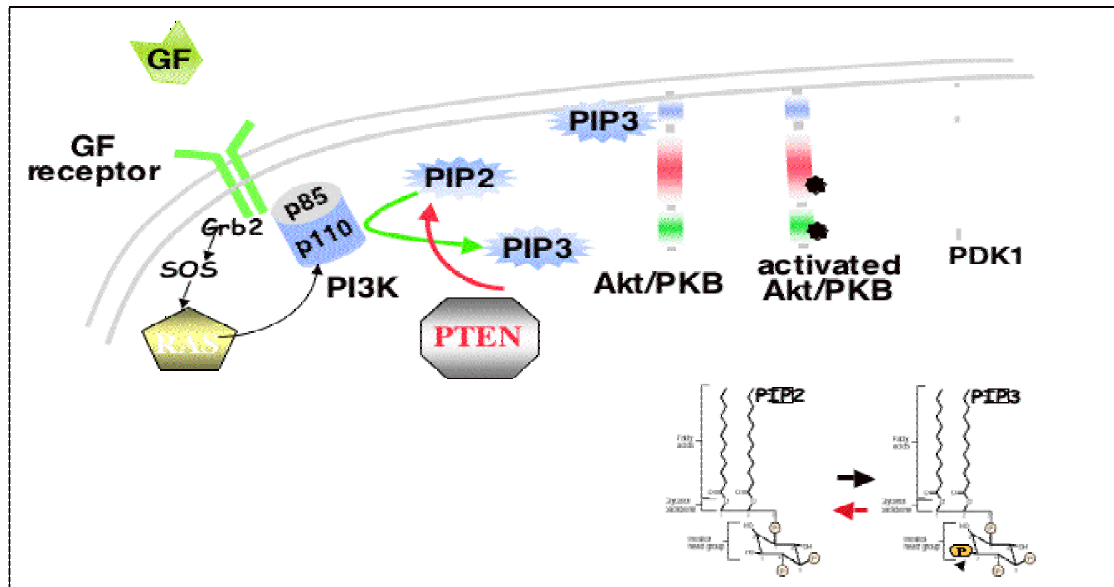


Figure 2: Activation of the serine/threonine kinase Akt (PKB).

Scheme demonstrates the activation of Akt following the activation of growth factors (GFR).

This event leads to the activation of the catalytic subunit p110 of PI3-kinase, which in turn phosphorylates phosphoinositides (PI) at the 3-position of the inositol ring to generate PIP2 (phosphatidylinositol-(3,4)diphosphat) and PIP3 (phosphatidylinositol-(3,4,5)triphosphat) (Vanhaesebroeck and Waterfield 1999). Ly94002 and wortmannin, two PI3-kinase inhibitors or dominant negative p110 of the catalytic subunit of PI3-kinase, reduce the level of PIP3 that is responsible for Akt activation (Chan et al. 1999).

The tumor suppressor protein PTEN (phosphatase and tensin homologue deleted on chromosome 10) reversed the production of phosphoinositides by PI3-kinase. Pten phosphoinositide phosphatase activity leads to inactivation of Akt by converting PIP3 to PIP2 (Maehama and Dixon 1998; Stambolic et al. 1998). Studies using Pten-deficient cells, in which the PI3-kinase pathway is activated owing to the up regulation of PIP3, indicated a constitutively activated mammalian target of rapamycin (mTOR) (Podsypanina et al. 2001).

2.1.2 PDK1, Akt activating kinase

PDK1 (3-phosphoinositide-dependent kinase1), a AGC kinase member, was purified and identified as a kinase, which phosphorylates Akt on Threonine 308 (Stephens et al. 1998) The structure of PDK1 is very similar to other AGC-kinases, especially its pleckstrin homology (PH) domain. For both Akt and PDK1 the translocation process to the plasma membrane is required for full activation (Andjelkovic et al. 1997; Anderson et al. 1998).

Phosphorylation sites on Akt were identified by using phospho mapping of quiescent cells and IGF-I stimulated cells. Stimulated cells are phosphorylated on Threonine 308 and Serine 473 and can be blocked completely by the PI3-kinase inhibitor wortmannin (Alessi et al. 1996). The kinase responsible for the phosphorylation on Serine 473 has not been identified and is still controversial. Phosphorylation on Serine 473 is dependent on PI3-kinase activity, as well as phosphorylation on Threonine 308, it would be logical that PDK1 also phosphorylated Threonine 473, however, this result was disapproved by using PDK1 knock out ES (embryonic stem) cells. It was shown that Serine 473 was phosphorylated similar to the wild type cells, whereas Threonine 308 phosphorylation was completely abolished in response to IGF-I stimulation (Williams et al. 2000).

3. Physiological roles of Akt (PKB)

Akt, the serine/threonine kinase, plays an important role in executing multiple cellular metabolic pathways, such as cell metabolism, cell survival and cell proliferation.

3.1 Metabolism

GSK3 β , the first physiological protein substrate identified for Akt, phosphorylates and inactivates glycogen synthases in response to insulin stimulation. Both isoforms GSK3 α and GSK3 β have the phosphorylation site Serine 9 and Serine

21 in the amino-terminal region and they are directly phosphorylated and inactivated by Akt (Burgering and Coffey 1995).

Akt phosphorylates and induces the activity of the heart 6-phosphofructo-2-kinase (PFK-2), which in turn stimulates glycolysis. The identified phosphorylation site is serine 466 (Deprez et al. 1997). Phosphodiesterase 3B (PDE3B) is phosphorylated by Akt on Serine 273, which in turn regulates the intracellular level of cAMP and cGMP in response to insulin (Kitamura et al. 1999).

Akt can also phosphorylate protein tyrosine phosphatases (PTP1B) on Serine 50 to inhibit its phosphatase activity towards the insulin receptor. PTP1B negatively regulates insulin sensitivity by dephosphorylating the insulin receptor. This acts as a feedback loop in response to insulin (Ravichandran et al. 2001). Akt can regulate several levels of glucose metabolism. It enhances glucose uptake in insulin-responsive tissue by affecting the glucose transporter GLUT1, GLUT3 and GLUT4. Akt was shown to increase the expression of the glucose transporter (Barthel et al. 1999); (Mazure et al. 1997) and the translocation of GLUT4 to the plasma membrane (Kohn et al. 1996; Cong et al. 1997; Tanti et al. 1997).

Akt phosphorylates TSC2 (tuberous sclerosis complex2) on four residues, inactivates it and thereby activates mTOR (Inoki et al. 2002; Manning et al. 2002; Potter et al. 2002). mTOR (mammalian target of rapamycin) activity appears to be dependent on intracellular ATP level (Dennis et al. 2001) and it was shown that ATP depletion activates AMP-activated protein kinase (AMPK), which in turn phosphorylates and activates TSC2 leading to the inhibition of mTOR activity (Inoki et al. 2003b). Akt is required for the phosphorylation of 4EBP1 (4E binding protein1) by mTOR (Gingras et al. 1998).

Rapamycin, an inhibitor of TOR/mTOR, down-regulates cap-dependent translation initiation. TOR/mTOR control protein synthesis by activating the translation initiation factor eIF4E (eukaryotic translation initiation factor 4E) (Barbet et al. 1996).

The rate-limiting step in mammalian translation initiation is the binding of the ribosome to mRNA. Almost all of the factors that are involved in the recruiting ribosome to the mRNA have phosphorylation states that are directly proportional to the translation and growth rate of the cell. 4EBP, the inhibitory protein of

elF4E, is similarly phosphorylated under the same circumstances. The mTOR pathway is mediating the phosphorylation of almost all of these factors, except elF4E (Gingras et al. 2001). mTOR activity is often measured by using the phosphorylation status of 4EBP1 and S6K.

3.2 Apoptosis

One of Akt's major functions is to promote growth factor-mediated cell survival and to block programmed cell death or apoptosis. Ectopically expression of a constitutive active form of Akt has been shown to promote cell survival in the absence of IGF-1 or serum (Kennedy et al. 1999). Mice lacking the Akt1 gene, have provided genetic evidence, that Akt is required for cell survival (Chen et al., 2001) Akt was shown to preserve mitochondrial integrity, and thereby to inhibit apoptosis. It requires glucose availability and is coupled to its metabolism. Hexokinase is known to bind VDAC (voltage dependent anion channel) and directly couple intra-mitochondrial ATP synthesis to glucose metabolism. Akt serves as downstream effector, which increases mitochondrial-associated hexokinase activity. The ability of Akt to maintain the mitochondrial integrity is dependent on glucose availability and through increased mitochondria hexokinase (mtHK) activity (Gottlob et al. 2001).

Growth factor withdrawal induced proteolytic cleavage of proapoptotic BCL-2 family member BID to yield its active truncated form tBID. Activated Akt inhibited mitochondrial cytochrom c release and apoptosis following BID cleavage. Akt also antagonized tBID mediated BAX activation and mitochondrial BAK oligomerisation. Both events have been shown to be critical for tBid-induced apoptosis. Glucose deprivation, which in turn impaires the ability of Akt to maintain mitochondrial-hexokinase association, prevents Akt from inhibiting BID mediated apoptosis (Majewski et al. 2004).

Bad is a member of the BCL-2 protein family, that binds to BCL-2 and BCL-X and inhibits their anti-apoptotic potential (Downward 1999). Akt can directly phosphorylate Bad on Serine 136 in vivo and in vitro (Datta et al. 1997; del Peso et al. 1997). Once phosphorylated, Bad is released from the BCL-2/BCL-X complex, which is localized on the mitochondrial membrane.

Phosphorylated Bad instead forms a complex with the chaperone 14-3-3 and remains cytosolic (del Peso et al. 1997).

Caspase 9 can initiate the apoptotic cascade; Akt can phosphorylate pro-caspase 9 on Serine 196 in a Ras-dependent manner that inhibits cytochrome c-induced cleavage of pro-caspase 9, which is required for enzymatic activity (Cardone et al. 1998). However, the Akt phosphorylation motif has not been found in caspase 9 from lower species, such as mouse or rat (Cardone et al. 1998).

3.3 Proliferation

P21/cip1/waf1 is a major cyclin/CDK inhibitor and was reported to be directly phosphorylated by Akt. Phosphorylation of p21 on Threonine 145 by Akt results in the inhibition of its potential to arrest the cell cycle. Inhibition and antagonizing of p21 by Akt targets nuclear localization of p21 and leads to activation of cyclin/CDK required for HER-2/neu-dependent tumor growth (Zhou et al. 2001).

P27/kip1 is also regulated by Akt-dependent phosphorylation on Threonine 157 in breast cancer cells. This activation by phosphorylation causes its nuclear localization signal (NLS), which excludes p27 from the nucleus and results in the activation of cyclin/CDK and cell cycle progression (Liang et al. 2002; Shin et al. 2002; Viglietto et al. 2002). It's a similar mechanism as described above for p21/cip1/waf1.

Akt can also regulate the expression level of p27 through mTOR. Down regulation of p27 in Akt-mTOR dependent manner was supported by the observation that Pten (Antagonist of Akt activity), which deactivates Akt, elicits growth arrest through elevation of the p27 protein level (Li and Sun 1998).

The tumor suppressor p53 is the best studied regulator of cell cycle progression and apoptosis in response to genotoxic stress (Vousden and Lu 2002). MDM2 (murin double minute2) is a ubiquitin E3 ligase that directly binds to p53 and targets p53 for ubiquitination. It was shown that Akt phosphorylates MDM2 and contributes to MDM2 nuclear localization (Mayo and Donner 2001). The precise effect of MDM2 is still controversial.

Akt is also required for the activation of mammalian target of rapamycin (mTOR), a large evolutionary conserved protein of about 300kD, a multifunctional kinase, that mediates protein synthesis (Gingras et al., 1998).

The loss of Akt or PI3K function results in impaired growth and smaller cells (Stocker et al., 2002; Weinkove et al., 1999), whereas the loss of PTEN function in *Drosophila* leads to an increased growth and larger cells. (Goberdhan et al., 1999; Huang et al., 1999).

4. Akt activity on mTOR controlled by growth factors

4.1 TSC1-TSC2 tumor suppressor

TSC1 and TSC2 proteins encoded by tuberous sclerosis complex 1 (TSC1) and tuberous sclerosis complex 2 (TSC2) genes are upstream of mTOR (Hay and Sonenberg 2004). These two tumor suppressor genes TSC1 (also known as hamartin) and TSC2 (also known as tuberin) encoded by two genes were associated with the autosomal dominant hamartoma syndrome (Cheadle et al. 2000a). Mutations in TSC1 and TSC2 genes contribute to sporadic TSC (van Slegtenhorst et al. 1997), and tuberous sclerosis patients have hamartomas in brain, skin, kidney and heart (Roach et al. 1998). Studies in mammalian cells have implicated these tumor suppressors TSC1 and TSC2 in cellular functions including cell cycle, endocytosis, cell adhesion and transcription (Pan et al. 2004).

Sequence-analysis revealed that rat TSC2 contains eight potential Akt consensus phosphorylation sites. For experiments, the group of Inoki et al obtained a rat cDNA, which contained only six putative Akt consensus phosphorylation sites because of an internal deletion (Inoki et al. 2002). Several groups have demonstrated that Akt directly targets TSC2 by direct phosphorylation in vitro and in vivo. Identified sites are Serine 939, Serine 1086/1088 and Threonine 1462/1422rat-short cDNA (Tee et al. 2002, Inoki et al. 2002)). Many reports have demonstrated that TSC1-TSC2 act to antagonize the insulin-signaling pathway through inhibition of S6K, which is downstream of mTOR (McManus and Alessi 2002).

Consistent findings of all studies in mammalian cells are that TSC1 and TSC2 form a complex (van Slegtenhorst et al. 1997; Nellist et al. 2002). The consequences of Akt-mediated TSC2 phosphorylation are not clear, there are reports supporting the model that Akt phosphorylation of TSC2 disrupts the TSC1-TSC2-complex (Dan et al. 2002; Potter et al. 2002) and mediates TSC2 degradation by ubiquitination (Inoki et al. 2002). Other reports indicate that Akt phosphorylation does not affect the complex between TSC1 and TSC2 (Manning et al. 2002).

Akt activity mediated by insulin and growth factors is significantly diminished in cells lacking TSC1 (Kwiatkowski et al. 2002) or TSC2 (Jaeschke et al. 2002), although Akt protein is expressed to the same extend compared to wildtype cells. The exact mechanism, how this intriguing phenomenon of a negative regulatory loop is occurring, is still unknown. One study suggested it is due to a reduced expression of PDGF alpha and PDGF beta (Zhang et al. 2003a).

Mammalian target of rapamycin (mTOR) is required for the regulation of a number of components of the translational machinery; the translational repressor 4E-BP1 (eukaryotic initiation factor 4E-binding protein1) and p70S6K (p70 ribosomal protein S6 Kinase), both are downstream targets of mTOR (Gingras et al., 2001; Schmelzle and Hall, 2000). The mTOR activity, measured by phosphorylation on p706K1 and 4E-BP1, was found to be constitutively phosphorylated in either TSC1^{-/-} or TSC2^{-/-} cells (Goncharova et al. 2002).

4.2 Rheb, a small G protein, activates mTOR

TSC1 and TSC2 do not have any sequence homologies with protein kinases or protein phosphatases and as a conclusion of this fact, the regulation to mTOR must be indirect. Sequence information of TSC2 has revealed a GTPase-activating protein (GAP) domain in its C-terminus (Krymskaya 2003). This GAP-domain is highly conserved from yeast to human (Hay and Sonenberg 2004). GAPs function is to down regulate the activity of small G proteins (small GTP-bound proteins) (Krymskaya 2003).

Small G proteins cycle in between active status GTP-bound and inactive status GDP-bound, whereas guanine nucleotide exchange factors (GEFs)

promote exchange between GDP and GTP on the small G protein. GAPs are responsible for the inactivation of small G proteins by exchanging GTP for GDP (Paduch et al. 2001). Genetic studies in *Drosophila* placed Rheb (Ras homolog enriched in brain), a small G protein, in the insulin-signaling pathway downstream of the TSC1-TSC2 complex and upstream of mTOR (Saucedo et al. 2003; Stocker et al. 2003; Zhang et al. 2003b). Using an RNAi-based screen in *Drosophila*, Zhang et al. could show a highly TSC2-GAP-specificity for the small GTP-binding protein Rheb. They found that only the inhibition of Rheb expression by RNAi, and none of the other 17 small G proteins abolished mTOR activity, measured by p70S6K phosphorylation on Threonine 389 (Zhang et al. 2003b).

Biochemical studies revealed that the ratio GTP to GDP bound on Rheb was decreased as shown by over-expression experiments using TSC1 and TSC2 cDNA in both mammalian and *Drosophila* cells (Castro et al. 2003; Garami et al. 2003; Inoki et al. 2003a; Zhang et al. 2003b). The role of TSC1 in the TSC1-TSC2-complex has been unclear, it was suggested it stabilized TSC2 to function as a GAP-protein (Li et al. 2004). The question that emerged from all studies is how Rheb activates mTOR?

Further biochemical studies showed that over-expression of Rheb increased mTOR activity measured by phosphorylation of p70S6K and 4EBP1 (Garami et al. 2003; Inoki et al. 2003a), and rapamycin, an inhibitor of mTOR activity, completely blocked the increased p70S6K phosphorylation induced by Rheb (Castro et al. 2003; Garami et al. 2003; Inoki et al. 2003a). Additionally, Inoki et al. observed increased phosphorylation of mTOR on Serine 2448, although the phosphorylation of this site accounting for mTOR activity is very controversial (Hay and Sonenberg 2004). It still needs to be addressed which factors are upstream and downstream of TSC1/2 and Rheb signaling.

4.3 TOR- target of rapamycin

The mammalian target of rapamycin (Figure 3), mTOR is a regulator for mRNA translation in the signaling pathways controlled by insulin, growth factors and availability of nutrients, such as amino acids (Myers et al. 1998).

TOR proteins, TOR1 and TOR2 were first cloned in yeast (Cafferkey et al. 1994) and originally named FRAP (FKBP-rapamycin and associated protein), RAFT (rapamycin and FKBP target), or RAPT1 (rapamycin target) (Brown et al. 1994; Chiu et al. 1994; Sabatini et al. 1994; Sabers et al. 1995). Rapamycin was isolated from the soil bacteria *Streptomyces hygroscopicus* and is a macrolide antibiotic with potent antifungal, immunosuppressive and antimitotic properties (Gregory et al. 1995). Rapamycin forms an inhibitory complex with FK506 binding protein (FKBP12), this FKBP12 complex then binds to a FRB (FKBP12-rapamycin binding) region in the carboxy-terminus of mTOR/TOR protein and inhibits their activity (Chen et al. 1995) (Choi et al. 1996).

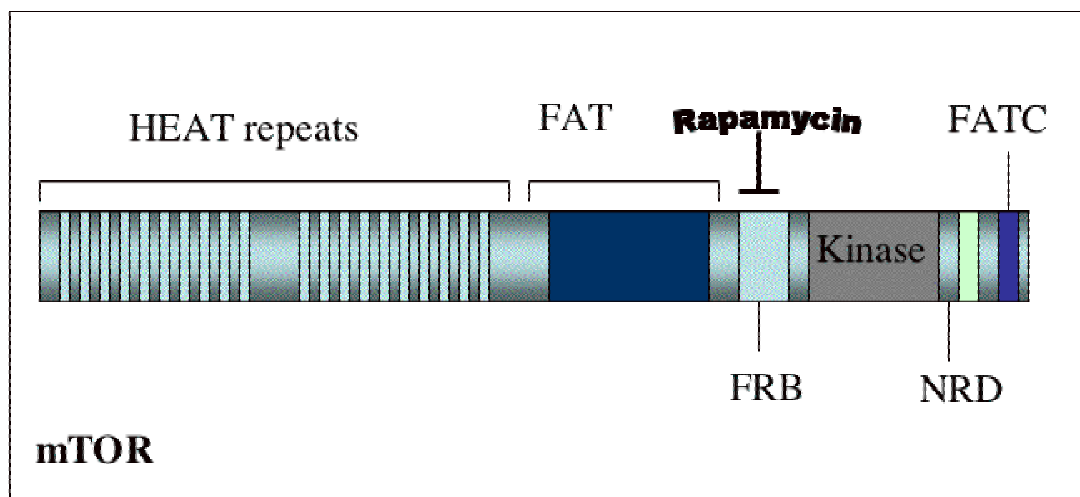


Figure 3: Structure of mammalian target of rapamycin (mTOR).

mTOR possesses 20 HEAT repeats in its amino-terminus, which are important for protein-protein interaction. The FAT domain, FRB domain, catalytic domain (kinase), NRD domain and FATC domains are located in the carboxy-terminus half of the protein TOR. The catalytic domain is very similar to the catalytic domain of the PI3-kinase.

The mammalian TOR protein (Figure 3), was cloned short after the yeast orthologue and has a similar structure exhibiting approximately 40% amino acid identity and conserved structural domain (Brown et al. 1994; Chiu et al. 1994; Sabatini et al. 1994).

TOR is a large evolutionary conserved protein of 2549 amino acids (depending on species) and about 280 kD of molecular weight. It possess 20 HEAT repeats (for Huntington, EF3, A-Subunit of PP2 A TOR1) in its amino-terminus, which are important for protein-protein interaction (Andrade and Bork 1995). The FAT domain, FRB domain, catalytic domain, NRD domain and FATC

domains are located in the carboxy-terminus half of the protein TOR (Figure 3). The catalytic domain is very similar to the catalytic domain of the PI3-kinase (Hay and Sonenberg 2004). The mammalian target of rapamycin displays an intrinsic serine/threonine kinase activity and can be autophosphorylated (Brown et al. 1995).

Insulin and activated Akt were shown to induce phosphorylation of mTOR *in vivo*. Two phosphorylation sites were identified for Akt, Threonine 2446 and Serine 2448. Serine 2448 was shown to be phosphorylated by Akt *in vitro* and *in vivo* (Scott and Lawrence 1998; Nave et al. 1999; Sekulic et al. 2000; Reynolds et al. 2002). However, mutation of both sites converted to alanine did not affect mTOR activity (Sekulic et al. 2000) and additionally, both phosphorylation sites are not conserved in *Drosophila* dTOR (Hay and Sonenberg 2004).

4.4 Downstream targets of mTOR

Akt is required for the phosphorylation and inhibition of 4EBP1 by mTOR (Gingras et al., 1998). TOR is responsible for the phosphorylation of p70S6K and activates it, whereas 4EBP1 activity is inhibited by phosphorylation of TOR. Both 4E-BP1 and p70S6K have been implicated in determining the cell size (Kozma and Thomas 2002). The phosphorylation of 4EBP1 and S6K is inhibited by rapamycin.

Thus, p70S6K accelerates global protein synthesis and phosphorylates the 40S ribosomal protein S6, which accelerates translation of mRNAs containing a terminal oligopolypyrimidine (TOP) track at the 5' end that encodes mainly for ribosomal protein and elongation factors (Jefferies et al., 1997).

The hypophosphorylated form of 4EBP1 binds to the translation initiation factor eIF4E (the cap-binding protein) and is a repressor of translation that inhibits the translation of cap-containing mRNAs. The full phosphorylation of 4EBP1 (hyperphosphorylated form) leads to the dissociation from eIF4E. Released eIF4E is able to interact with the cap region of the mRNA.

5. Control of mTOR by nutrients and energy metabolism

How cell growth, cellular energy level and nutrient availability are coordinated is a fundamental question in cell biology. The protein mTOR appears to control various cellular signaling in response to mitogens, nutrients (such as amino acids) and energy.

5.1 Protein-protein interaction with mTOR senses nutrient availability?

TOR or mTOR possess about 20 HEAT repeats in their amino-terminus, which are likely to be involved in protein-protein interaction (Andrade and Bork 1995). In addition to possessing kinase activity, TOR in yeast and mTOR in mammalian cells have been shown to interact with other proteins, which modulate mTOR/TOR kinase activity to its downstream effectors S6K and 4EBP.

TOR builds complexes with other proteins, which are likely for 'sensing' the availability of nutrients. Studies in yeast revealed TOR-complex1 and TOR-complex2 (TORC1 and TORC2), whereby TORC1 contains TOR1, TOR2, KOG1 and LST8. The mammalian orthologue of KOG1 is named Raptor (regulatory associated protein of mTOR), and builds a complex with the mammalian orthologue of LST8 (mLST8) and mTOR (Hara et al. 2002; Kim et al. 2002). Similar to TORC1 in yeast this complex has been named 'nutrient sensitive' complex (Kim et al. 2002).

mLST8, identified as a G protein β -subunit like protein, interacts specifically and independently of Raptor with the kinase domain of mTOR and plays a positive role in regulating mTOR activity (Kim et al. 2003). Raptor binds to mTOR on its amino-terminal domain containing the HEAT repeats and is required for interaction with the mTOR-Raptor complex (Kim et al. 2002). RNAi experiments in mammalian cells suggested a positive role for mTOR-activity regulation (Hara et al. 2002; Kim et al. 2002). Nutrient withdrawal resulted in an increased association of Raptor with mTOR (Kim et al. 2002). Raptor appeared to serve as an adaptor protein that recruits mTOR targeting S6k and 4EBP1 (Schalm and Blenis 2002). Changing conformation of the mTOR-Raptor complex

mediated by availability of nutrients, such as amino acids, affected mTORs ability to interact with the substrates S6K and 4EBP (Hay and Sonenberg 2004).

TORC2 in yeast contains TOR2, AVO-1, AVO-2 and AVO-3, whereas AVO-1 contains a Ras binding domain (RBD) of Ras targets and AVO-2 possesses a Ras-GEFN-domain (guanine nucleotide exchange factor) that has been found in exchange factors and activating proteins for Ras-like small GTPases (Loewith et al. 2002).

The exact mechanism, how mTOR or TOR senses nutrients, are still not clear and whether growth factor or insulin activation of mTOR is involved in this process.

5.2 Energy sensor mTOR, regulation through AMPK?

Translation (protein synthesis) requires both amino acids and a substantial amount of metabolic energy. The translation rate of mRNA was shown to be regulated by multiple signaling pathways, including intracellular ATP, nutrients, growth factor and environmental stress (Proud 2002).

Dennis et al. linked mTOR-activity to the availability of intracellular energy in form of ATP (Dennis et al. 2001). They showed that ATP depletion by reduced glucose availability or inhibition of mitochondrial respiration inhibites mTOR-activity. The interpretation of this effect was due to a low K_m of mTOR-kinase activity for the substrate ATP. However, under physiologically conditions, reduced glucose availability did not dramatically diminish ATP levels (Hay and Sonenberg 2004).

A sensor for even moderate changes of the intracellular ATP level is AMPK (AMP-activated kinase), which senses the status of the intracellular ratio of adenine nucleotides AMP and ATP. The AMPK-structure is built by a heterotrimeric complex composed of a catalytic α subunit and non-catalytic subunits β and γ . Activation of AMPK under hypoxia, exercise, ischemia, heat shock, and low glucose and is regulated allosterically by AMP-ATP ratios caused by a rising AMP level and by phosphorylation of the catalytic α subunit by one or more AMPK-kinases on Thr-172. The phosphorylation site of AMPK is located in the 'T-loop' of the catalytic subunit α (Hardie et al. 1998; Kemp et al. 1999) and

can be used as a read out for AMPK-activity (Kimura et al. 2003). Even a small reduction in ATP can result in elevation of cellular AMP through the activation of adenylate kinase, which is predominantly located in the mitochondrial matrix (Ryazanov et al. 1997) .

Activated AMPK directly phosphorylates multiple downstream substrates aimed to conserving the ATP-level. The goal of AMPK is to further reduce ATP-consumption by inhibiting key enzymes in the biosynthesis pathways such as ACC (acetyl-Co-A carboxylase) in fatty acid synthesis (Kemp et al 1999).

Kimura et al. showed for the first time that activation of AMPK decreased mTOR activity. AICAR (5-aminoimidazol-4-carboxiamide ribonucleoside), widely used as an AMPK activator, induced AMPK activity and impaired insulin-mediated phosphorylation of S6K. In addition, over expression of dominant negative AMPK increased S6K phosphorylation, whereas a constitutively active AMPK decreased S6K activity (Kimura et al. 2003).

Inoki et al 2003 provided more evidence for a link between ATP level (energy availability), AMPK and mTOR. TSC2 was found to be the mediator of energy status in response to AMPK. TSC2-KO (knock out) cells were more refractive to ATP depletion when compared to wild type cells. To elucidate the mechanism of how TSC2 is regulated by AMPK, an in vivo labeling and two-dimensional phosphopeptide mapping of TSC2 was performed. By using 2-deoxyglucose to induce AMPK activity, two important phosphorylation sites for AMPK, Threonine 1227 and Serine 1345 were found on TSC2. Over expression of a mutant TSC2, in which all AMPK phosphorylation residues were substituted by alanine, S6K phosphorylation (mTOR-activity) was more resistant to depletion of ATP (Inoki et al. 2003b). Whether GAP-activity of TSC2 was changed by AMPK phosphorylation, has not been determined yet.

5.3 LKB1 potentiates the effect on AMPK

LKB1, a serine/treonine kinase, is a tumorsuppressor, which is mutationally inactivated in the autosomal Peutz-Jeghers syndrome (PJS) (Boudeau et al. 2003a) (Boudeau et al. 2003b) as well as in some sporadic lung adenocarcinoma (Sanchez-Cespedes et al. 2002). LKB1 heterozygosity in mouse results in

sporadic hamartomatous gastrointestinal polyps, which phenocopy those in PJS patients (Rossi et al. 2002).

Hamartomas are benign tumors that display normal cellular differentiation but disorganized tissue architecture, which are very similar to hamartomas occurring in tuberous sclerosis complex and Cowden's disease (Shaw et al. 2004). The 55kDa protein LKB1 was shown to be required for repression of mTOR under low ATP conditions in cultured cells in AMPK and TSC2 dependent manner. Lkb1 null MEFs (mouse embryo fibroblasts) and hamartomatous gastrointestinal polyps from Lkb1 mutant mice showed elevated signaling downstream of mTOR (Shaw et al. 2004).

Biochemical studies confirmed the relationship between LKB1 and AMPK and showed that LKB1 potentiates the effects of increased intracellular AMP or reduced intracellular ATP by direct phosphorylation on Threonine 172 of the AMPK (Corradetti et al. 2004).

Using a phospho-mapping method, of co-transfected 293 cells with TSC1/TSC2 and mutant (kinase dead) LKB1, showed increased phosphorylation on Serine1345/Threonine1227 on TSC2 under ATP depletion. This result established the molecular mechanism of LKB1 function through TSC2 (Corradetti et al. 2004).

5.4 Amino acid sensor mTOR, AMPK-sensing mechanism?

A very crucial element involved in the translation initiation and protein synthesis are the protein substrates themselves i.e., amino acids. Among amino acids, leucine has been reported to have the most impact on mTOR activity (Hara et al. 1998). It was proposed that leucine activates mTOR activity, in part, by serving both as a mitochondrial fuel through oxidative carboxylation and by allosteric activation of glutamate dehydrogenase (Xu et al. 2001). This hypothesis supports a model, in which leucine modulates mTOR activity by regulating mitochondrial function and AMPK. Thus, energy and amino acids (leucine) responses are regulated by a similar mechanism: through the regulation of intracellular levels of ATP and/or AMP, which are mediating AMPK activity (Tokunaga et al. 2004).

6. Conclusion

Figure 4 depicts the regulation of the PI3-kinase-Akt-mTOR pathway, based on the available knowledge in the literature (described in CHAPTER I 2-5).

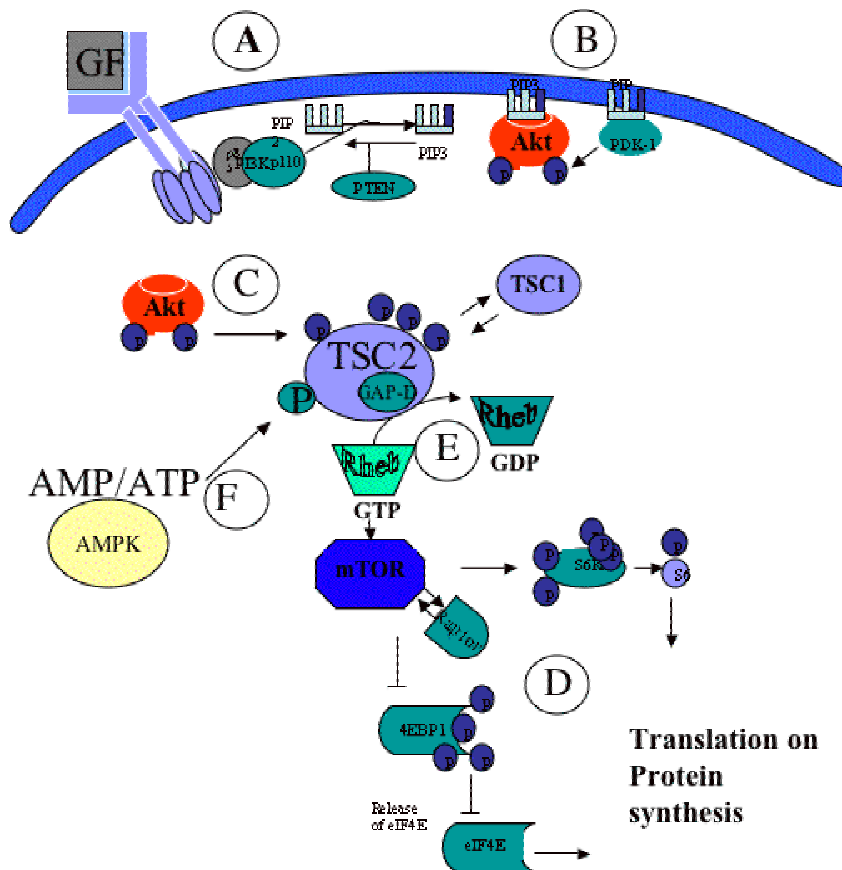


Figure 4: Scheme of the Akt-TSC2-mTOR pathway summarizing current literature.

Binding of growth factor leads to activation of the growth factor receptor, which in turn activates PI3-kinase (Figure 4 A). Activated PI3-kinase converts the second messenger PIP2 to PIP3. The rate-limiting step in the activation of Akt is the binding of PIP3 to the PH domain of Akt. Akt is then translocated to the plasma membrane, where it is phosphorylated on two residues, a threonine in the catalytic domain and a serine in the carboxy-terminal regulatory domain, for full activation. PDK1, which also possesses a PH domain, is the kinase that phosphorylates Akt on Threonine 308. Another yet unknown PI3K-dependent

kinase phosphorylates Akt on Serine 473 in the carboxy-terminus of Akt, are able to phosphorylate and thereby to activate Akt. Fully activated Akt phosphorylates TSC2 by direct phosphorylation on four sites (Figure 4C), which leads to a separation of the inhibitory complex between TSC1 and TSC2, and activates mTOR.

The kinase mTOR affects its downstream target 4EBP1 and S6K1, both are phosphorylated by its kinase activity and increasing protein synthesis (Figure 4 D). The small GTPase Rheb, which is in its active state GTP-bound, has been shown to activate mTOR. TSC2 inhibits activation of Rheb by exerting its GAP activity and converting Rheb-GTP bound to Rheb-GDP bound (Figure 4 E). AMPK was shown to phosphorylate TSC2 and to decrease mTOR activity under ATP depletion condition, hypothetically due to increased GAP-activity toward Rheb (Figure 4 F).

II. Practical- Effect of Akt (PKB) on the activity of mammalian target of rapamycin (mTOR)

1. Introduction

The serine/threonine kinase Akt, also known as protein kinase B (PKB), is a multifunctional kinase (Kandel and Hay 1999; Hanada et al. 2004). The primary structure of Akt is depicted in Figure 1. This dissertation is focused on the PI3-kinase/Akt/mTOR axis. The PI3-kinase-Akt-mTOR pathway plays an important role in development, cell growth and cell division. Deregulation of this pathway can lead to cancer, metabolic diseases, diabetes and obesity in humans. Especially, the process of tumorigenesis is the result of a disturbed balance between cell division and cell growth on the one hand, and programmed cell death (i.e., apoptosis) on the other. Activation of mTOR was shown to contribute to genesis of cancer, by loss of function of the tumor suppressor PTEN or by amplification of genes encoding catalytic subunits of PI3-kinase or Akt [reviewed in (Hay and Sonenberg 2004)].

What actually determines cell size? Availability of nutrients, energy in form of ATP, growth factors or physically stimuli induced cell growth? Increasing body of evidence placed mTOR as a central regulator of cell growth (size), proliferation and more recently, survival. Akt is required for the phosphorylation of 4EBP1 by mTOR (Gingras et al. 1998). However, despite this observation that Akt may act downstream of mTOR, there was no genetic evidence that Akt is required for mTOR activity, and it is not clear how Akt exerts its effect on mTOR. A very important question is whether TSC2 phosphorylation by Akt is sufficient to fully activate mTOR. mTOR activity is also dependent on intracellular ATP levels and AMPK activity. AMPK inhibits mTOR through the phosphorylation and inactivation of TSC2.

A better understanding of how Akt exerts its effect on the mTOR-signaling pathway may lead to the design of new drugs against cancer, metabolic diseases, diabetes and obesity. A relatively new mTOR-inhibitor or drug is rapamycin, which is in clinical trials to treat cancer, arthritis and heart diseases.

1.1 Objective

The focus of this thesis is to verify the activity of Akt on mTOR and how ATP availability affects the pathway in correlation with the effect on TSC2.

How does Akt regulate cell mass (size)?

Skeletal muscle cells of Akt1/Akt2 DKO mice show severe atrophy and a decrease in cell size (Peng et al. 2003). Increasing body of evidence placed mTOR as a central regulator of cell growth (size) and proliferation. The kinase mTOR affects its downstream targets 4EBP1 and S6K1, both are phosphorylated by its kinase activity and increasing protein synthesis (Kozma and Thomas 2002). Akt phosphorylates TSC2 on four residues, inactivates it and thereby activates mTOR (Inoki et al. 2002; Manning et al. 2002; Potter et al. 2002). Design of experiments to investigate the status of mTOR activity and TSC2 phosphorylation in Akt1/Akt2 DKO MEFs vs. WT may establish genetic evidence that Akt is required for the activation of mTOR by growth factor.

Does Akt regulate mTOR activity by a mechanism related to energy metabolism?

mTOR activity appears to be dependent on the intracellular ATP level (Dennis et al. 2001) and it was shown that ATP depletion activates AMP-activated protein kinase (AMPK), which in turn phosphorylates and activates TSC2 leading to the inhibition of mTOR activity (Inoki et al. 2003b). It was also shown that cells expressing activated Akt have a significantly higher level of ATP (Gottlob et al. 2001). It might be possible to underlie this observation by experiments that will determine if Akt deficiency reduces the intracellular level of ATP and how a decreased ATP level affects the AMP/ATP ratio and AMPK activity. To prove previous findings, experiments may uncover how AMPK attenuates Akt's ability to activate mTOR under ATP-depletion conditions. Furthermore, it is not known whether a reduced or high ATP-level mediated by Akt affects AMPK activity and which are potential downstream effectors. Experiments that determine the effect of Akt's ability to regulate the intracellular level of ATP and AMPK on downstream effectors, such as TSC2 or mTOR, will explore the mechanism.

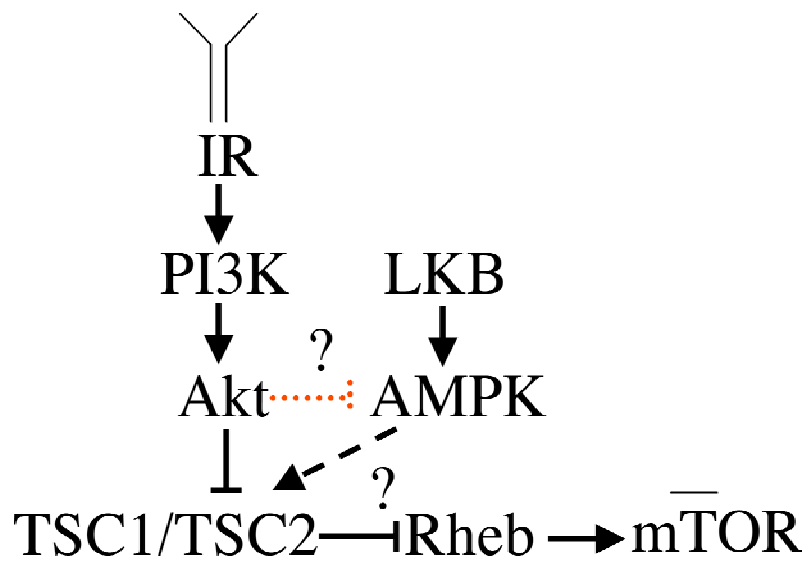
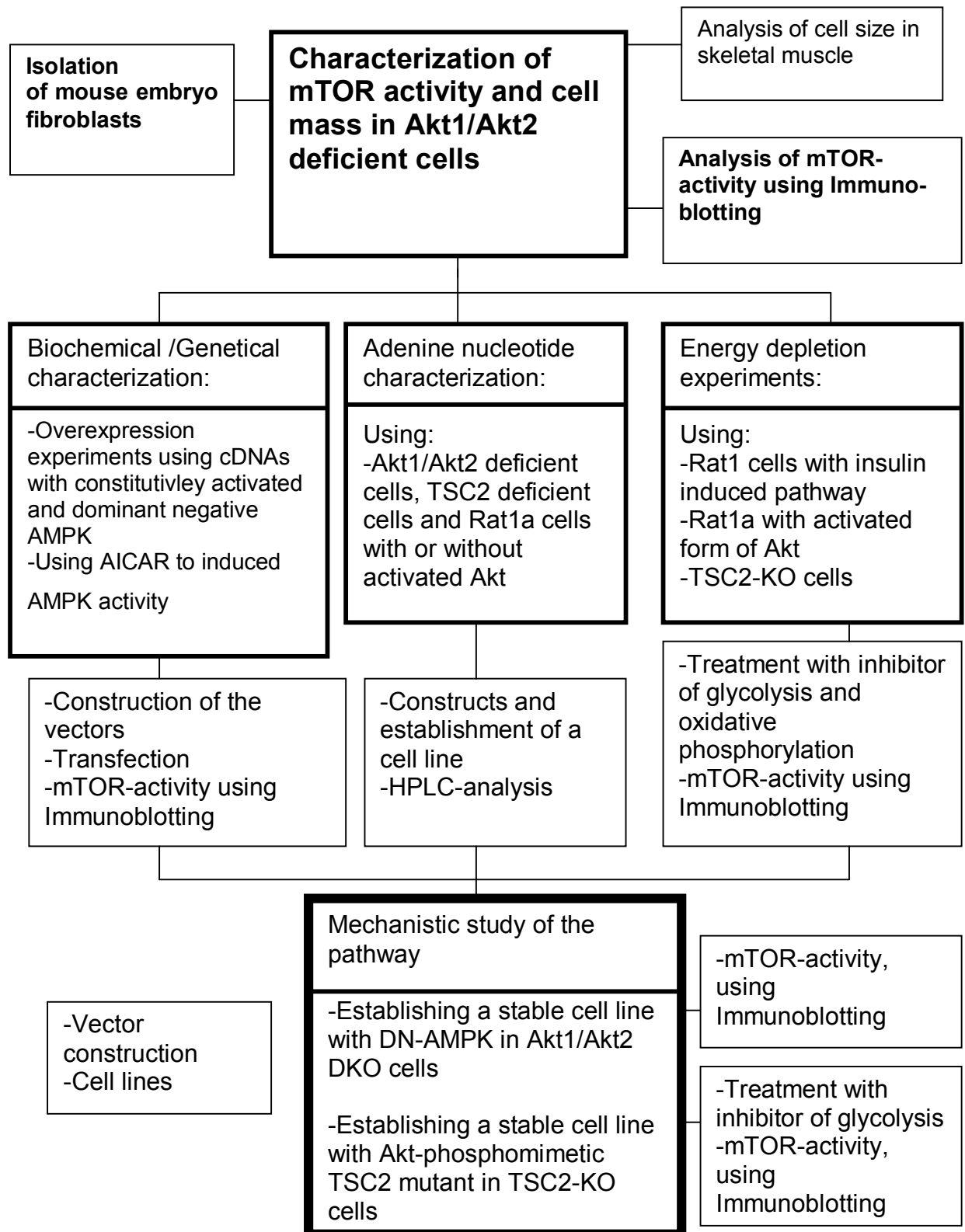


Figure 5: Hypothetical scheme for the regulation of the AKT-TSC2-mTOR pathway.

Activation of Akt leads to the direct phosphorylation of TSC2. Does Akt regulate mTOR by a mechanism related to energy metabolism and AMPK? And if so, which are the downstream targets for this regulation, e.g., TSC2, or more downstream targets?

IR (Insulin-receptor), (PI3K-phosphatidylinositol-3-kinase), Akt (serine /threonine activated protein kinase), TSC1 (tuberose sclerosis complex1-hamartine), TSC2 (tuberose sclerosis complex2-tuberin), AMPK (AMP-activated kinase), LKB1 (AMPK-kinase), Rheb (Ras homologue enriched in brain), mTOR (mammalian target of rapamycin).

2. Network



3. Materials and Methods

3.1 Materials

Chemicals

Acrylamide/bis-Acrylamide (29:1), 30% Solution	Sigma, St. Louis, MS, USA
AICAR	TRC Inc., Toronto/Canada
Agarose	Fisher, Fair Lawn, USA
Ampicilline	Fisher, Fair Lawn, USA
Ammonium Persulfate	Sigma, St. Louis, MS, USA
Bacto-Agar	Difco, USA
Bromphenol blue	Sigma, St. Louis, MO, USA
β -glycerolphosphate	Sigma, St. Louis, MO, USA
Chloroquine	Sigma, St. Louis, MO, USA
Chromatography paper	Fisher, Fair Lawn, USA
Coomassie Brilliant BlueR250	Sigma, St. Louis, MO, USA
DEAE	Sigma, St. Louis, MO, USA
Dextran	Sigma, St. Louis, MO, USA
2-deoxy-D-glucose	Sigma, St. Louis, MO, USA
DMEM	Invitrogen, Grand Island, NY, US
DMSO	Fisher, Fair Lawn, USA
ATP	Sigma, St. Louis, MO, USA
ADP	Sigma, St. Louis, MO, USA
AMP	Sigma, St. Louis, MO, USA
DTT	Sigma, St. Louis, MO, USA
Okadaicacid	Sigma, St. Louis, MO, USA
EDTA	Sigma, St. Louis, MO, USA
EGTA	Sigma, St. Louis, MO, USA
Ethidiumbromide	Sigma, St. Louis, MO, USA
Fetal Bovine Serum	AtlantaBiologicals, Oakbrook, USA
β -glycerolphosphate	Sigma, St. Louis, MO, USA

Glycerol	Sigma, St. Louis, MO, USA
HEPES	Sigma, St. Louis, MO, USA
IPTG	Sigma, St. Louis, MO, USA
Leupeptin	Sigma, St. Louis, MO, USA
Lipofectamin 2000	Invitrogen, Carlsbad, CA, USA
Lysozym	Sigma, St. Louis, MO, USA
2-Mercaptoethanol	Fisher, Fair Lawn, USA
MgCl ₂	Sigma, St. Louis, MO, USA
Na ₃ VO ₄	Sigma, St. Louis, MO, USA
NaCl	Sigma, St. Louis, MO, USA
NaF	Sigma, St. Louis, MO, USA
Nonidet NP-40	Sigma, St. Louis, MO, USA
PBS	Gibco, Invitrogen, USA
Penicillin/Streptomycin	Cambrex Bioscience, Walkersville, MD, USA
protease inhibitor cocktail complete	Boehringer Ingelheim, Mannheim/Germany
PMSF	Sigma, St. Louis, MO, USA
Pure Nitrocellulose (0,2 µm)	Schleicher & Schuell, Protran, USA
BSA	Fisher, Fair Lawn, USA
Rotenone	Sigma, St. Louis, MO, USA
Saccharose	Sigma, St. Louis, MO, USA
Skim milk	BD Difco, Sparks, USA
SDS	Fisher, Fair Lawn, USA
TEMED	Fisher, Fair Lawn, USA
5-thio-D-glucose	ICN, Biochemicals, Eschwege Germany
Rotenone	Sigma, St. Louis, MO, USA
Tris	Fisher, Fair Lawn, USA
Triton X-100	Fisher, Fair Lawn, USA
Trypsin/EDTA	Cellgro Mediatech, USA
Tween 20	Fisher, Fair Lawn, USA

3.1.2 Enzymes and kits

Dye Reagent (Bradford)	BIO-RAD Laboratories, USA
Calf Intestine Alkaline Phosphatase	MBI Fermentas
Gel extraction kit	Qiagen
Qiagen Maxiprep kit	Qiagen
Qiaquick gel extraction kit II	Qiagen
Rainbow Marker	Amersham UK, Buckinghamshire
Restriction endonucleases	MBI Fermentas
RNaseA	MBI Fermentas
T4-DNA Ligase	MBI Fermentas
T4-DNA Ligase Buffer	MBI Fermentas
Western-Blot detection kit	ECL detection reagent 1+2, Amersham UK, Buckinghamshire

3.1.3 Equipment

Centrifuge	Beckman Model J2-21M
Centrifuge Table	Eppendorf 5415 D
Centrifuge 4 °C	Thermo Electron Corporation
Electrophoresis system (DNA)	EC-135-90EC Apparatus Cooperation Electrophoresis system
Electrophoresis system	Hoefer 600 vertical Amersham Bioscience (PROTEIN)
Fridge and Freezer	Kelvinator -4°C, -20°C, -80°C
Incubator 37°C	mammalian cell culture, Forma Scientific CO ₂ waterjacketed incubator
Incubator 37°C	bacteria culture Precision Gravity Convection incubator
Microscope	Nicon, FRYET COMPANY INC
Fluorescence microscope	LEICA DM IRB and ARC-Lamp HBO

N ₂ -storage	XLC-440
Polaroid Gel camera	Gel CAMP POLAROID
Protein Wet Transfer chamber	BIO-RAD Trans-blot-cell
Stirrer	PC-353 Stirrer CORNING
Scales	Sartorius laboratory
Sterile guard hood	Class II Typ A/B3, The Baker company
Shaker, orbital	Bellco
Spectrophotometer	Beckman DU 640
Water bath 37°C	VWR Scientific model 12252
UV-Transilluminator	UVP (USA)
X-ray film exposure cassettes	Du Pont CRONEX

3.1.4 Plasmids and constructs

Expression vector:

- pcDNA3 (Invitrogen)

Retroviral vector:

- pLPCX (Clontech Laboratories, San Diego/CA)

- pBabe-Puro puromycin resistance gene (Morgenstern and Land 1990)

- pBabe-eGFP (Eves et al. 1998) was replaced with enhanced green fluorescence protein (eGFP)

Constructs:

- pcDNA3-AMPKalpha-II-DN-K45R-myc (Mu et al. 2001)

- pcDNA3-AMPKalpha-I-CA-Thr172D-myc (Woods et al. 2000)

- pcDNA-4EBP1-HA (Gingras et al. 1998)

- pBabe-Puro-mycAkt expressing an activated form of Akt/PKB encoding myristolated Akt (mAkt)

To eliminate the rate-limiting step in the activation of Akt, a myristolation signal was linked in frame to the amino-terminus of Akt. This constitutively activated form of Akt, termed MyrAkt, still requires the phosphorylation of the serine and threonine residues for full activation.

- pBabe- eGFP-mAkt (Eves et al. 1998; Kennedy et al. 1999)

- pcDNA3-HA-TSC2-2D-4E (S939D/S1086D/S1088D/T1422E (Inoki et al. 2002)

- pBabe-puro-AMPKalpha-II-K45R(DN-AMPK) new constructed
- pBabe-eGFP- AMPKalpha-II-DN-K45R (DN-AMPK) new construct
- pLPCX-TSC2-4D new construct

3.1.5 Enzymes and Antibodies

Antibodies were obtained from Cell Signaling Technologies (Beverly, MA) and included:

- phospho-acetyl-CoA carboxylase (Ser79) antibody # 3661
- Akt antibody # 9272, phospho-Akt (Ser473) antibody #9271
- phospho-4E-BP1 (Ser65) antibody #9451
- p70S6 kinase antibody #9202
- phospho-p70S6 (Thr389) antibody #9205
- phospho-tuberin (TSC2) (Thr1462) antibody #3611
- AMPK-alpha antibody #2532
- phospho-AMPK-alpha (Thr172) antibody #2531,
- S6 ribosomal protein antibody #2212
- phospho-S6 ribosomal protein (Ser235/236) antibody #2211
- phospho-(Ser/Thr) Akt substrate antibody #2974.

Antibody obtained from Santa Cruz Biotechnology (Santa Cruz, CA):

TSC2 (tuberin, C-20)

Antibodies obtained from Sigma-Aldrich:

- Anti-beta-actin
- anti-Myc #9E10

Secondary antibodies obtained from Zymed (San Francisco, CA):

- HRP-labeled goat anti-rabbit
- HRP-labeled rabbit anti-mouse

Antibodies provided by other laboratories:

- 4EBP1-antibody was provided by N. Sonenberg, University of Montreal, CA

Sequencing:

Sequencing was conducted by the DNA Sequencing facility at the University of Illinois in Chicago. Analysis of the sequence was performed by using the

software program “DNA-strider” and all available databases on the internet, for example Pubmed .

Primer for Sequencing :

Constructs in pcDNA3

-T7-Primer 5'-TAATACGACTCACTATAGGG-3'

-Sp6-Primer 5'-ATTTAGGTGACACTATAG-3'

Construct of TSC2 wt/TSC2-2D2E

-Upper primer: 5'-CGGAAGGATTTTGTCCCTTATATCA-3'

-Lower primer: 5'-GGTGAATGGTAGAGCTGTAGGAACA-3'

3.1.6 Bacteria and Cell lines

Cell lines:

# Name/Genotype	Cell type:	Original/Vector
01. iMEFs WT (Akt1+/+Akt2+/+) GFP	mouse embryo fibroblast	Lab-stock,
02. iMEFs DKO (Akt1-/-Akt2-/-) GFP	mouse embryo fibroblast	Immortalized by
03. iMEFsDKO (Akt1-/-Akt2-/-) AMPKalpha-II-DN	mouse embryo fibroblast	dominant negative - p53 (pBabe-Puro- GSE56) pBabe-Puro- GSE56 pBabe-GFP- empty vector pBabe- Puro-GSE56 pBabe- GFP-AMPK-alpha-II- DN
Rat1a	rat fibroblasts	Lab-stock Lab-stock,
Rat1aMyrAkt	rat fibroblasts	pBabe-Puro-mAkt
HEK293	human embryonic kidney	Lab-stock Lab-stock,
HEK293MAkt	cell human embryonic kidney cell	pBabe-Puro-mAkt
08. Phoenix cells, ecotropic	human embryonic kidney cell transfomed	Lab-stock created by placing into 293T constructs of producing gag-pol, and envelop protein
09.TSC2 +/- MEFs	mouse embryo fibroblast	from D.Kwiatkowski
10.TSC2-/- MEFs	mouse embryo fibroblast	
11. TSC2-/-MEFs	mouse embryo fibroblast	from D.Kwiatkowski
12. TSC2-/- MEFs MAkt	mouse embryo fibroblast	pBabe-Puro pBabe- Puro-mAkt
13. TSC2-/- MEFs TSC2- 4D 14. TSC2-/- MEFs	mouse embryo fibroblast	from D.Kwiatkowski
TSC2-4D MAkt	mouse embryo fibroblast	pLPCX-TSC2-3D-1E pLPCX-TSC2-3D-1E, pBabe-GFP-mAKT

Bacteria:

DH5 alpha

ϕ 80dlacZ Δ M15, recA1, endA1, gyrA96, thi-1, hsdR17 (r_k^- , m_k^+), supE44, relA1, deoR, Δ (lacZYA-argF) U169 (see PROMEGA, catalogue 1995)

Primary Cells:

Primary DKO (Akt1^{-/-}Akt2^{-/-}) and WT (Akt1^{+/+}Akt2^{+/+}) MEF (mouse embryo fibroblast) cells were isolated and cultured as previously described in (Chen et al. 2001).

3.1.7 Media, agarose plates, antibiotica and materials

For all cell lines DMEM high glucose (Dulbecco's modified Eagle medium from Invitrogen, Carlsbad/CA) containing 10% (v/v) FBS (fetal bovine serum from Atlanta, Norcross) and 1% (v/v) Penicillin/Streptomycin (c=10,000U/ml Penicillin, c=10 μ g/ml Streptomycin) from Cambrex Bioscience was used. DMEM (with L-glutamine, without glucose, without sodium pyruvate, # 11966-025 from Invitrogen, Carlsbad/CA) with 10% FBS dialyzed (# SH30079.02 from Hyclone, Logan) was supplemented with 5.5 mM glucose and used for cell lines in ATP-depletion experiments.

X-ray film	KODAC
Syringes	Falcon Becton Dickinson, Lakes USA
Tubes 1.5 ml, 2.0ml	Eppendorf
Tubes 15ml, 50ml	Falcon Becton Dickinson, Lakes USA
Cell lifter	Corning Incorporated, Corning USA
Cryotubes	Nalgene
Pipettes	Falcon Becton Dickinson, Lakes, USA

3.1.8 Buffers and solutions

All stock solutions were prepared with ddH₂O (Millipore) double distilled water and autoclaved or sterile filtered. Media and buffer were autoclaved or sterile filtered before using. ddH₂O (was generated by using a Millipore filtersystem (#CPMQ004D2) and stored at 4°C.

RNase A:	10mM Tris-HCl pH 7,5; 15mM NaCl solved to a concentration of 10mg/ml; to inactivate DNases the solution was incubated for 15 minutes and slowly cooled to room temperature, aliquoted and stored at -20°C
Ampicillin:	- solved to a concentration of 100mg/ml with ddH ₂ O, sterile filtered, aliquoted and stored at -20°C
Lysozyme:	- solved to a concentration of 20 mg/mL in TE pH 8.0 (10mM Tris 1mM EDTA) , sterile filtered, aliquoted and stored at -20°C

<u>20 x TBS pH 7.4</u>	<u>TE</u>
using HCl, 3M NaCl 1M Tris	10mM Tris/HCl, pH 7.5, 1mM EDTA
6X SDS-loading buffer	<u>20x PBS-Puffer pH 7.2</u>
	6M NaCl, 140mM Na ₂ HPO ₄ , 60mM NaH ₂ PO ₄ x 2 H ₂ O
1x TRIS pH 7.4-8.0 1M Trisbase	<u>1X TrisHCl pH 6.8</u>
	for SDS-stacking gel 1M Tris pH 6.8 using HCl
<u>1x Tris HCl pH 8.8</u>	<u>50X TAE</u>
for SDS-separation gel 1.5M Tris pH 8.8 HCl	2M Trisbase, 57.1ml Acetic Acid (1M), 0.5M EDTA (pH 8.0)
<u>0.5 M EDTA pH 8.0</u>	<u>DNA loading buffer</u>
using NaOH	0.25% Bromphenolblue, 0.25% Xylene cyanol FF 30% Glycerol 5mM EDTA

<u>Lysis buffer</u> protect phosphorylation status of proteins 20 mM Tris HCL (pH 7.5), 100 mM KCl, 20 mM beta-glycerolphosphate, 1mM DTT, 0.25 mM Na ₃ VO ₄ , 10 mM NaF, 1mM EDTA, 1mM EGT, 1mM PMSF, 10mM Na-pyrophosphate, 10 nM Okadaicacid, Protease inhibitor cocktail complete	
---	--

3.2 Cell culture methods

3.2.1 Culture conditions, stimulations and Inhibitions

1.5x10⁶ primary DKO (Akt1^{-/-}Akt2^{-/-}) and WT (Akt1^{+/+}Akt2^{+/+}) MEFs (passage 3) were plated in 15-cm-plates in DMEM with 10% FBS and deprived of serum for 24h. Cells were stimulated with insulin (1µg/ml), 10% FBS and 20% FBS for 60 min and intracellular ATP, ADP and AMP concentrations were analyzed by HPLC (see CHAPTER 3.9). For Western analysis cells were stimulated with 10% FBS and 20% FBS for 30 and 60 minutes.

Rat1a, TSC2 ^{+/}- MEFs and TSC2^{-/-} MEFs (1x10⁶ /10-cm-plate) were plated in DMEM (5.5 mM glucose) with 10% FBS (dialyzed) and deprived of serum for 24h, stimulated with insulin (1µg/ml) for 30 minutes and either further stimulated with insulin (1µg/ml) for 30 minutes or ATP-depleted by using different concentrations of 5-thio-D-glucose, 2-deoxy-D-glucose and rotenone.

Rat1a MAkt cells (1x10⁶ /10-cm-plate) expressing activated Akt were deprived of serum for 24h in DMEM (5.5 mM glucose) and treated with different concentrations of 5-thiogluucose, rotenone and AICAR for 30min.

293MAkt (1x10⁶ /6-cm-plate) were plated in DMEM with 10% FBS and transfected with increasing concentrations of pcDNA3-AMPKalpha-I-CA-Thr172D-myc (5, 10, 15, 20 µg DNA) and 2.5 µg pcDNA-4EBP1-HA per 1x10⁶ cells by using Lipofectamine 2000, (CHAPTER 3.5.2).

3.2.2 Maintenance of cell lines

All cell culture work was done under sterile conditions (sterile guard hood Class II Type A/B3, Baker company Inc.). For pipetting sterile serological pipettes (Falcon, BD) and automatic pipette aids were used. Supernatants of cultured cells and solutions were vacuumed by using sterile Pasteur pipettes. All cell lines were cultured at 37°C using a CO₂ water jacketed incubator for mammalian cell culture from Forma Scientific. The culture of all incubated mammalian cells were controlled every day to observe confluence status by using a light microscope (Microscope Nikon, FRYET COMPANY INC). The culture medium DMEM with 10% (v/v) FBS and 1% (v/v) Penicillin/Streptomycin was replaced every third day of culture. Cultured cells were used shortly after plating and expansion, to avoid long-term effects, such as mutations.

Splitting of cell lines was performed by washing the plates two times with PBS solution and incubating the cell plates with 1-3ml Trypsin/EDTA, dependent on the size of the plate for 1-5 minutes. After cells had been detached, DMEM with 10% FBS was added and cells were gently resuspended and split to a ratio 1:3 or 1:5 depending on the growth rate of the cell line.

3.2.3 Storage of cells

Cell lines were stored for long-term use in liquid nitrogen or for short-term use in a freezer at -80°C. For storage of cell lines, cells of interest were trypsinized when confluence reached 70%, centrifuged at 1000rpm for 5 minutes, resuspended in ice cold freezing solution and aliquoted in cryotubes. Tubes were transferred immediately into an -80°C freezer for short-term use and stored in liquid nitrogen for long-term use.

Frozen cell lines were thawed at 37°C in a waterbath. Immediately after thawing, the cell-solution was transferred into a 10 ml Falcon tube and resuspended in DMEM with 10% FBS, centrifuged at 1000rpm for 5min, the supernatant discarded and cells resuspended in fresh DMEM with 10% FBS and plated.

Freezing solution:

90% FCS

10% DMSO

3.3 Mouse embryo fibroblast (MEF) isolation

Mouse embryo fibroblasts were produced using the protocol from (Chen et al. 2001). The first step for the production of mouse embryo fibroblast (MEFs) is to sacrifice the bearing animal in the embryonic stage between days 12-14. With sterile techniques and solutions, the uterus containing embryos was removed and placed in DMEM. After transfer into a laminar flow hood, the embryos were placed into a 15ml conical tube and rinsed 3 times with 5 ml DMEM.

The top half of the embryo head and the internal organs were removed and stored in a separate conical tube for genotyping. With forceps and a fresh disposable scalpel the remaining parts of the embryo were minced very well and transferred into a 15 ml conical tube containing 5ml 0.05% trypsin-0.02% EDTA. The tube was inverted for several times and then placed for 5 min in a 37°C water bath (every minute the tube was inverted and returned to the water bath).

The supernatant was placed in a 15 ml conical tube containing 5 ml DMEM with 10% FBS and with 1% Penicillin/Streptomycin. 5ml of trypsin was added to the embryo and incubated for 5 min. The two tubes were combined (total volume was 15ml) and centrifuged for 5min. After the supernatant had been discarded, the pellet was resuspended in 10 ml of DMEM with 10% FBS-PS and put into a 10 cm dish overnight.

On the next day, the plate was nearly confluent and split into 2x15 cm plates. Once grown to confluence, primary MEF cells were frozen down in 4 cryovials per 15 cm plate and stored at -80°C in a freezer.

3.4 Transfection of adherent mammalian cells for recombinant expression

3.4.1 Calcium phosphate method

1-1.5x10⁶ adherent 293 cells or 293 MAkt cells were plated in 6 cm plates in DMEM with 10% FBS one day before the transfection. 30min before the transfection, the media was changed to 3ml DMEM with 10% FBS. The amount of DNA was dissolved in 440µl of 0.1X TE (pH 8.0) by mixing and allowing to sit for 5 minutes in a 1.5ml eppendorf tube. After 5 min, 500 µl HBS (pH 7.05) buffer was added to each tube and mixed. Using a 1ml pipettor hooked up to a taped pipette aid, the DNA-TE-HBS solution was bubbled and 62µl of 2M CaCl₂ was drip wise added. To increase the transfection efficiency, chloroquine (25µM) was added to each plate. The final step was to drip each of the 1.0 ml transfection aliquots of precipitate onto one plate and to mix the media with this aliquot by rotating the plates. After 1 hour there were salt crystals detectable by using a light microscope. The transfected plates were incubated overnight at 37°C. On the next day, the 293 or 293 MAkt cells were washed with PBS and the media was replaced with DMEM with 10% FBS. Expression of the ectopic protein was dependent on the construct and had to be addressed before starting the actual experiment (Sambrook 1998).

3.4.2 Lipofectamine 2000 method

Transient overexpression of cDNA constructs into eukaryotic cells was performed with Lipofectamine 2000 from Invitrogen, specifically by co-transfection of two or three different constructs (according to the manufacturer's instructions).

Liposomes are microscopic spherical vesicles that form when phospholipids are hydrated. When mixed in water under low shear conditions, the phospholipids arrange themselves in sheets, the molecules aligning side by side in like orientation, "heads" up and "tails" down. These sheets then join tails-to-tails to form a bilayer membrane, which encloses the DNA in a phospholipids sphere.

One day before transfection, cells were plated in 6cm plates using DMEM with 10% FBS. The next day, the media was changed to DMEM without FBS and without Penicillin/Streptomycin (1h before transfection). At the same time the suitable DNA-constructs were prepared in 300µl DMEM without FBS and without Penicillin/Streptomycin by gently mixing and incubating for 5 minutes at room temperature. Lipofectamin (20µl) was added to 300µl DMEM without FBS and without Penicillin/Streptomycin. Immediately the DNA-DMEM-solution was added to the Lipofectamin-DMEM-solution and incubated for 20 minutes at room temperature. After incubation the transfection-mix was added on the prepared plates and placed back into the incubator at 37°C for 5 hours. Finally, after incubation, 1ml DMEM with 20% FBS was added to each plate. Transfected cells were used for treatment 24 hours post-transfection.

3.4.3 DEAE-Dextran-Chloroquine method

293 cells were transfected by using the DEAE-Dextran-Chloroquine method (Gonzalez und Joly 1995). The expression vector containing the cDNA of interest or the empty vector for ectopically expression experiments was prepared in 50µl TE pH 7.5. The amount of DNA varied dependent on the experiment. $1-1.5 \times 10^6$ adherent cells were plated in 25 cm² flasks with resealable lids in DMEM + 10% FBS and cultured for 24h. 15ml Falcon tubes were used to set up the transfection-mix for each sample by transferring 2.5ml DMEM without FBS and 100µl DEAE-Dextran-Chloroquine solution. Before transfection, media in the cell culture plates were replaced with DMEM without FBS (1h before transfection). DNA-TE-buffer and transfection-mix were mixed under sterile conditions and incubated at room temperature for 5 minutes.

After the media were removed from the plates, the ready-transfection- mix was applied to the plates, the lid was closed and incubated for 2h at 37°C. Closing of the lid causes a drop of the pH-level of the media, which in turn increases the efficiency of the transfection. After 2h incubation the transfection-mix was removed and replaced with PBS-buffer+10% DMSO for 2 minutes and washed with PBS-buffer. Finally, normal DMEM with 10% FBS and

Penicillin/Streptomycin was added and the plates were placed into the incubator for overnight incubation.

<u>DEAE-Dextran-Chloroquine</u> 10mg/ml DEAE-Dextran in PBS 2.5mM Chloroquine

3.5 Retrovirus production and infection

For the production of high virus titers of pLPCX-Puro-TSC2-4D, pBabe-eGFP-AMPKalpha-II-DN-K45R, pBabe-eGFP-mAkt and pBabe-eGFP, packaging ecotropic Phoenix cells were transfected by a calcium phosphate method (CHAPTER 3.5.1). Cells were plated one day before transfection at approximately 50% confluence in 15-cm-diameter tissue culture plates. Two days after transfection, viral supernatants were collected and concentrated by ultrafiltration (membrane # PBVK06210 from Millipore, Bedford). Concentrated virus solution was first passed through 0.22 μ m filter units (Millipore) and mixed with DMEM with 10% FBS (1:1). The solution was added to the cells of interest in the presence of polybrene 8 μ g/ mL (Kennedy et al. 1999) . Cells were selected by puromycin and cells expressing 85-95% GFP were used as polyclonal cell lines for further experiments. Polyclonal cell population that displayed lower transfection rates were sorted by FACS (Vantage Becton Dickinson, San Jose, CA) for enhanced green fluorescence protein signal (eGFP) to ensure high expression levels of the respective plasmids.

3.6 Modification and amplification of DNA

3.6.1 Methods of *in vitro* modification of DNA

Conditions and buffers were used according to the manufacturer's instructions. Restriction of DNA with endonucleases (Sambrook 1998) was used for control of ligations (Miniprep-Plasmid-DNA) and for preparative use. To each DNA-digestion 1 μ g DNA in a volume of 20 μ l was added with 3-5 Units of restriction endonucleases and buffers according to the manufacturer's instructions.

Reactions with more than one endonuclease enzyme were possible using the same buffer conditions. If reaction buffers had different requirements for NaCl concentrations, the lowest NaCl concentration and the second endonuclease enzyme were added after the NaCl concentration was adjusted to the higher salt concentration. If the reaction buffers required different ions, agarose electrophoresis was used to separate the DNA-fragments after the first digestion. The necessary DNA-fragment was cut out and purified by using the gel extraction kit (CHAPTER 3.2.1). The second incubation with the endonuclease enzymes were performed using the buffer according to the manufacturer's instructions. For Mini-preparation-plasmid-DNA the digestion-reaction contained 0.5µl RNase-standard solution.

3.6.2 Preparation of vector-DNA

Vector-DNA was used in a concentration of 1µg pro 20µl total volume and digested with the suitable endonucleases. The reaction was incubated for 1-3 hours with 3-5 Units/µg DNA and the buffer according to the manufacturer's instructions. After digestion, the linearized Vector-DNA was dephosphorylated.

The approach was set up to use 20 µl total digestion-volume and add up to a total volume of 50µl with 1x CIAP-buffer and 1 unit Calf Intestine Alkaline Phosphatase for 30 minutes at 37°C. The stop reaction was performed at 85°C for 15 minutes or by phenol/chloroform extraction followed by ethanol precipitation. Dephosphorylation of the vector was controlled during the ligation reaction by using vector-DNA without insert-DNA (cDNA of interest, „Self-ligation“). The number of colonies in the vector-only reaction occurring after transformation on the LB-agarose plate compared to the number of colonies occurring in the vector-insert reaction were validating the dephosphorylation process. If there were less colonies on the 'vector-only-reaction' plate compared to the 'vector-insert reaction' plate, the ligation reaction was successful.

Ligation of DNA fragments (vector and insert) was performed at 22°C for 2-3 h using T4-DNA-ligase and T4-DNA Ligase buffer according to the manufacturer's instructions.

The inactivation of T4-DNA Ligase was accomplished by incubation at 65°C for 10 minutes. 50% of the ligation reaction was used for the transformation process, the other 50% were stored at -20°C.

3.6.3 Gel electrophoresis

Plasmid-DNA and DNA-Fragments were separated on horizontal agarose gels 7*10*0.5 cm (width*length*thickness), in 1x TAE-buffer (Sambrook 1998). Concentrations of agarose gels were dependent on the size of DNA-fragments to be separated ranging from 0.7%(w/v) - 1.5%(w/v). Restricted DNA-samples were mixed with loading buffer (CHAPTER 3.1.8) and loaded on the agarose gel. The gels were run 1-3 hours with 80-100 V with a DNA-size marker 1kb DNA-ladder. Agarose gels with ethidium bromide-stained DNA-fragments were visualized under UV illumination (366 nm).

3.6.4 Isolation of restriction fragments from gel slices

To obtain the desired DNA fragments the gel was cut by using a scalpel and transferred to an Eppendorf tube.

3.6.5 Phenol extraction and ethanol precipitation of DNA

Separation of DNA solution from protein, which could disturb the transfection process of mammalian cells, was performed by phenol-chloroform-isoamyl alcohol (24:24:1, v/v/v) extraction. The aqueous phase was mixed with an equal volume of TE saturated phenol-chloroform-isoamyl alcohol for 30 seconds. The solution was centrifuged at 12,000rpm for 5 minutes and the upper aqueous phase was mixed a second time with the phenol-chloroform-isoamyl alcohol phase for 30 seconds and centrifuged again. To remove all remaining phenol the upper phase was removed and placed in a new Eppendorf tube and extracted with chloroform-isoamyl alcohol. After centrifugation at 12,000rpm for 5 minutes,

the transferred upper aqueous phase was precipitated by adding 1/10 volume 3M-sodium acetate (pH 5.2) and 2.5 fold volume of ethanol (96%, v/v). The mixture was stored at -20°C for 30 minutes or by -80°C for 10 minutes. After centrifugation at 12,000 rpm for 15 min at 4°C , the pellet was washed with 70% (v/v) ethanol, air dried and redissolved in TE (appropriate volume).

3.6.6 Quantitative determination of DNA concentration

To determine the amount and quality of the preparative DNA, 5 μl were measured spectro-photometrically at 260nm in a dilution of 1:500 in TE-buffer. The ratio A_{260}/A_{280} describes the purity of the sample. Because the DNA was intended to be used for transfection of mammalian cells, the ratio needed to be >1.8 .

3.6.7 Production of competent bacteria cells for transformation

Competent bacteria are needed to transform ligation products to select for the right construct and to amplify the construct.

Using the classical method, competent cells were prepared by treatment with CaCl_2 as described by Janssen et al. 1994. 10 ml of an overnight culture of DH-5 α *E.coli* were inoculated in 300 ml LB-media and incubated again by 37°C and shaken until the OD_{600} reached 0.6. After incubation on ice for 10 minutes the culture was centrifuged at 4000 rpm at 4°C for 5 minutes.

The supernatant was discarded and the pellet was resuspended in 40 ml ice-cold 100mM CaCl_2 buffer and incubated on ice for 10 minutes. This step was repeated two times. Lastly, the pellet was resuspended in 8 ml ice-cold 100mM CaCl_2 buffer, incubated on ice for 10 minutes and aliquoted in Eppendorf tubes. Aliquots of 100 μl cell suspension were snap frozen in liquid nitrogen and stored at -80°C until usage. Transformation efficiencies of 10^6 to 10^8 transformed cells per supercoiled plasmid DNA were obtained. CaCl_2 competent bacteria cells were stored up to 6 months in 100mM CaCl_2 at -80°C .

3.6.8 Transformation of vector or plasmid DNA in competent bacteria

Competent bacteria cells (approximately 100 μ l) and 10 μ l of total 20 μ l ligation reaction were gently mixed and incubated on ice for 30 min. The remaining 10 μ l of each reaction were stored at -20°C . After 30min a heat shock was performed at 42°C for 2 minutes. Addition of 900 μ l LB-Media without antibiotics and shaking of the bacteria solution at 200 rpm (37°C) for 30 minutes led to a recovery and continued growth. 100 μ l of each bacteria culture were transferred to a LB-agarose plate with antibioticum (dependent on the expression vector). The remaining culture was centrifuged at 6000rpm and only the pellet was plated on a LB-agarose plate with antibioticum. This step served to increase the number of bacteria colonies per plate. All plates were incubated at 37°C overnight.

3.6.9 Mini-preparation

Mini-preparation was used for analytical approaches. After transformation of the desired plasmid or ligation reaction, one to 30 positive colonies were picked from a LB-agarose plate with a toothpick and cultured in 2.5 ml liquid LB-medium with antibioticum at 37°C and 220rpm overnight. 1.5ml of each culture, which represent one plasmid/colony, were used to pellet the bacteria by centrifugation. The pellet was resuspended in 400 μ l Stet-buffer, mixed with 32 μ l of Lysozyme and boiled for 50 seconds. After bacteria cells were lysed, the sample was centrifuged at 15,000rpm for 15 min and the pellet of lysed bacteria cells was removed with a sterile toothpick. 400 μ l of isopropanol was added to the solution and stored for 20 min at -20°C .

After precipitation of the DNA with isopropanol, the solution was centrifuged for 15 minutes at the maximum speed (13,000rpm). The supernatant was discarded and the resulting DNA-pellet was washed with 70% (v/v) ethanol. After the pellets were dried, the DNA was resuspended in 10-30 μ l TE-Buffer (CHAPTER 3.1.8) dependent on the size of the pellets (DNA yield). Mini-preparation-DNA was used to screen for the right construct after cloning of cDNAs, for example DN-AMPK into the pBABEpuro vector. Control restriction protocols included the use of RNases, because RNA was still present in Mini-preparation-DNA solution.

Stet-buffer

8% Saccharose (w/v), 5% Triton (v/v)

50 mM EDTA, 50 mM Tris HCl pH 8.0

3.6.10 Maxi-preparation

For preparative use, a Qiagen-kit Pack-500 tip was used according to the manufacturer's instructions.

1.5 ml overnight culture or Mini-Preparation-culture was inoculated to 250 ml LB-media with antibiotica and cultured at 37°C and 220rpm overnight. The bacteria culture was centrifuged for 15 minutes at 6000 rpm at 4°C and the supernatant was discarded. After resuspension of the bacteria pellet by vortexing or pipetting up and down with 10 ml P1 buffer, 10ml P2 buffer (Qiagen-kit) was added and mixed gently but thoroughly by inverting the tube 4-6 times. An incubation time of 5 minutes allowed for lysis of the bacteria cells. Adding 10ml P3 buffer and inverting the tube 4-6 times neutralized the solution. Incubation of the solution for additional 20 minutes led to separation into two phases, one with fluffy white material. The precipitated material contains genomic DNA, protein, cell debris and SDS.

Centrifugation for 30 minutes at 20,000g at 4°C separated the fluffy white material from the solution, at the same time a Qiagen-tip 500 column was equilibrated by applying 10ml of QBT-buffer, and allowed to empty by gravity force. The supernatant was transferred to the column and after the supernatant passed through the column, QC-buffer was used to wash the resin two times by applying 30ml each time. Using 15ml QF-buffer the DNA was eluted into a 50ml Falcon tube, which contained 10.5ml isopropanol for precipitation of the DNA. Immediately after precipitation the solution was mixed and centrifuged at 15000g for 30 minutes at 4°C. The supernatant was removed and the pellet was carefully washed with 70% (v/v) ethanol. Then, the air-dried pellet was redissolved in 205µl TE-buffer. To determine the amount and quality of the preparative DNA, 5µl were measured spectrophotometrically at 260nm in a dilution of 1:500 in TE-buffer. The ratio A_{260}/A_{280} describes the purity of the sample. Because the DNA

was intended to be used for transfection of mammalian cells, the ratio needed to be >1.8. Otherwise, an additional phenol-chloroform-isoamyl alcohol extraction (24:24:1, (v/v/v) had to be performed (CHAPTER 3.7.4).

3.7 Protein Methods

3.7.1 Whole-Cell Lysate Preparation

Cells were washed with ice cold PBS after treatment and scraped into 1.5ml-2.0ml Eppendorf tubes using a sterile cell lifter, centrifuged at 2000rpm for 2 minutes at 4°C and the supernatant was discarded. Cells ($1-2 \times 10^6$) were resuspended in 100-200µl lysis buffer (20mM Tris HCl (pH 7.5), 100mM KCl, 20 mM beta-glycerolphosphate, 1mM DTT, 0.25mM Na₃ VO₄, 10mM NaF, 1mM EDTA, 1mM EGTA, 1mM PMSF, 10mM Na-pyrophosphate, 10nM Okadaicacid and protease inhibitor cocktail complete (Boehringer Ingelheim, Mannheim/Germany), and the cell lysis was prepared by thaw-freeze-cycle extraction. All working steps were performed on ice. Three thaw-freeze-cycles have been carried out on dry ice and a 37°C waterbath in rotation, thereby the cell debris was never warmed up over 4°C. The debris was centrifuged at 13,000 rpm at 4°C and the supernatant was transferred into new Eppendorf tubes; aliquots for protein measurements were taken before the samples were stored at -20°C.

<u>6x SDS-Loading-buffer</u>	<u>Lysis-buffer</u>
1.95ml 1M Tris pH 6,8	20mM Tris HCl (pH 7.5)
0.9g SDS	100mM KCl
1.5ml -Mercaptoethanol	20mM beta-glycerolphosphate
5% Bromphenolblue	1mM DTT, 0.25mM Na ₃ VO ₄
ad 5ml dd H ₂ O	10mM NaF
	1mM EDTA
	1mM EGTA
	1mM PMSF
	10mM Na-pyrophosphate
	10nM Okadaicacid and protease inhibitor cocktail complete

After having determined protein concentrations of each sample using the Bradford method, 6x SDS-Loading-buffer was added to the lysate. The suitable amount of protein was loaded on a SDS-PAGE.

3.7.2 Quantification of proteins

For the quantification of proteins the Bradford method was performed using a ready mixed dye from BIO-Rad. The dye containing Coomassie brilliant blue G250 binds to aromatic and basic amino acids. Each sample was measured 3 to 4 times and averages over all measurements were used to calculate the concentration. 1-12µg BSA per ml were used for the standard curve. The color has been allowed to develop for at least 5 minutes, but not longer than 30 minutes. The measurements were performed in a spectrophotometer at 595nm.

3.7.3 SDS-PAGE

Polyacrylamide-gel-electrophoresis (SDS-PAGE) was used to separate proteins by molecular weight. The SDS-PAGE contains a lower phase, separating-gel and an upper phase, the stacking-gel. All ingredients needed for the chosen percentage were mixed and poured quickly into the gel casting (Hoefer 600 vertical Amersham Bioscience). Approximately 2 centimeters below the bottom of the comb were left for the stacking gel. For the polymerization process water saturated butanol was used to layer the top of the gel. The layer also removed the bubbles at the top of the gel and ensured that this part did not dry out. 30 minutes were needed for the gel to polymerize completely. The use of fresh ammonium persulfate usually leads to a quick gel polymerization and is therefore more reliable. While waiting for polymerization of the separating-gel or running-gel, the reagents for the stacking-gel were mixed. After the running gel was polymerized, butanol was washed out completely. Quickly after pouring the stacking gel the combs were inserted and the gel polymerized within 30 minutes

to 1 hour. The percentage of acrylamide was chosen based on the molecular weight range of the expected proteins:

% Gel	M.W. Range
8	50 kDa - 500 kDa
10	20 kDa - 300 kDa
12	10 kDa - 200 kDa
15	3 kDa - 100 kDa

After polymerization the gel casting was stored at 4°C or used immediately. Before usage, the comb was removed and the pockets were washed with SDS-running buffer. The equipment used for electrophoresis was the electrophoresis system Hoefer 600 vertical from Amersham Bioscience.

Samples and marker were loaded and 10-15mA were initially applied to collect the samples until they reached the border of the stacking-separation gel. Then, 20-30mA were used to separate the proteins. The cooling system of the electrophoresis system was used to avoid heating of the gel. A Rainbow marker (Amersham) was also loaded and used to determine the size of proteins and to observe the separation process. Unloaded gel pockets were filled with 1X SDS-loading buffer. For overnight electrophoresis, 40 volts were constitutively applied until the next morning.

Examples of recipes for Polyacrylamide-gels:

<u>SDS-stack</u>		<u>SDS-Separation</u>	<u>12%</u>	<u>15%</u>	<u>1x SDS-</u>
ddH ₂ O	4.1ml	ddH ₂ O	5.7ml	4.6ml	<u>Running buffer</u>
5% Acrylamide	1.0ml	Acrylamide	7.0ml	10ml	25mM Tris
1.0M Tris pH 6,8	0.75m	1.5M Tris pH 8.8	4.45ml	5.ml	Base pH 6.8
10% SDS	60µL	10% SDS	175µl	200µl	192mM Glycin
10% APS	60µl	10% APS	175µl	200µl	3.7mM SDS
TEMED	6µl	TEMED	7µl	8µl	

3.7.4 Protein transfer

Proteins were transferred to nitrocellulose membranes (0.2µm or 0.4µm) from Schleicher & Schuell (Dot Scientific, Inc.) using a protein wet transfer chamber from BIO-RAD (Trans-blot-cell wet transfer apparatus). 3 Liters of 1X transfer buffer were prepared and filter paper (4 sheets for each gel) was cut according to the size of the membrane. The gel was transferred for 1 minute in a plastic container containing 1X transfer buffer. The gel was then placed bubble-free in a sandwich-blotting chamber.

Order:

<u>Cathode</u>
Spanch-pad
2 times 3MM filter paper
polyacrylamid-gel
nitrocellulose-membran
2 times 3MM filter paper
Spanch-pad
<u>Anode</u>

Transfer conditions used: 2 hours 75V and 14V overnight.

After transfer the blotted membrane was stained with Ponceau S solution from Sigma to determine a successful delivery of proteins to the membrane. The staining on the membrane was removed by using TBST-buffer for 10-15 minutes on a shaker.

<u>1X Transfer-buffer</u>	<u>20x TBS</u>	<u>TBST</u>
25mM Tris Base	1M Tris/ HCl pH 7.4	0.02% Tween-20 in
187mM Glycin	3M NaCl	1x TBS
20% (v/v) Methanol		

Proteins from lysates were separated by using 15% SDS-PAGE for 4EBP and Akt immunoblotting, 12% SDS-PAGE for p70S6K, AMPK and S6 immunoblotting, 8% SDS-PAGE for TSC2 and 6% SDS-PAGE for mTOR immunoblotting.

3.7.5 Immunoblotting and Development

The membrane was transferred to a small container containing blocking milk solution and incubated for 1-1.5 hours at room temperature on a shaker to decrease unspecific binding of the primary antibody. Immediately after blocking, the diluted primary antibody-blotting solution was added and incubated in a closed plastic container either at room temperature for 2 hours or at 4°C overnight. The next step included three washing steps in TBST for 15 minutes.

After washing the membrane, the secondary antibody was incubated for 2 hours at 22°C and washed again three times with TBST for 15 minutes.

For developing the membrane the Western-Blot detection kit ECL reagent 1+2 from Amersham was used according to the manual.

<u>Blocking solution</u>

5% dry milk

1% BSA (fraction V, Sigma)

0.2% Tween-20 in 1X TBS

The phosphospecific antibody was always used in the first round of immunoblotting. After stripping the membrane with stripping buffer (62mM Tris HCl (pH 6.8), 100mM beta-mercaptoethanol, 2% SDS) the antibodies that recognized the total amount of the specific protein were used.

The 0 to 45kD size range sections of the membranes were blotted with p-4EBP1 or p-S6 and after stripping with 4EBP1-regular or S6-regular antibodies. The 30-220kD sections of the membranes were blotted with p-Akt, p-p70S6K or p-TSC2 antibodies. After stripping the membrane blots were immunoblotted again with corresponding regular antibodies Akt, p70S6K and TSC2. Immunoblotting with beta-actin served as protein loading control.

3.7.6 Immunoprecipitation

Immunoprecipitation is a technique that permits the purification of specific proteins for which an antibody has been raised. This primary antibody is either already bound to agarose or can be bound to protein A/G agarose beads during the procedure in order to physically separate the antibody-antigen complex from the remaining sample.

Adherent cells were washed twice on the plate with ice-cold PBS and drained off PBS. Lysis-buffer (1-1.5ml) was added to the cells ($1-1.5 \times 10^6$) and the adherent cells were scraped into a 2ml Eppendorf tube and the suspension was incubated on either a rocker or an orbital shaker at 4°C for 15 minutes to lyse the cells. The lysate was centrifuged at 14,000 x g in a pre-cooled centrifuge at 4°C for 15 minutes. Immediately after transfer the supernatant fraction was transferred to a fresh centrifuge tube and the pellet was discarded. To prepare protein A or G agarose/sepharose, the beads were washed twice with PBS and restored to a 50% (v/v) slurry with PBS solution.

The cell lysate was pre-cleared by adding 100 microliters of either protein A or G agarose/sepharose beads slurry (50%) per 1 ml of cell lysate and incubated at 4°C for 10 minutes on a rocker or orbital shaker. Pre-clearing the lysate reduced non-specific binding of proteins to agarose or sepharose when it was used later on in the assay. The protein A or G beads were removed by centrifugation at 14,000xg at 4°C for 10 minutes and the supernatant was transferred to a fresh centrifuge tube.

To determine the protein concentration of the cell lysate a Bradford assay was performed (CHAPTER 3.7.2). The cell lysate was diluted at least 1:10 before determining the protein concentration because of the interference of the detergents in the lysis buffer with the Coomassie-based reagent. The cell lysate was diluted to approximately 1mg/ml total cell protein with PBS to reduce the concentration of the detergents in the buffer.

The recommended volume of the immunoprecipitating antibody was added to 1ml of cell lysate. The optimal amount of antibody that quantitatively immunoprecipitated the protein of interest was empirically determined for each cell model. The cell lysate/antibody mixture was incubated overnight at 4°C using

an orbital shaker. Capturing the immunocomplex was performed by adding 100 microliters protein A or G agarose/sepharose bead slurry (50 microliters packed beads) and gently rocking on an orbital shaker for 2 hours. The agarose/sepharose beads were collected by pulse centrifugation (5 seconds in the microcentrifuge at 14,000 rpm) and the supernatant fraction was discarded. Beads were washed 3 times with 500µl ice-cold washing buffer. Agarose beads were resuspended in 2x Laemmli sample buffer and boiled for 5 minutes to dissociate the immunocomplexes from the beads.

The beads were then collected by centrifugation and an SDS-PAGE was performed with the supernatant fraction. Alternatively, the supernatant fraction was transferred to a fresh microcentrifuge tube and stored frozen at -20°C for later use. Frozen supernatant fractions were reboiled for 5 minutes directly prior to loading on a gel.

<u>Lysis buffer:</u>	<u>Wash-buffer:</u>
20mM Tris	20mM HEPES
150mM NaCl	150mM NaCl
1mM MgCl ₂	50mM NaF
1mM DTT	1mM EDTA
50mM beta-glycerolphosphate	1% NP 40
50mM NaF	1mM DTT
1mM PMSF	50mM beta-
1% NP40	glycerolphosphate
10% Glycerol	Protease inhibitor cocktail
Protease inhibitor cocktail	

Immunoprecipitation and Immunoblotting of MEFs:

1.5x10⁶ primary DKO (Akt1^{-/-}Akt2^{-/-}) and WT (Akt1^{+/+}Akt2^{+/+}) MEFs (passage 3) were plated in 15-cm-plates in DMEM 10% FBS and deprived of serum for 24h. The cells were lysed after treatment for 30 min or 60 min with DMEM containing 20% FBS. Cell lysates were prepared in 1000µl lysis buffer. Lysates were incubated with the precipitating antibody TSC2/tuberin (1:200) overnight, followed by 2h incubation with 30µl of protein A/G plus agarose affinity gel slurry

from Santa Cruz Biotechnology (Santa Cruz, CA). The immune complex was then washed 5 times with wash buffer and boiled in 2x Laemmli sample buffer. The whole sample volume was used to separate the proteins by a 6% SDS-PAGE. Proteins were then transferred to nitrocellulose membranes (0.2 μ m), the 66-220kD sections of the membranes were blotted with Phospho-Akt-S/T-substrate antibody and after stripping membranes were probed with TSC2-regular.

3.8 Adenine nucleotide analysis

Adenine nucleotide measurements and statistical analysis:

1-2x10⁶ cells were quickly harvested into PBS buffer (100 mM Tris-HCl (pH 7.75), 4mM EDTA) and immediately centrifuged for 2 minutes at 1,000g (4°C). Pellets were resuspended in 150 μ l PCA (Perchloracetic acid, 4% (v/v) and incubated on ice for 30 minutes. Within 1h the pH of the lysates was adjusted between 6 and 8 using a solution made of 2M KOH/ 0.3M MOPS and incubated for 30 minutes on ice. Precipitated salt was separated from the liquid phase by centrifugation at 13,000g for 10 minutes. Aliquoted samples were stored at -80°C.

Adenine nucleotide measurements were conducted using an HPLC (high pressure liquid chromatography, HPLC-Pro Star from Varian, Walnut Creek, CA). Samples were eluted after 17 min with a flow rate of 1.0mL/ min (isocratic elution) and nucleotides were detected spectrophotometrically at λ =254 nm (separation column: Spherisorb, ODS II, 5 mm, 0.46 x 25 cm, Z22.697-1, Sigma). The order of eluted nucleotides was ATP, ADP and AMP. Internal standards with known nucleotide concentrations (7.5 μ M ATP, ADP and AMP in ddH₂O) were used to quantify the samples. HPLC running buffer (mobile phase) contained 25mM Na₄P₂O₇, 10 H₂O, 25mM H₄P₂O₇, the pH was adjusted to 5.75 with a saturated solution of Na₄P₂O₇.

4. Results

4.1 Cellular atrophy of skeletal muscle and impaired mTOR activity in Akt1/Akt2 DKO cells

4.1.1 Cellular atrophy of skeletal muscle in Akt1/Akt2 DKO cells

Embryos were dissected from anesthetized females. Embryos and newborn were perfused and embedded in paraffin. Sections of 5-7 μm were stained with hematoxylin and eosin. The muscle fiber cross-sectional area and fiber diameter were measured from presternum, intercostal muscle and diaphragm. Digitized muscle images were taken, and size (diameter) of individual cells were determined by the number of pixel within manually outlined fiber boundaries (Figure 6B, (Peng et al. 2003)).

The histopathological analysis revealed that skeletal muscle tissues in DKO E18.5 embryos and newborn are significantly thinner than those of WT and DHet (double heterozygote) littermates (Figure 6A, (Peng et al. 2003)). This is mostly caused by cellular atrophy. Interestingly, there is not a significant decrease in the number of muscle fiber, at least in the respiratory muscle, whereas the size of the individual muscle is markedly decreased. Notable, the diaphragm of the DKO mice is extremely thin. Calculation of the relative cross-section area (described above) of individual muscle cells in the diaphragm and presternum as well the diameter of the intercostal muscle showed that DKO muscle are ~50% smaller than WT cells and DHet cells are of intermediate size.

These results established genetic evidence that Akt is required for determining cell growth or cell mass in mammalian cells (Peng et al. 2003).

4.1.2 Status of mTOR-activity in AKT1/AKT2 DKO cells

The results of the skeletal muscle DKO cells showed severe muscle atrophy. The mTOR pathway has been shown to determine that cell mass in particularly skeletal muscle (Bodine et al. 2001; Rommel et al. 2001; Fingar et al. 2002; Pallafacchina et al. 2002).

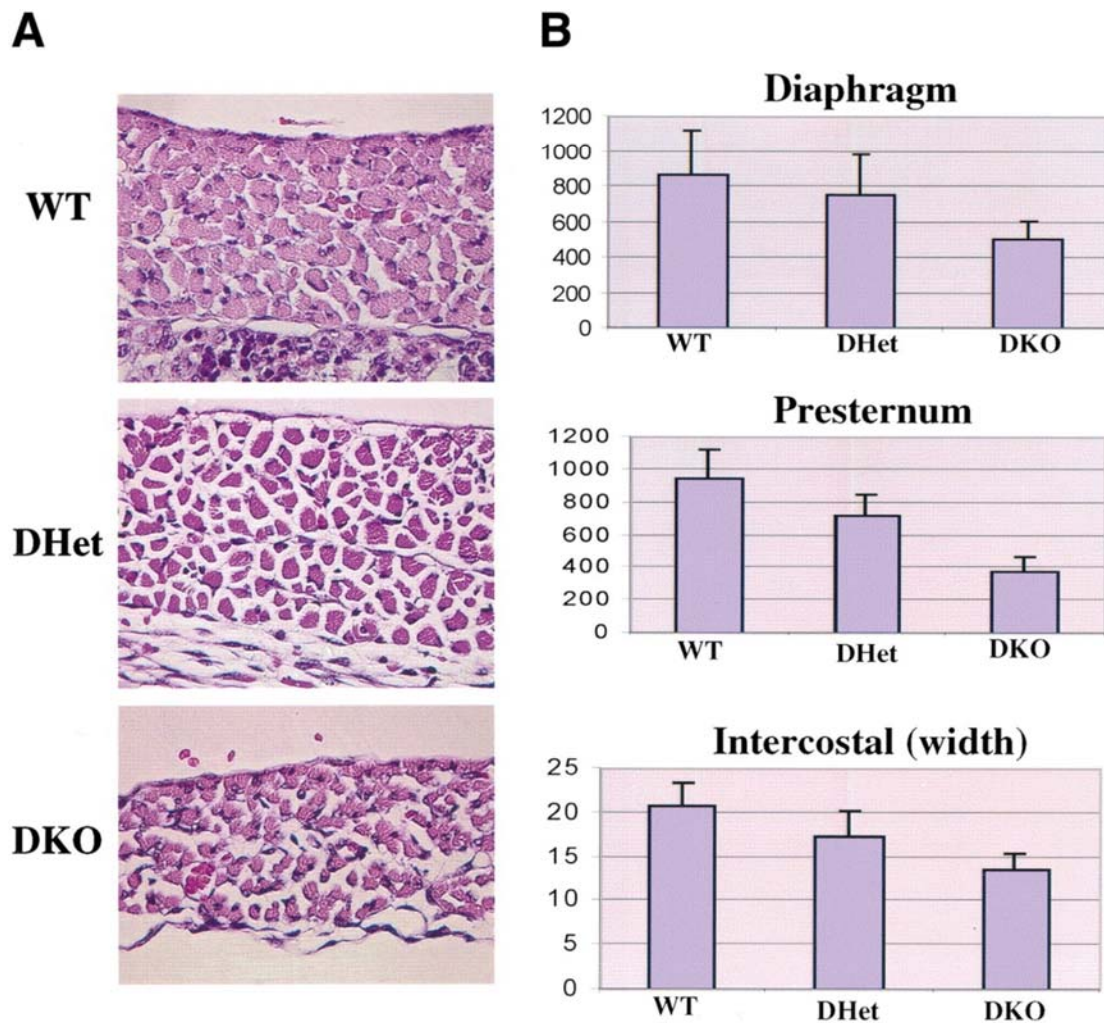


Figure 6: Skeletal muscle atrophy in Akt1/Akt2 DKO mice.

(A) Image of standard H&E-staining diaphragms from WT, DHet and DKO E18.5 littermate embryos (630x magnification). (B) Histograms show the size and diameter of muscle cells. Digitized images of skeletal muscle were analyzed as described in chapter 4.1.1. Results are mean \pm S.E.M., expressed as the number of pixels in cross-sectional areas of diaphragm and presternum muscle cells or within the width of intercostals muscle. Twenty cells in three random fields were analyzed for each. (The figure is part of Dr. Xiao-ding Peng's results, (Peng et al. 2003)).

Gingras et al. have shown that Akt is upstream of mTOR (Gingras et al. 1998) and mTOR's ability to determine the cell size is dependent on its downstream effectors, 4EBP1 and S6K1, that regulate protein synthesis (Dufner and Thomas 1999). Those facts are critical findings that led to the investigation of mTOR activity in Akt1/Akt2 KO cells compared to WT cells. The neonatal lethality

of Akt1/Akt2 DKO mice precludes the analysis of the Akt-mTOR pathway in skeletal muscles of DKO mice.

Mouse embryo fibroblasts were isolated using the protocol described in Material and Methods (CHAPTER 3.4). Isolated MEFs (mouse embryo fibroblasts) from WT and Akt1/Akt DKO cells were plated and expanded for 3-5 days before the mTOR activity experiment was conducted. For serum stimulation of WT and Akt1/Akt DKO cells, 1.5×10^6 primary MEFs (passage 4) were plated in 15-cm-plates in DMEM with 10% FBS and deprived of serum for 24h. Cells were then stimulated with 20% FBS for 30 and 60 min. Cell lysates were subjected to immunoblot analysis (CHAPTER 3.8).

Total Akt expression, measured by anti-Akt antibody that recognize all three isoforms of Akt, in WT compared to Akt1/Akt2 DKO MEFs reflects the status of knockout in MEFs on the protein level. The remaining Akt3 isoform is expressed at a much lower level than Akt1 or Akt2 isoforms (Figure 7, compare lane1 with lane 2, and lanes 3-5 with lanes 6-8. Akt activity, measured by anti-phospho Akt Serine 473 in Akt1/Akt2 DKO MEFs, is almost diminished in proliferating cells (Figure 7, compare lane 1 with lane 2) compared to the WT, but after 30 minutes serum induction with DMEM/20% FBS, there was Akt activity (phosphorylation) due to the remaining Akt3 isoform in Akt1/Akt2 DKO cells (Figure 7, lane 7). After 60 minutes this phosphorylation of Akt in Akt1/Akt2 DKO cells was completely abolished (Figure 7, lane 8).

Using antibodies against phospho-Ser65 of 4EBP1 and phospho-Thr389 of S6K, the steady-state levels of phosphorylation 4EBP1 and S6K in proliferating WT and Akt1/Akt2 DKO MEFs were examined. There is a marked reduction of mTOR activity measured by phosphorylation status of 4EBP1 and S6K in Akt1/Akt2 DKO cells (Figure 7, lanes 1 and 2).

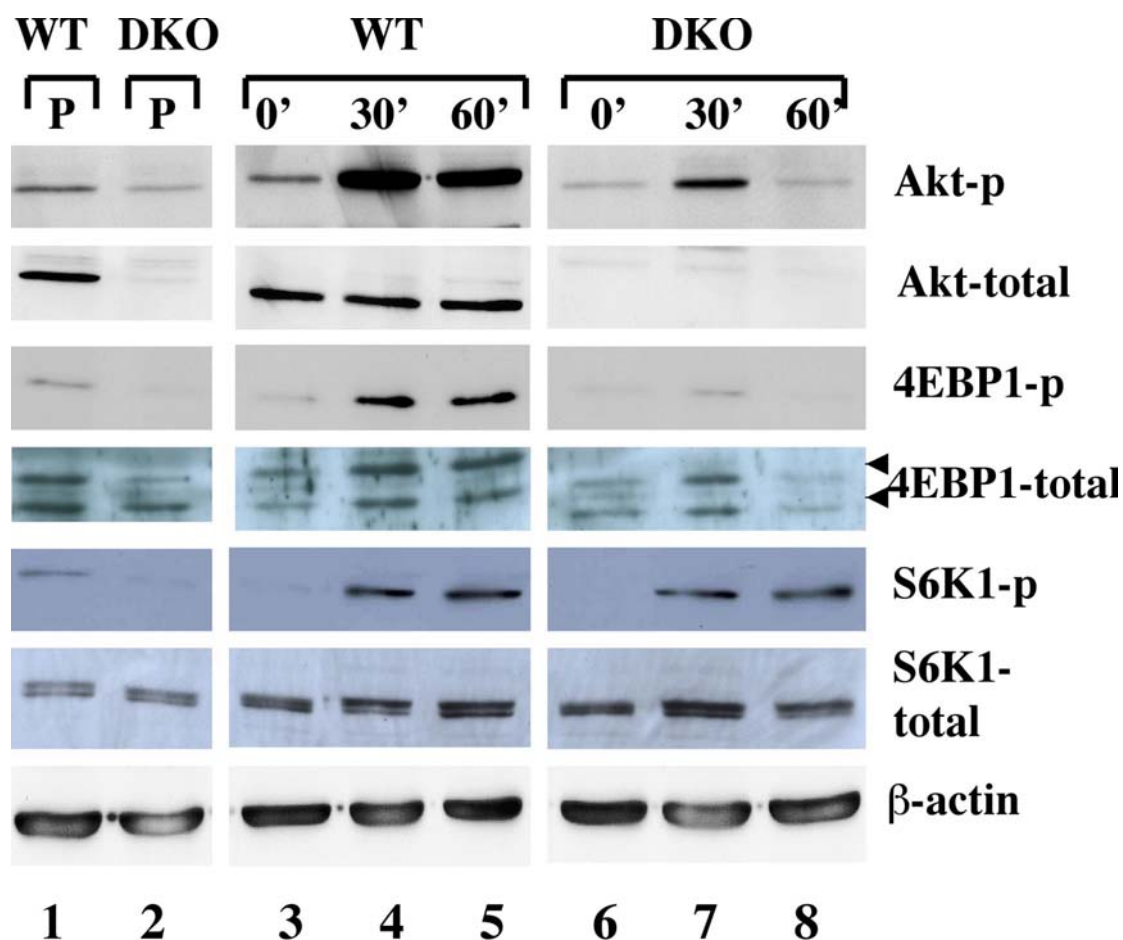


Figure 7: mTOR activity in WT and Akt1/Akt2 DKO MEFs.

Phosphorylation and protein levels were determined by immunoblotting. (Lanes 1/2) Proliferating (P) cells (passage 4) were plated in DMEM/10% FBS and analyzed 24h after plating. (Lanes 3,6) Primary wild type (WT) and Akt1/Akt2 DKO MEFs were plated in DMEM/10% FBS for 24 h, then deprived of serum for 24 h. (Lanes 4,5,7,8) after serum deprivation, cells were stimulated with DMEM/20% FBS for 30 or 60 min, respectively. Cell lysates isolated prior (0') and 30' and 60' following serum stimulation were subjected to immunoblotting using anti-p-Akt-S473, anti-p4E-BP1-S65, anti-p-S6K-Th389, anti-pan-Akt, anti-pan-S6K, anti-pan-4EBP1 and anti-β-actin (loading control) antibodies.

The reduction in 4EBP1 phosphorylation was also visible by different migrating forms of 4EBP1 or mobility shift detected by anti-4EBP1 antibodies. Hyperphosphorylated 4EBP1 migrates slower on a SDS-Page than hypophosphorylated 4EBP1. In proliferating Akt1/Akt2 DKO cells the faster migrating, hypophosphorylated form of 4EBP1 was predominant, whereas in

proliferating WT cells the slower migrating form was more dominant (Figure 7, lanes 1 and 2).

Stimulation of serum deprived WT and Akt1/Akt2 DKO cells with DMEM containing 20% FCS for 30 and 60 min showed a severely impaired mTOR activity in DKO cells, measured by 4EBP1 phosphorylation (Figure 7, lanes 6-8). Under this condition the S6K1 phosphorylation was not impaired, suggesting there may have been another kinase phosphorylating this kinase, or the threshold of Akt activity for S6K1 phosphorylation was relatively low (Figure 7, lane 6-8). It was recently shown that PDK1 and PKC ζ are able to mediate Thr 389 phosphorylation in an mTOR dependent manner (Romanelli et al. 2002).

The total protein level was determined using method in chapter 3.8. by anti- β -actin antibody to confirm equal protein levels in each sample (Figure 7, lanes 1-2).

This result established the first genetic evidence that Akt is required for mTOR-mediated phosphorylation.

4.1.3 Status of TSC2 phosphorylation by Akt in Akt1/Akt2 DKO MEFs

Akt was shown to phosphorylate and inactivate TSC2 (Inoki et al. 2002; Manning et al. 2002; Potter et al. 2002) and thereby activating mTOR. In Chapter 4.1.2. it was shown that in mouse embryo fibroblasts (MEF), deficient for Akt1 and Akt2, mTOR activity is impaired, as measured by 4E-BP1 phosphorylation following serum stimulation (Figure 7). The same experimental set up as described in chapter 4.1.2 was used to investigate TSC2 phosphorylation on Threonine 1462, which is directly phosphorylated by Akt (Inoki et al. 2002) in Akt1/Akt2 DKO MEFs compared to WT cells using immunoblotting analysis.

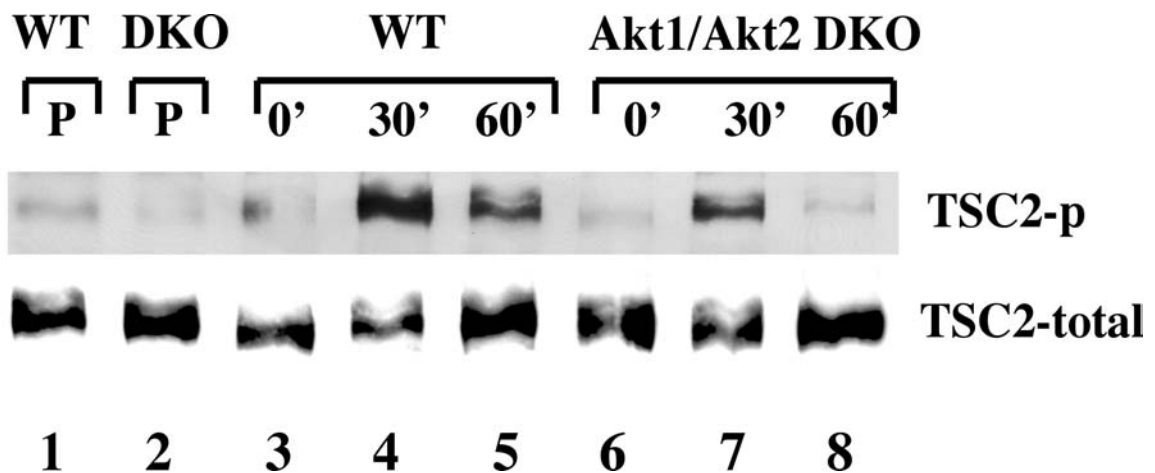


Figure 8: TSC2 phosphorylation in WT and Akt1/Akt2 DKO cells, immunoblotting. Phosphorylation and protein levels were determined by immunoblotting. (Lanes 1,2) Proliferating (P) cells (passage 4) were plated in DMEM/10% FBS and analyzed 24h after plating. (Lanes 3,6) Primary wild type (WT) and Akt1/Akt2 DKO MEFs were plated in DMEM/10% FBS for 24 h, then deprived of serum for 24 h. (Lanes 4,5,7,8) after serum deprivation, cells were stimulated with DMEM/20% FBS for 30 or 60 min, respectively. Cells lysates isolated prior (0') and 30' and 60' following serum stimulation were first subjected to immunoprecipitation with anti-phospho-TSC2-Thr 1452 and anti-TSC2-antibodies.

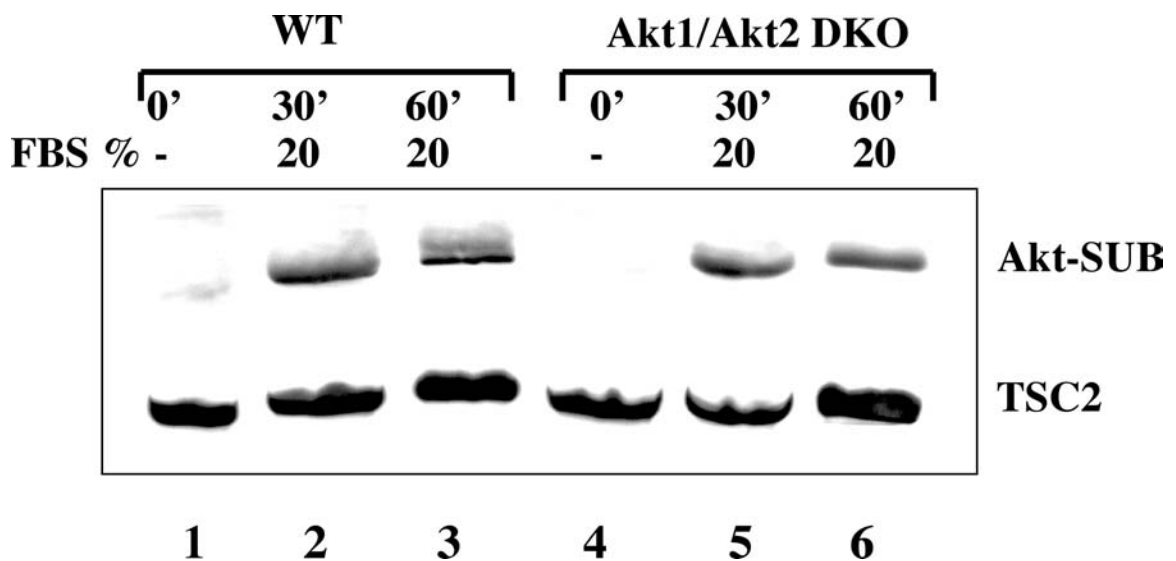


Figure 9: TSC2 phosphorylation in WT and Akt1/Akt2 DKO cells, immunoprecipitation.

Primary WT and Akt1/Akt2 DKO MEFs were deprived of serum for 24 h and then stimulated by addition of 20% FBS. Cells lysates isolated prior (0') and 30' and 60' following serum stimulation were first subjected to immunoprecipitation with anti-TSC2 antibodies. Immunoprecipitates were then subjected to immunoblotting using anti-Akt-p-S/T substrate and anti-TSC2 anti-bodies.

Proliferating Akt1/Akt2 DKO cells have a decreased phosphorylation on this site, measured by anti-phospho-TSC2-Thr1462 antibody (Figure 8, lanes 1 and 2), correlating with the Akt activity shown in Figure 7, lanes 1 and 2. Induction of the Akt-mTOR pathway after growth factor starvation with 20 % serum also showed a correlating result of phosphorylation on TSC2 Threonine 1462 (Figure 8, lanes 3-8).

Because TSC2 displays four important phosphorylation sites for Akt (Threonine 1462, Serine 939, Serine 1086 and Serine 1088, (Inoki et al. 2002)), the measurement of only one site wouldn't show the status of TSC2 phosphorylation by Akt. Therefore, TSC2 was immunoprecipitated by anti-TSC2 antibody in WT and Akt1/Akt2 DKO MEFs after 24 hours growth factor starvation and induction with DMEM containing 20% serum for 30 and 60 minutes.

Equal amounts of protein were subjected to an SDS-Page and immunoblotted with anti-phospho-Serine/Threonine Akt substrate antibody. Figure 9 shows the results by measuring all Akt-phosphorylation sites on TSC2. There was almost no reduction of phosphorylation of the Akt-sites on TSC2 in Akt1/Akt2 DKO MEFs compared to the WT. The functions of those sites are not clear yet (Hay and Sonenberg 2004), it was shown that the phosphorylation by Akt disrupts the association of TSC2 with TSC1 and causes increased mTOR activity (Dan et al. 2002; Inoki et al. 2002; Potter et al. 2002,; Tee et al. 2002). It raises the question, of the importance of this step for the actual mTOR activity and if there is another mechanism by which Akt affects mTOR activity. 4EBP1 phosphorylation was dramatically reduced in Akt1/Akt2 DKO cells (Figure 7), but phosphorylation of all Akt-sites on TSC2 was not impaired (compare Figure 7 and Figure 9).

These results suggest; first, that the remaining Akt activity in Akt1/Akt2 DKO cells (Figure 7) is sufficient to elicit significant TSC2 phosphorylation and second, that TSC2 phosphorylation may not be sufficient for Akt to fully activate mTOR. Thus, these results led to the hypothesis that an additional function of Akt, which was required to fully activate mTOR, and was impaired in Akt1/Akt2 DKO cells.

4.2 Akt maintains the intracellular level of ATP and regulates AMPK activity

4.2.1 Akt deficiency significantly reduce intracellular ATP level and increases AMP/ATP ratio

It was shown that mTOR activity is dependent on the intracellular ATP level (Dennis et al. 2001), and it was suggested that this is due to the low K_M of mTOR-kinase-activity for its substrate ATP for. However, another recent publication linked AMPK to TSC2, showing that TSC2 is phosphorylated by activated AMPK, which in turn leads to inhibition of mTOR-activity (Inoki et al. 2002).

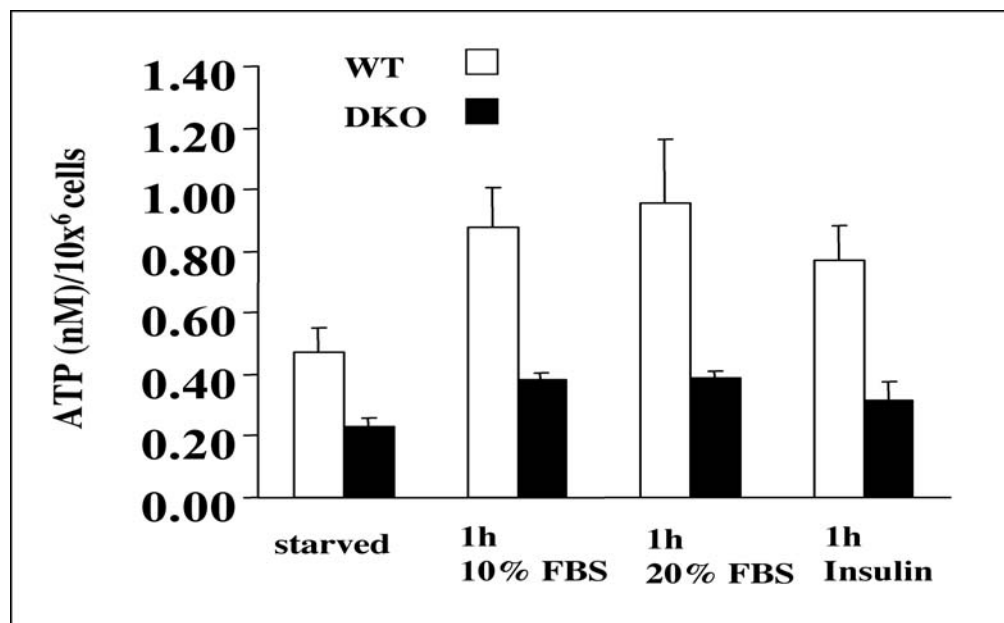


Figure 10: ATP level is reduced in Akt1/Akt2 DKO cells vs. WT.

Primary WT and Akt1/Akt2 DKO MEFs were plated in 10% FBS and deprived of serum for 24h. Cells were stimulated with 10% FBS, 20% FBS for 60 min or insulin 1 μ g/ml, and intracellular ATP concentrations were analyzed by HPLC as described in Methods. Results represent the average of three independent experiments (Error bars indicate SD).

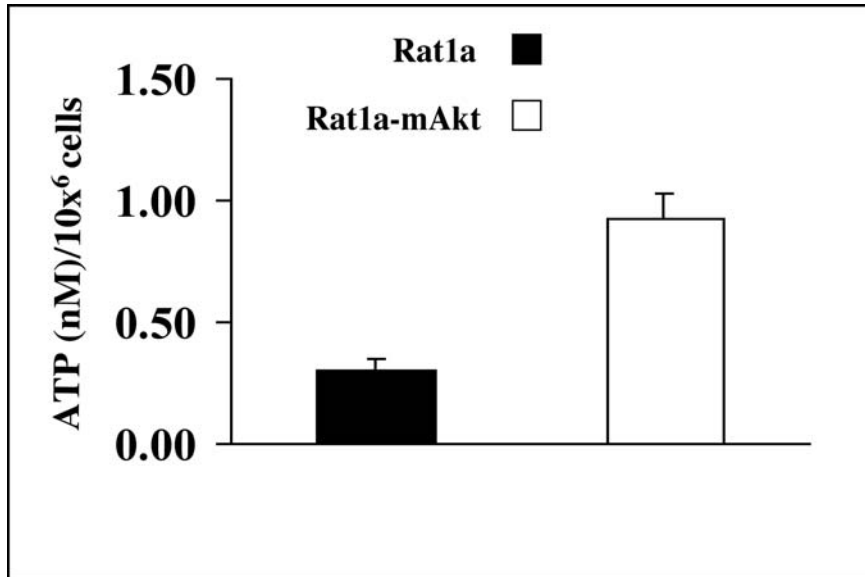


Figure 11: ATP level in cells expressing activated Akt vs. control cells.

To eliminate the rate-limiting step in the activation of Akt, a myristoylation signal was linked in frame to the amino-terminus of Akt. This constitutively activated form of Akt, termed mAkt, still requires the phosphorylation of the serine and threonine residues for full activation. Proliferating Rat1a and Rat1a-mAkt cells were analyzed for intracellular ATP concentrations analyzed by HPLC as described in Methods. Results represent the average of three independent experiments (Error bars indicate SD).

It was also shown before, that cells expressing activated Akt have significantly higher levels of ATP compared to control cells (Figure 11, (Gottlob et al. 2001)). To underlie this observation the experiments were setup to determine whether cells deficient for Akt have a reduced level of the intracellular ATP.

For serum or insulin stimulation of WT and Akt1/Akt2 DKO cells, 1.5×10^6 primary MEFs (passage 4) were plated in 15-cm-plates in DMEM with 10% FBS and deprived of serum for 24h. Cells were stimulated with insulin ($1 \mu\text{g/ml}$), 10% FBS and 20% FBS for 60 min and intracellular ATP, ADP and AMP concentrations were analyzed by HPLC (described in CHAPTER 3.9).

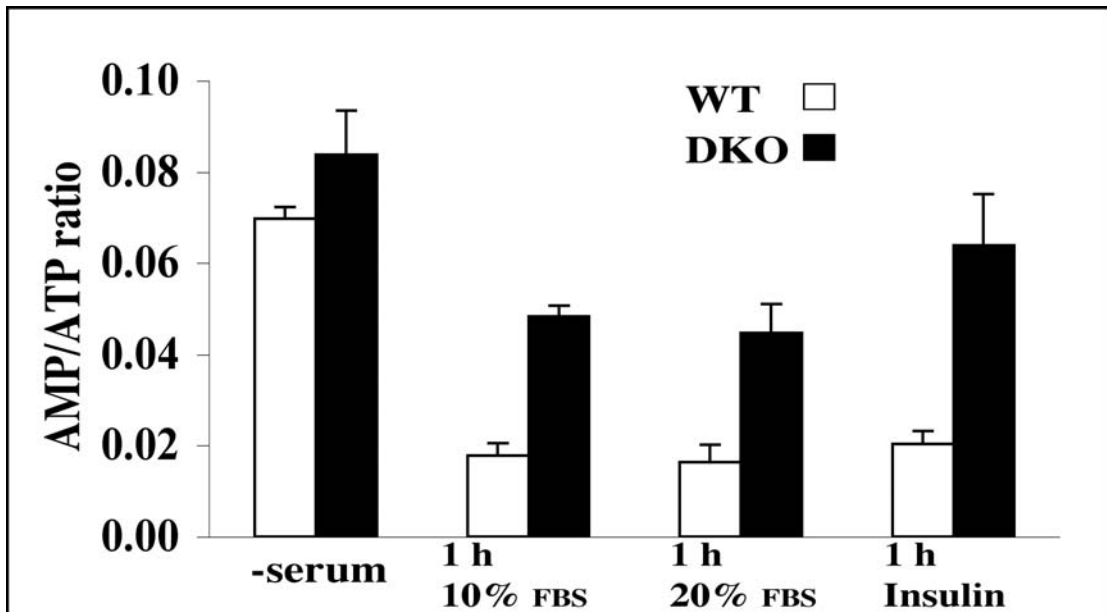


Figure 12: AMP/ATP ratio in Akt1/Akt2 DKO cells vs. WT.

Primary WT and Akt1/Akt2 DKO MEFs were subjected to analysis as described in and AMP/ATP ratio was calculated using intracellular ATP and AMP concentration.

As shown in Figure 10, the ATP level is lower in serum deprived Akt1/Akt2 DKO cells when compared to WT cells. Following insulin or serum stimulation the ATP level was increased in WT cells, whereas in Akt1/Akt2 DKO cells, it was retained at a markedly reduced level, 2-3 fold lower than in WT cells.

The activity of AMPK is dependent on the AMP/ATP ratio (Hardie et al. 1998; Kemp et al. 1999). To determine a potential link for the regulation of AMPK by Akt activity, the AMP/ATP ratio was more suitable than only the ATP concentration. Figure 12 shows the ratio of AMP/ATP (under the same condition as described above). Akt1/Akt2 DKO cells exhibited a higher AMP/ATP ratio compared with WT under starvation condition and under serum/insulin stimulation. The AMP/ATP ratio was consistent with the lower ATP level in Akt1/Akt2 DKO cells (Figure 10), except under starvation conditions. The AMP/ATP ratio in WT cells was also elevated. Under growth factor starvation Akt was not active. These results demonstrate, that Akt is required to maintain the intracellular level of ATP and thereby to decrease the AMP/ATP ratio.

4.2.2 Akt deficiency markedly increases AMPK activity

The ratio of AMP/ATP was markedly higher in Akt1/Akt2 DKO cells in the presence of growth factors when compared with WT cells (Figure 12). Investigation of AMPK activity in Akt deficient cells in the presence of growth factor and under growth factor withdrawal was the next step to establish a functional link between Akt and AMPK.

1.5×10^6 primary Akt1/Akt2 DKO and WT MEFs (passage 4) were plated in 15-cm-plates in DMEM with 10% FBS and deprived of serum for 24h. For Western analysis Akt1/Akt2 DKO and WT MEFs were harvested under proliferating conditions in the presence of growth factor and after growth factor starvation. After quantification of the protein content, equal amounts of lysate were subjected to a SDS-page and immunoblotted (CHAPTER 3.8) with different antibodies (Figure 13).

Total Akt expression, measured with anti-Akt antibody that recognized all three isoforms of Akt, reflects the knockout status in Akt1/Akt2 DKO and WT MEFs on the protein level (Figure 13 compare lanes 1-3 with lanes 2-4). The remaining Akt expression in Akt1/Akt2 DKO MEFs was due to the Akt3 isoform. In the presence of growth factor and using anti-phospho Akt Ser473 antibody, Akt activity was retained in WT cells (Figure 13, lane1), whereby in Akt1/Akt2 DKO MEFs the phosphorylation on this site was abolished (Figure 13, lane2). After growth factor starvation Akt-activity measured with anti-phospho Akt for Serine 473 was abolished in both Akt1/Akt2 DKO and WT MEFs (Figure 13, lane 3-4).

The question was, if growth factor/serum withdrawal and decreased Akt-activity had an impact on AMPK activity? Indeed, the AMPK activity, as measured by its phosphorylation on Thr172 (Hawley et al. 1995) and by the phosphorylation of the AMPK target Acetyl-CoA carboxylase (ACC) on Ser79 (Ha et al. 1994), was markedly increased in Akt1/Akt2 DKO cells when compared with WT cells in the presence of serum (Figure 13, lanes 1-2). Serum withdrawal also increase of AMPK activity in WT MEFs, which established that this effect was growth factor dependent, measured by the phosphorylation of the AMPK target Acetyl-CoA carboxylase (ACC) on Ser79 (Ha et al. 1994). Results show that Akt is required to maintain low AMPK activity.

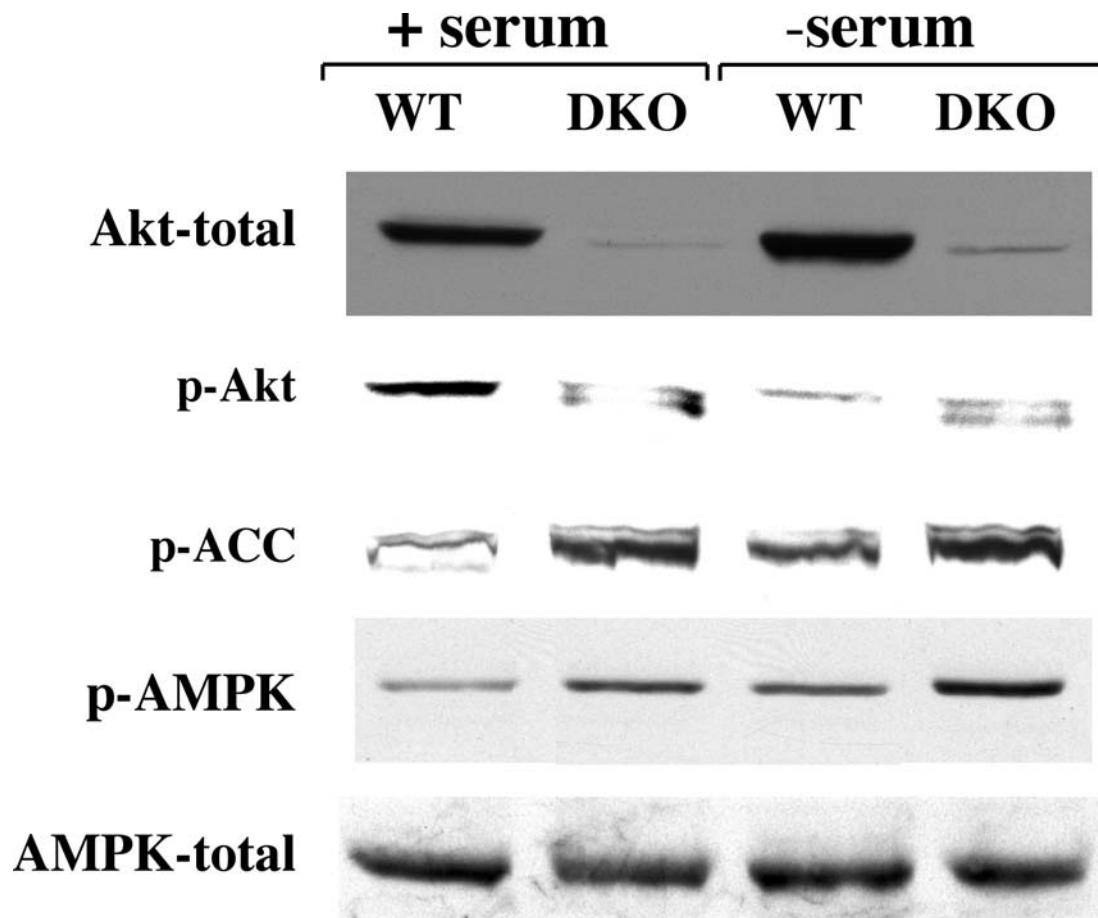


Figure 13: AMPK activity in Akt1/Akt2 DKO cells vs. WT.

Cell lysates from primary WT and Akt1/Akt2 DKO MEFs grown in 10% FBS or in 0.1% FBS (serum deprived) for 24h were subjected to immunoblotting using anti-pan Akt, anti-p-Akt-S473, anti-p-ACC-S79, anti-p-AMPK-T172, and anti-AMPK antibodies.

4.2.3 Expression of activated Akt increases intracellular ATP level, reduces AMP/ATP ratio and affects AMPK activity

To eliminate the rate-limiting step in the activation of Akt, a myristoylation signal was linked in frame to the amino-terminus of Akt. This constitutively activated form of Akt, termed mAkt, still requires the phosphorylation of the serine and threonine residues for full activation (Kandel and Hay 1999).

Cells that express activated myristoylated Akt have a significantly higher level of ATP (Gottlob et al. 2001, Figure 11). To confirm this result, the intracellular level of ATP in proliferating Rat1a cells was compared to Rat1a cells expressing the myristoylated, activated form of Akt was measured by using HPLC (see

CHAPTER 3.9). Figure 11 shows an approximately 2-fold higher intracellular level of ATP in Rat1a cells expressing activated Akt when compared to control cells.

1.5×10^6 Rat1a and Rat1mAkt were plated in 10-cm-plates in DMEM with 10% FBS. For western analysis and adenine nucleotide analysis, Rat1a and Rat1mAkt cells were harvested under proliferating conditions in the presence of growth factor and after growth factor starvation. After quantification of the protein content, equal amounts of lysate were subjected to a SDS-page and immunoblotted (CHAPTER 3.8) with several antibodies (Figure 15).

Adenine nucleotide analysis using HPLC showed that the AMP/ATP ratio in Rat1a cells expressing activated Akt (Rat1a-mAkt) was about 3-fold lower than in control cells (Figure 14) in the presence or in the absence of serum.

Comparison of Western analysis and adenine nucleotide analysis shows that when control Rat1a cells were deprived of serum, the AMP/ATP ratio was markedly increased with a concomitant increase in AMPK activity as measured by phosphorylation of AMPK on Thr172 (Hawley et al. 1995) (Figure 14 and Figure 15, lane 3).

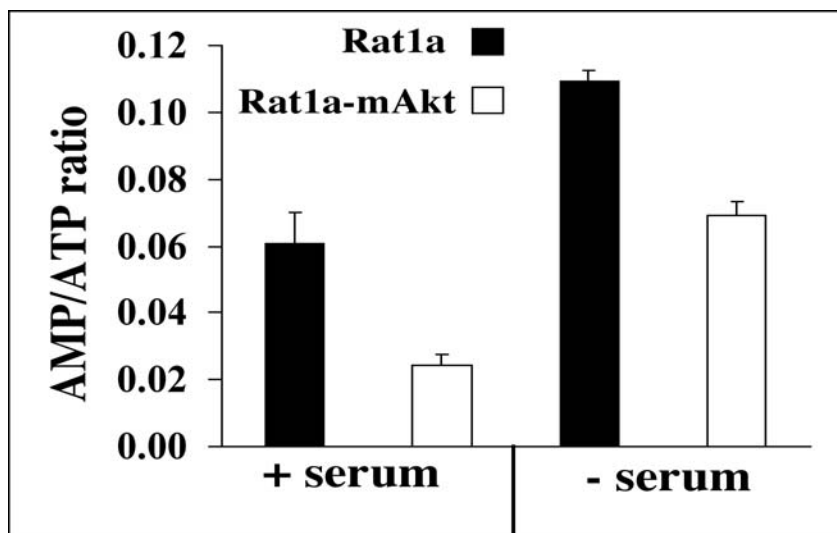


Figure 14: AMP/ATP ratio in cells expressing activated Akt vs. control cells.

Rat1a and Rat1a-mAkt cells grown in DMEM/10 % FBS or in DMEM/0.1% FBS (serum deprived) for 48 h were subjected to ATP and AMP analysis and AMP/ATP ratios were determined.

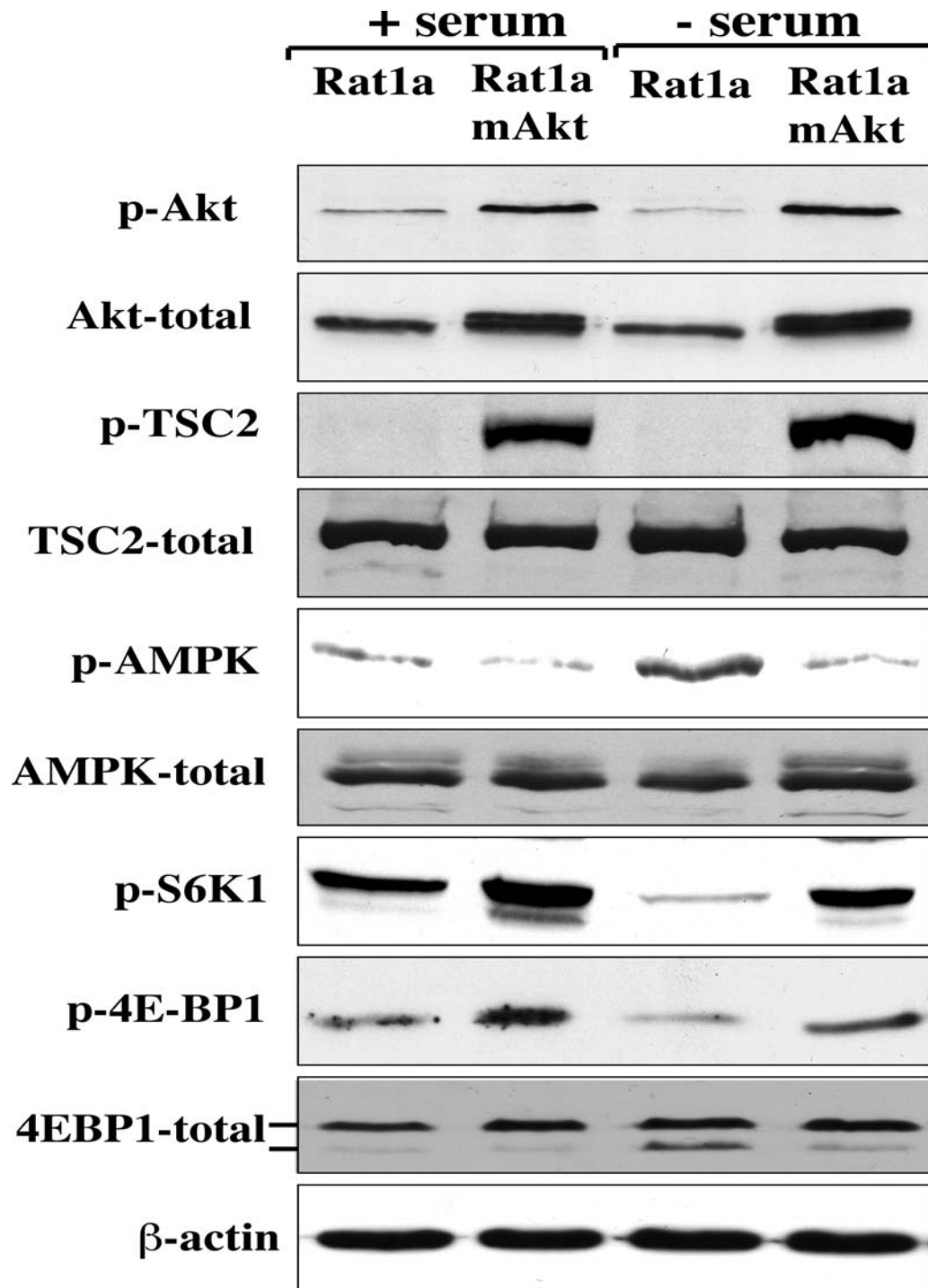


Figure 15: AMPK activity in cells expressing activated Akt vs. control cells and correlation with mTOR activity.

Cell lysates from proliferating and serum deprived Rat1a and Rat1a-mAkt cells were subjected to immunoblotting using anti-p-Akt-S473, anti-p-TSC2-T1462, anti-pAMPK-T172, anti-AMPK, anti-p-S6K1-T389, anti-p-4EBP1-S65, anti-4EBP1 and anti-β-actin antibodies.

However, although the AMP/ATP ratio was also increased in Rat1a-mAkt cells, this increase did not significantly exceed the AMP/ATP ratio of the control cells in the presence of serum. Thus, AMPK activity was not significantly increased (Figures 14 and 15 lane 4), because cells that maintain an AMP/ATP ratio below a certain threshold level also displayed high mTOR activity (Fig. 14 and 15 lanes 1, 2, 4). The increase in AMP/ATP ratio and AMPK activity correlated with a decrease in mTOR activity, as determined by S6K1 and 4EBP1 phosphorylation and by 4EBP1 mobility shift (Figure 15, lane 3).

This result further established the role of Akt as a regulator of cellular ATP and AMPK activity. Interestingly, TSC2 phosphorylation by Akt was not impaired in Rat1-mAkt cells following serum deprivation, while S6K1 and 4EBP1 phosphorylation, although maintained at higher level, was only modestly impaired (Figure 15 lanes 1 and 3).

4.3 ATP depletion and activation of AMPK attenuates Akts ability to activate mTOR

4.3.1 ATP depletion in Rat1a cells expressing activated Akt

To find out whether the increase of the intracellular ATP level and the decrease of the AMP/ATP ratio mediated by Akt is required for Akt to activate mTOR, activated Akt expressing cells were subjected to ATP depletion using inhibitors of glycolysis and oxidative phosphorylation.

1.0×10^6 Rat1aMyAkt cells were plated in 10 cm plates in DMEM (5.5mM Glucose) with 10% FBS. Before treatment with inhibitors to deplete ATP, cells were starved for 24h with DMEM (5.5mM glucose) without serum (Figure 16, lanes 1 and 6). Growth factor withdrawal did not decrease mTOR activity, measured with anti-phospho-4EBP1 antibody (Figure 16, lanes 1 and 6). In cells expressing activated myristoylated Akt, mTOR was constitutively active even in the absence of growth factors as determined by 4E-BP1 phosphorylation and mobility shift ((Gingras et al. 1998) and Fig. 15, 16, 18 and 19).

Akt was constitutively active even in the presence of inhibitors of glycolysis and oxidative phosphorylation (Figure 16, lanes 1-10). The Akt-

mediated 4E-BP1 phosphorylation was inhibited when ATP was depleted following addition of the glucose analogue 5-thiogluco (5,10, 20, 40mM 5-TG) (Figure 16 lanes 2-5) or the oxidative phosphorylation inhibitor, rotenone (1, 5, 10, 20 μ M rot), (Figure 16, lanes 7-10). Interestingly, TSC2 phosphorylation by Akt was not changed under this condition (Figure 16).

These results suggest that Akt's ability to mediate mTOR activity was dependent on its function to increase the intracellular ATP level, which subsequently down regulated AMPK.

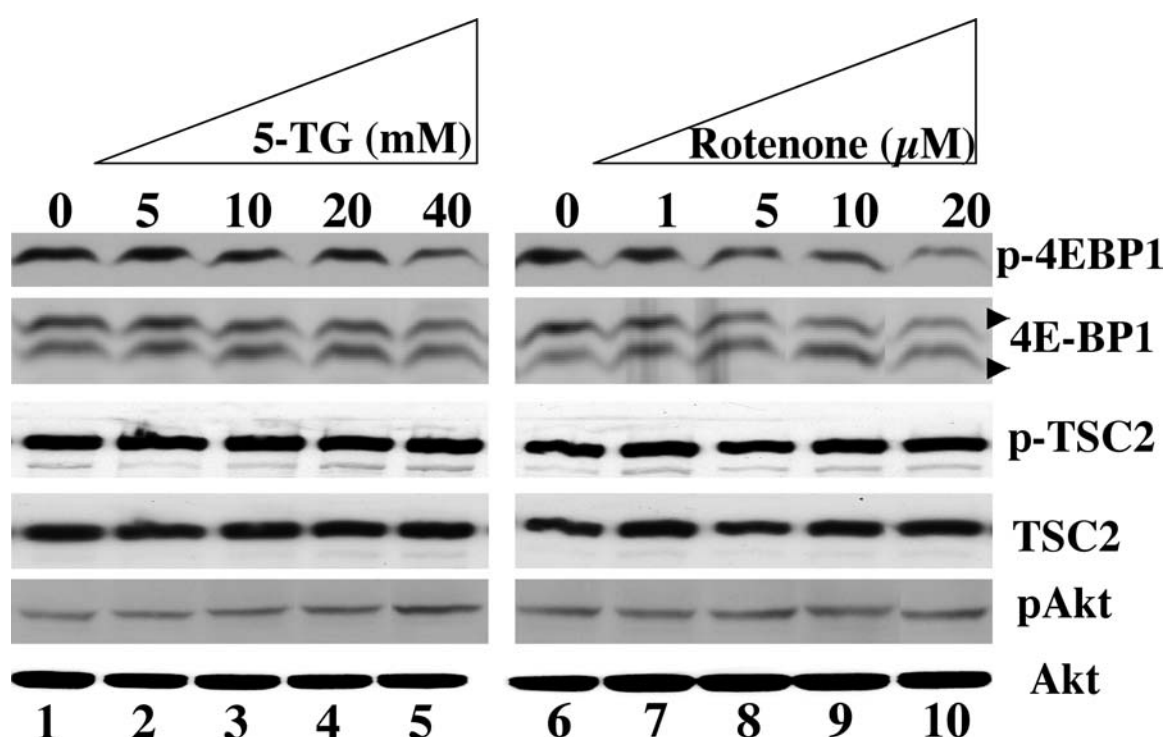


Figure 16: ATP depletion attenuates the ability of activated Akt to activate mTOR. Rat1a-mAkt cells were plated in DMEM (5.5 mM glucose) with 10% FBS (dialyzed), deprived of serum for 24h, and treated with different concentrations of 5-thiogluco (5-TG) (lanes 1-5) and rotenone (lanes 6-10) for 30min. Cell lysates were prepared from serum starved or treated Rat1a-mAkt cells and subjected to immunoblotting using anti-p-4E-BP1-S65, anti-4E-BP1, anti-pTSC2-T1462, anti-TSC2, anti-p-Akt-S473, and anti-Akt antibodies.

4.3.2 ATP depletion of insulin-stimulated Rat1a cells

Proliferating Rat1a cells had a lower intracellular ATP level compared to Rat1 cell expressing activated Akt (Figure 11). We expected that depletion of ATP in Rat1a cells after insulin-stimulation would decrease mTOR activity to a higher extent than in Rat-mAkt cells using the same concentration of inhibitor.

1.0×10^6 Rat1a cells were plated in 10 cm plates in DMEM (5.5mM Glucose) with 10% FBS. Before treatment with the inducer of ATP (5-TG) depletion, cells were starved for 24h with DMEM (5.5mM glucose) without serum (Figure 17, lane 1). Growth factor withdrawal decreased Akt and mTOR activity, measured with anti phospho-Akt antibody and anti-phospho-4EBP1 antibody (Figure 17, lane 1) and stimulation with DMEM (5mM glucose) with 1 μ g/ml Insulin induced Akt and mTOR activity (Figure 17, lane 2). The induction of 4EBP1 phosphorylation by insulin was almost abolished by ATP depletion with 20 mM and 40 mM 5-Thiogluucose (Figure 17, lanes 3 –4).

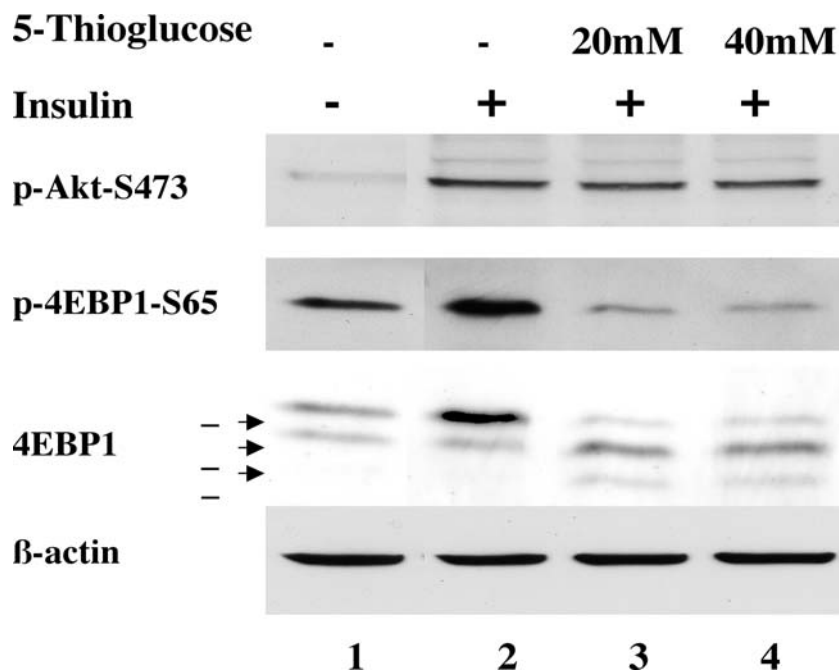


Figure 17: ATP depletion of insulin-stimulated Rat1a cells, and its inhibition of the growth-factors-dependent activation of mTOR.

Rat1a cells were plated in DMEM (5.5 mM glucose) with 10% FBS (dialyzed), then deprived of serum for 24h (lane 1). Cells were stimulated with insulin (1 μ g/ml) for 30min and (lane 2) then either untreated or treated with 5-thiogluucose (5-TG) for additional 30min. (20mM–lane 3, 40mM–lane 4).

Higher concentrations of 5-TG were required to impair mTOR activity in cells expressing activated Akt. 4E-BP1 phosphorylation mediated by insulin stimulation in Rat1a cells was more severely impaired by ATP depletion (Figure 17, lanes 3-4) compared to Rat1a-mAkt cells expressing activated Akt (Figure 16, lanes 4-5). Furthermore, adding high levels of 2-deoxyglucose (2-DOG) to cells expressing activated Akt inhibited mTOR activity (data not shown).

However, 100mM 2-DOG that impaired Akt-mediated mTOR activity could also induce osmotic stress and therefore, we used 5-TG instead. 5-TG was probably a more effective inhibitor because, unlike 2-DOG, 5-TG is a competitive inhibitor that cannot be phosphorylated by hexokinase which leads to inhibition of glycolysis and then ATP depletion.

4.3.3 Activation of AMPK by AICAR in Rat1a cells expressing activated Akt

Recent publications suggest that AMPK (AMP-activated protein kinase) is involved in the PI3K/PTEN/Akt pathway (Inoki et al. 2003b; Kimura et al. 2003). It has been shown that AMPK suppressed protein synthesis through mTOR. For this study, AICAR (5-aminoimidazole-4-carboxamide-ribose) has been used to activate AMPK (treatment of animal skeletal muscle). AICAR-treatment resulted in an activation of AMPK and a reduction in protein synthesis, this decline was associated with the decreased activation of mTOR (Bolster et al. 2002).

AICAR (5-aminoimidazole-4-carboxamide-ribose) is an adenosine analogue, which activates AMPK after its phosphorylation to 5-aminoimidazole-4-carboxamide-ribotide, an AMP analogue. Incubation of the cells with AICAR has the advantage of activating AMPK without affecting the adenine nucleotide level (Meisse et al. 2002), thus allowing to investigate the effect on mTOR activity without ATP depletion.

To determine the possibility that AMPK is a downstream effector of Akt leading to mTOR activation, 1×10^6 Rat1a-mAkt cells were deprived of serum and treated with AICAR, which activates AMPK and was shown to impair insulin-mediated phosphorylation of S6K1 (Kimura et al. 2003).

As shown in Figure 18, treatment of Rat1a-mAkt cells, in which mTOR is constitutively active, with increasing concentrations of AICAR elevated AMPK

activity, as measured by AMPK and ACC phosphorylation using anti-phospho Thr172 AMPK and anti-phospho Ser79 ACC antibodies, with a concomitant decrease of 4E-BP1 phosphorylation.

These results demonstrated that activation of AMPK by AICAR impairs the constitutive mTOR-activity in Rat1a-mAkt cells.

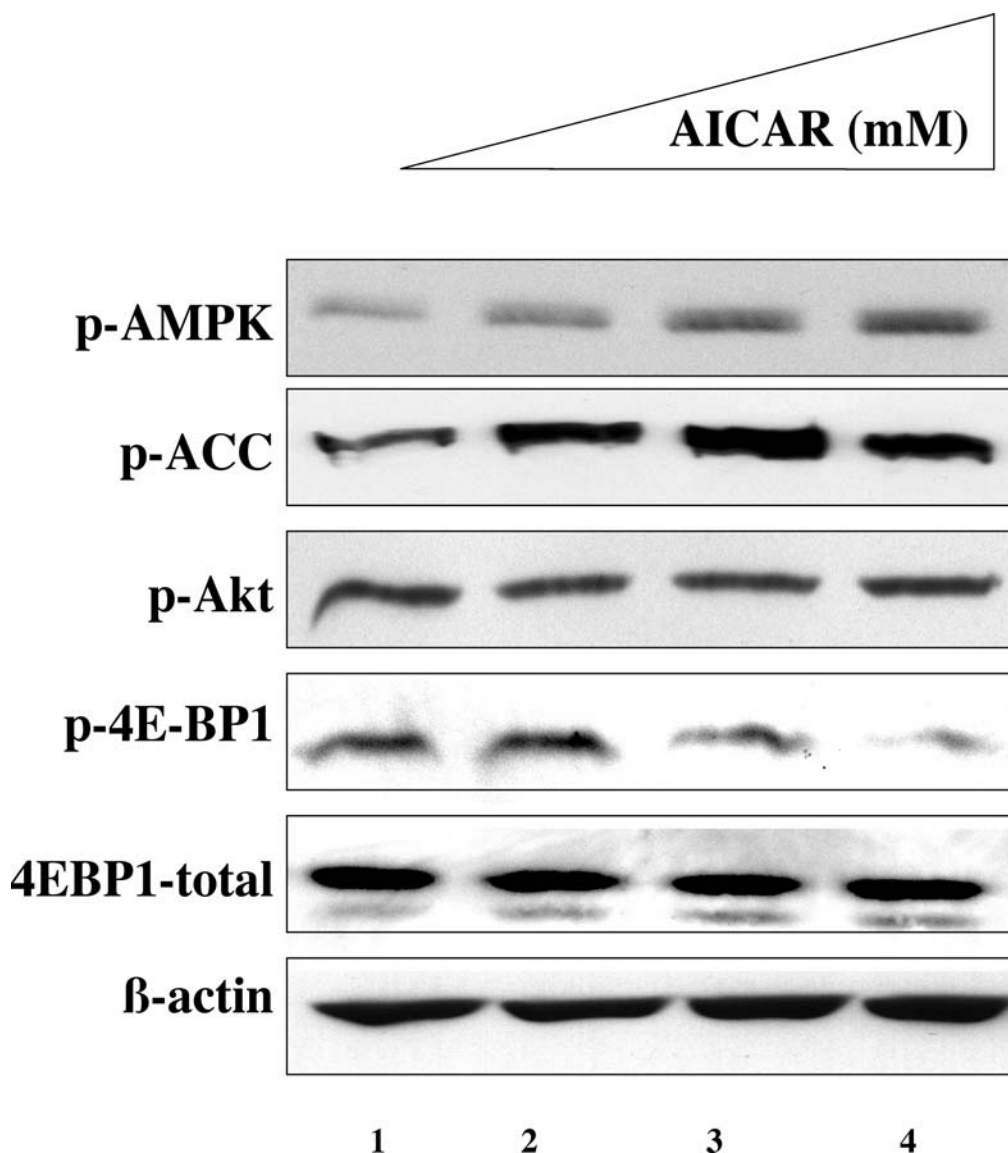


Figure 18: Dose-dependent activation of AMPK by AICAR.

Rat1a-mAkt cells were deprived of serum for 24 h and then treated with increasing concentrations of AICAR for 60 min. Following treatment cell lysates were subjected to immunoblotting using anti-p-AMPK-T172, anti-p-ACC-S79, anti-p-Akt-S473, anti-p-4E-BP1-S65, anti-4EBP1 and anti-β-actin antibodies.

4.3.4 Co-expression experiment with constitutively activated AMPK and 4EBP1

A co-expression experiment with a constitutively active form of AMPK (pcDNA3-Myc-AMPK1³¹²T172D) and 4EBP1 (pcDNA3-HA-4E-BP1), both in pcDNA3 expression vectors using HEK293 and HEK293-mAkt cells expressing activated myristoylated Akt, was performed. The plasmid pcDNA3-HA-4E-BP1 has been previously described (Gingras et al. 1998).

The expression vector for the Myc-tagged activated AMPK, pcDNA3-Myc-AMPK1³¹²T172D was obtained from D. Carling (Woods et al. 2000). This experiment was performed to further establish the role of AMPK in mediating mTOR activity by Akt's ability to increase the intracellular level of ATP.

For transient transfection of HEK293 and HEK293-mAkt cells, 1×10^6 cells per 6-cm-plate were plated in DMEM with 10% FBS and transfected without and with increasing concentrations of pcDNA3-Myc-AMPK1³¹²Thr172D (15, 20 μ g DNA) and 2.5 μ g pcDNA-4EBP1-HA per 1×10^6 cells using Lipofectamine 2000 (CHAPTER 3.5.2). Lysates were prepared 24 hours after transfection under proliferation condition in DMEM with 10% FBS.

Whether an activated form of AMPK can alleviate the ability of Akt to activate mTOR as measured by phosphorylation of 4EBP1 or 4EBP's different migrating forms or mobility shift detected with anti-HA antibody. Hyperphosphorylated 4EBP1 migrates slower on a SDS-Page than hypophosphorylated 4EBP1.

In contrast to control HEK293 cells, HEK293-mAkt cells showed constitutively phosphorylated 4E-BP1 even in the absence of insulin stimulation (Gingras et al. 1998), compare Figure 19 lanes 1 and 4). Following expression of activated AMPK, 4EBP1 phosphorylation (down shift toward faster migrating form) was impaired (Figure 19 lanes 2-3 and lanes 5-6). Due to higher ATP level in HEK293-mAkt cells, the effect on 4EBP1 (downshift and phosphorylation) was less pronounced in HEK293-mAkt cells compared to 293 cells. This result established the down-regulation of AMPK by Akt as function of increasing ATP-levels. Activated AMPK inhibits the ability of Akt to activate mTOR.

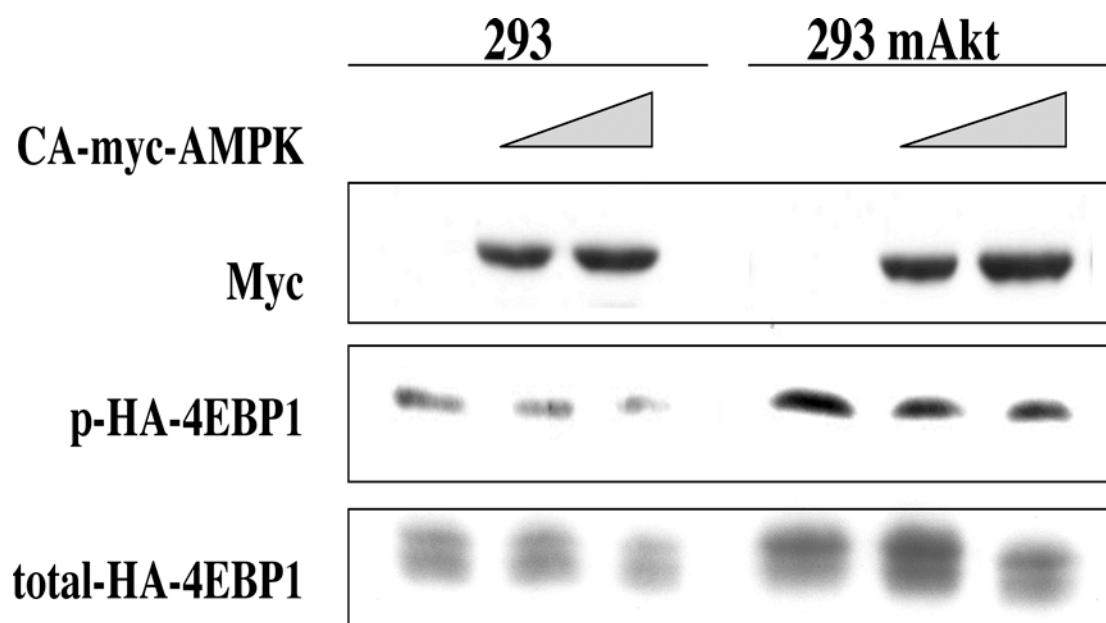


Figure 19: Co-expression of activated AMPK and 4EBP1 in HEK293 and HEK293MAkt cells.

HEK293 cells with mAkt (lanes 1-3) or without mAkt (lanes 4-6), were transfected with increasing amounts of constitutively activated AMPK mutant (CA-AMPK) (lanes 2 and 5, 15 μ g and lanes 3 and 6, 20 μ g) and HA-4EBP1 (lanes 1-6 2.5 μ g). Downshift of co-transfected HA-4EBP1 was determined by using anti-HA-antibody. CA-AMPK expression induced, a fast migrating 4EBP1 isoform.

4.4 Reduced AMPK activity by over expression of dominant negative AMPK restores mTOR activity in Akt1/Akt2 DKO MEFs

4.4.1 Stable Akt1/Akt2 DKO MEF cell line expressing dominant negative AMPK restores mTOR activity

Previous experiments showed that activation of AMPK by AICAR or a constitutively expressed AMPK decreased mTOR activity in an Akt-dependent manner. In chapter 4.1.2 mTOR activity has been found to be profoundly reduced in Akt1 and Akt2 deficient cells. The question that arose at this point of investigation was, whether the expression of a dominant negative form of AMPK would be able to increase mTOR activity in Akt1/Akt2 DKO MEFs, which would prove an Akt-dependent regulation of AMPK mediated by the intracellular level of ATP. A dominant negative form of AMPK exerts no kinase activity, this is due to

a point mutation on K (Lysin) 45 to R (Arginine), which disables ATP to bind to this region; therefore, the allosteric regulation of this protein is still functional (Mu et al. 2001).

For this experiment, immortalized Akt1/Akt2 DKO and WT MEFs were generated by infection with pBabe-Puro-GSE5 expressing a dominant negative form of p53 (Ossovskaya et al. 1996) followed by selection with puromycin to generate polyclonal cell lines. The retroviral vectors pBabe-Puro have been previously described (Kennedy et al. 1997; Eves et al. 1998). The retroviral vectors pBabe-Puro-DN-AMPK and pBabe-eGFP-DN-AMPK were constructed using previously described dominant negative AMPK (DN-AMPK). The rat Myc-tagged AMPKalpha2-K45R was excised from pcDNA3-Myc-AMPKalpha2-K45R (Mu et al. 2001) and inserted into the EcoR1 sites of pBabe-puro and pBabe-eGFP.

High titer retrovirus was generated in phoenix cells as previously described (CHAPTER 3.6, and (Kennedy et al. 1999)). To generate Akt1/Akt2 DKO polyclonal cell lines expressing DN-AMPK, immortalized Akt1/Akt2 DKO MEF were infected with high titer pBabe-eGFP-AMPKalpha2-K45R or control pBabe-eGFP followed by sorting with FACS (using facility at the UIC).

If Akt's ability to activate mTOR was dependent on its ability to increase the ATP level and to inhibit AMPK kinase activity, it was expected that inhibition of AMPK activity in Akt1/Akt2 DKO cells would partially restore the impaired *in vivo* mTOR activity as measured by 4E-BP1 phosphorylation (determined by shift of different forms of 4EBP1 using anti-4EBP1 antibody).

To explore this possibility, cell lines of immortalized Akt1/Akt2 DKO, DKO (DN-AMPK) and WT MEFs were plated in 15 cm plates in DMEM with 10% FBS. After one day of proliferation, cells were harvested and lysed.

Immortalized WT and Akt1/Akt2 DKO MEFs (expression of dominant-negative form of p53) were used. As in primary cells (Figure 7, lanes 1-2), mTOR activity was impaired in Akt1/Akt2 DKO immortalized cells (Figure 20, lanes 1-2).

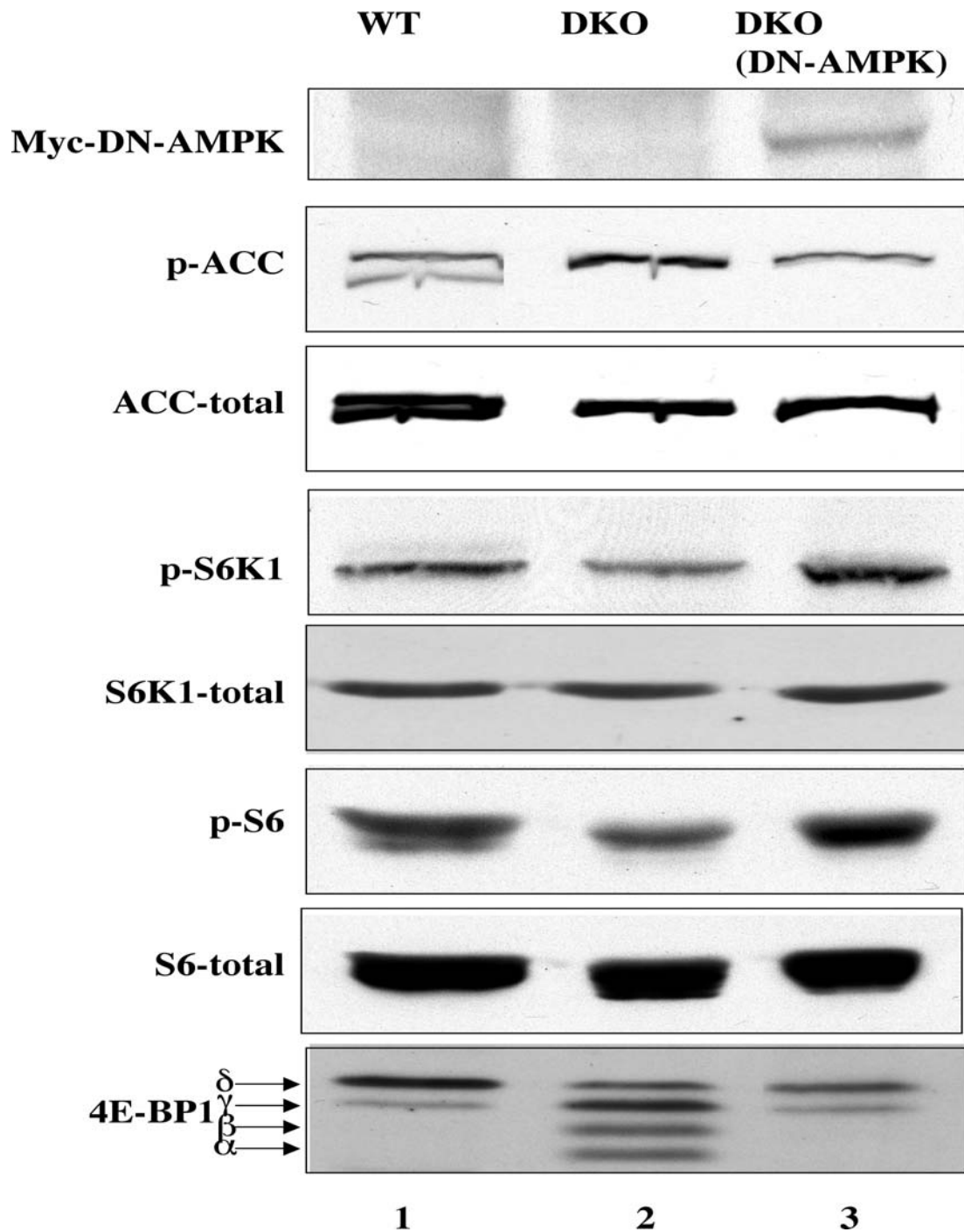


Figure 20: Expression of dominant-negative AMPK in Akt1/Akt2 DKO cells vs. WT. Cells lysates from proliferating immortalized WT, Akt1/Akt2 DKO, and Akt1/Akt2 DKO expressing Myc-tagged DN-AMPK were subjected to immunoblotting using anti-Myc 9E10, anti-p-ACC S79, anti-ACC, anti-pS6K1-T389, anti-S6K, anti-pS6-S235/236, anti-S6 and anti-4E-BP1 antibodies.

As shown in Figure 20, expression of DN-AMPK in Akt1/Akt2 DKO MEFs almost restored mTOR activity in proliferating cells as determined by S6K1, S6 and 4EBP1 phosphorylation/shift (Figure 20, lanes 2-3) compared to WT (Figure 20, lane 1).

These results demonstrated that mTOR activity in Akt1/Akt2 DKO cells was also impaired because of the inability to sufficiently increase the intracellular ATP level by insulin and growth factors and to decrease AMPK activity.

4.4.2 Increasing expression of dominant negative AMPK in Akt1/Akt2 DKO MEFs restores mTOR activity

To investigate dose dependability in restoring mTOR activity, dominant negative AMPK and 4EBP1 were co-expressed in AKT1/AKT2 DKO MEFs by using increasing concentrations of pcDNA3-Myc-AMPKalpha2-K45R (Mu et al. 2001) and pcDNA3-HA-4EBP1 (Gingras et al. 1998), shown in Figure 18. The amount of 2.5 µg pcDNA3-HA-4EBP1 and 10, 15 and 20 µg pcDNA3-Myc-AMPKalpha2-K45R per 1×10^6 cells were transfected using Lipofectamine 2000 (CHAPTER 3.5.2).

In the absence of DN-AMPK, mTOR activity was reduced (Figure 21, lane 1), measured by phospho-shifting of exogenous HA-4EBP1 using anti-HA antibody. Increasing expression of DN-AMPK restores mTOR activity, visible by an up-shift of the hyperphosphorylated form of exogenous HA-4EBP1 (Figure 21, lanes 2-4).

These results further established a role for AMPK in mediating the energy response on mTOR under a decreased level of intracellular ATP in Akt1/Akt2 DKO MEFs.

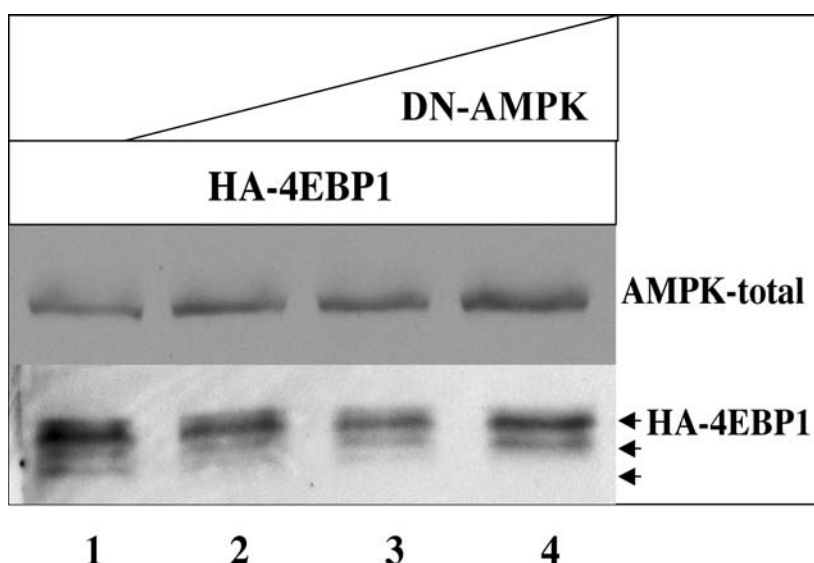


Figure 21: Dose-dependent co-expression of dominant-negative AMPK and 4EBP1 in Akt1/Akt2 DKO MEFs.

Akt1 and Akt2 DKO MEFs were transfected with increasing amounts of dominant negative AMPK mutant (DN-AMPK) and HA-4EBP1. Up-shift of co-transfected HA-4EBP1 was determined by using anti-HA-antibody. DN-AMPK expression induced slowly migrating 4EBP1-form.

4.5 Akt's ability to activate mTOR by inhibiting AMPK is dependent on TSC2

4.5.1 TSC2 deficiency renders cells almost resistant to ATP depletion

It was recently shown that TSC2 is phosphorylated and activated by AMPK, establishing one potential mechanism by which ATP and AMPK regulate mTOR activity (Inoki et al. 2003b).

To further confirm this finding of TSC2 as a mediator of cellular energy, MEFs, which were deficient for TSC2 (TSC2^{-/-}/p53^{-/-} MEFs and TSC2^{+/-}/p53^{-/-} MEFs), were used to study the Akt-mTOR pathway. TSC2^{+/-}/p53^{-/-} MEFs expressing TSC2 were used as control cell line, because the wild type was not available (Figure 22).

A very similar experiment to the experimental set-up in chapter 4.3.1 was carried out with a TSC2 deficient cell line. 1.0×10^6 TSC2^{-/-}/p53^{-/-} and TSC2^{+/-}

/p53-/- MEFs were plated in 10 cm plates in DMEM (5.5mM Glucose) with 10% FBS.

Before treatment with inhibitor for ATP depletion (5-Thiogluucose and 2-Deoxyglucose), cells were starved for 24h with DMEM (5.5mM glucose) without serum (Figure 22, lanes 1 and 5). Growth factor withdrawal decreased Akt and mTOR activity in TSC2+/-/p53-/- MEFs, measured with anti-phospho-Akt, anti-phospho-S6K1, anti-phospho-S6, and anti-4EBP1 antibody (Figure 22, lane 5). In TSC2-/-/p53-/- MEFs, however, there was no reduction of mTOR activity (Figure 22, lane 1) and Akt activity (anti-phospho-Akt antibody) was reduced even in the presence of insulin (Figure 22, lanes 1-4).

Under stimulation conditions with 1 μ g Insulin per ml DMEM (5.5mM glucose), Akt and mTOR activity in TSC2+/-/p53-/- MEFs were induced (Figure 22, lane 6). The induction of 4EBP1 phosphorylation by insulin was highly reduced by ATP depletion with 50 mM 2-Deoxyglucose and 50 mM 5-Thiogluucose in TSC2+/-/p53-/- MEFs (Figure 22, lanes 7–8). ATP depletion had only a moderate effect on mTOR activity in TSC2-/-/p53-/- MEFs under these conditions, suggesting that the ATP level regulates mTOR activity predominantly through TSC2 (Figure 22, lanes 3-4).

These results clearly demonstrate, that TSC2-/-/p53-/- MEFs are almost resistant to ATP depletion in comparison to TSC2+/-/p53-/- MEFs, and furthermore, TSC2 mediates the energy response, which is consistent with previous results (Inoki et al. 2003b).

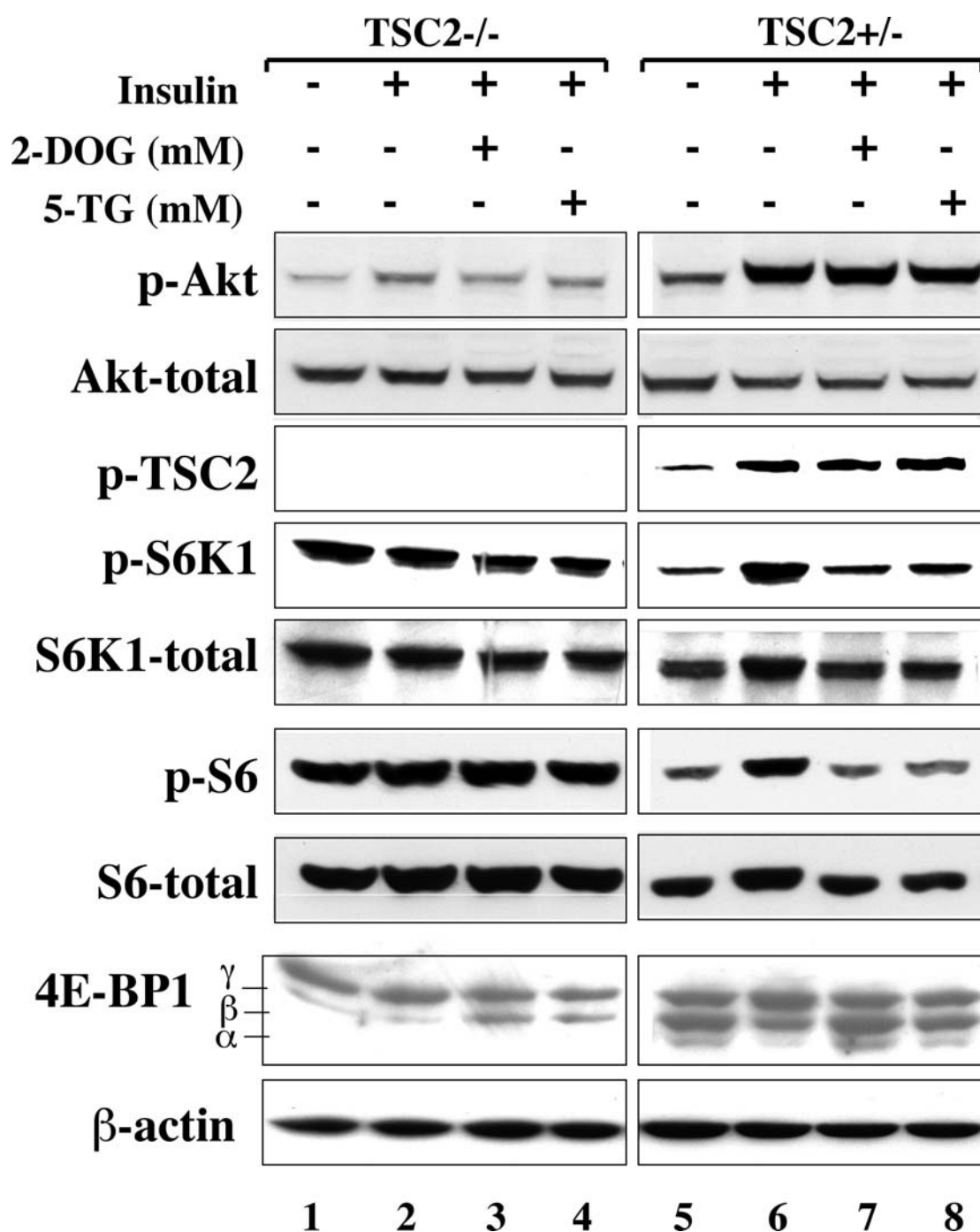


Figure 22: mTOR activity in TSC2^{-/-} vs. control cells following ATP depletion .

mTOR activity in TSC2^{-/-} cells is refractive to ATP depletion. TSC2^{-/-} and TSC2^{+/-} MEF were plated in DMEM (5.5 mM glucose) with 10% FBS (dialyzed), deprived of serum for 24h. Cells were stimulated with insulin (1μg/ml) for 30min and then either untreated or treated with 2-deoxyglucose (2-DOG, 50mM) or 5-thioglucon (5-TG, 50 mM) for additional 30min. Cell lysates from serum deprived cells (lanes 1 and 5), insulin stimulated cells (lanes 2 and 6), insulin stimulated, 2-DOG treated cells (lanes 3 and 7), and from insulin stimulated 5-TG treated cells (lanes 4 and 8) were subjected to immunoblotting using anti-p-Akt-473, anti-pan-Akt, anti-p-TSC2-T1462, anti-pS6K1-T389, anti-S6K, anti-pS6-S235/236, anti-S6, anti-4E-BP1 and anti-β-actin antibodies.

4.5.2 TSC2 KO cells exert a high AMP/ATP ratio and the expression of activated Akt is able to decrease this ratio

Interestingly, in TSC2^{-/-}/p53^{-/-} MEFs, there was a pronounced reduction of Akt activity (see Figure 22, lanes 1-4). Akt activity mediated by insulin and growth factors has been found to be significantly diminished in cells lacking TSC1 (Kwiatkowski et al. 2002) or TSC2 (Jaeschke et al. 2002).

If Akt activity was required to maintain the intracellular level of ATP, it was expected that the AMP/ATP ratio in TSC2^{-/-}/p53^{-/-} MEFs compared to control cells would be increased and that over expression of the activated form of mAkt in TSC2^{-/-}/p53^{-/-} MEFs would restore the AMP/ATP ratio to the level of control cells.

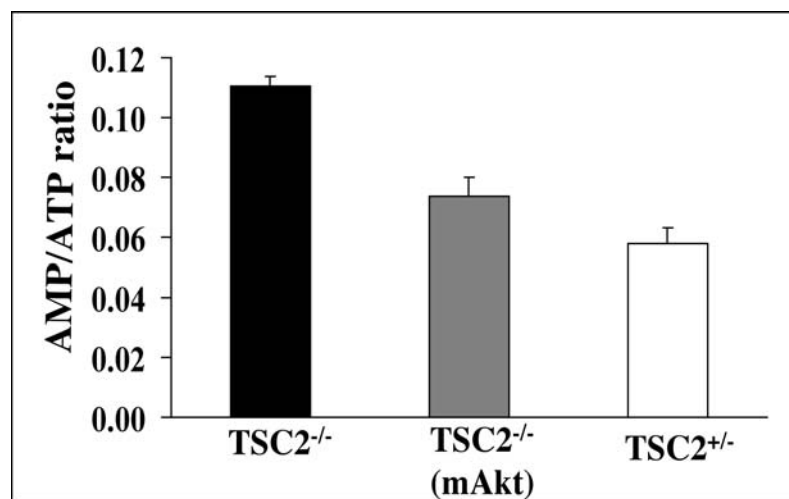


Figure 23: AMP/ATP ratio in TSC2^{-/-}, mAkt-TSC2^{-/-} and TSC2^{+/-} cells.

ATP and AMP levels were analyzed in a TSC2^{-/-} MEF, TSC2^{-/-} polyclonal MEF cell line expressing mAkt, and TSC2^{+/-} MEFs as described in Fig. 14. AMP/ATP ratios were determined and the results represent the average of three independent experiments (+/- SD).

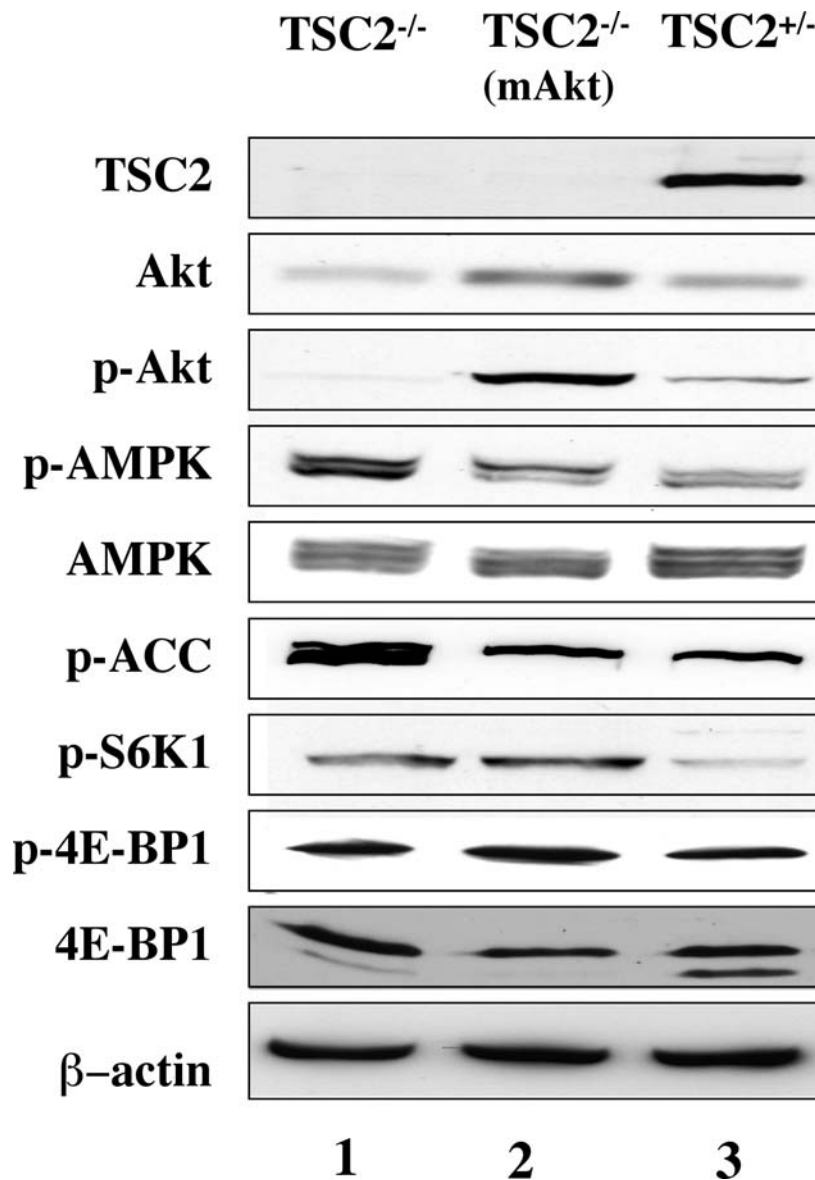


Figure 24: Akt and AMPK activity in TSC2^{-/-}, mAkt-TSC2^{-/-} and TSC2^{+/-} cells.

Cells lysates from TSC2^{-/-} MEFs, a TSC2^{-/-} polyclonal MEF cell line expressing mAkt, and TSC2^{+/-} MEFs were subjected to immunoblotting using anti-TSC2, anti-pan-Akt, anti-p-Akt-S473, anti-p-AMPK-T172, anti-AMPK, anti-p-ACC-S79, anti-p-S6K1-T389, anti-p-4E-BP1-S65, anti-4E-BP1, and anti- β -actin antibodies.

Figure 23 shows the AMP/ATP ratio of TSC2^{-/-}/p53^{-/-}, mAkt-TSC2^{-/-}/p53^{-/-} and TSC2^{+/-}/p53^{-/-} MEFs under proliferating condition in DMEM (5.5mM Glucose) with 10% FBS, measured by HPLC (see CHAPTER 3.9). In addition, cells under this condition were taken and lysed for immunoblotting analysis as

shown in Figure 24.

The AMP/ATP ratio and AMPK activity, measured by anti-phospho-AMPK antibody at Threonine172 (Hawley et al. 1995), was markedly higher in TSC2^{-/-}/p53^{-/-} cells when compared to TSC2^{+/-}/p53^{-/-} cells (Fig. 23 and Fig. 24, lanes 1 and 3). The higher AMP/ATP ratio and higher AMPK activity in TSC2^{-/-}/p53^{-/-} cells could be due to a reduced Akt activity in these cells (Figure 22, lanes 1-2 and 5-6, Figure 24, lanes 1 and 3) due to a feedback loop mechanism (Jaeschke et al. 2002; Zhang et al. 2003a). Indeed, when activated Akt was stably expressed in TSC2^{-/-}/p53^{-/-} cells, the AMP/ATP ratio was restored with concomitant decrease in AMPK activity similar to that in TSC^{+/-}/p53^{-/-} cells (Figure 23 and 24, lane 2). These results further established a role of Akt to mediate and maintain a low AMP/ATP ratio and to inhibit AMPK activity.

In TSC2-deficient cells mTOR was constitutively active, measured by the phosphorylation status of 4EBP1, p70S6K and S6, despite a high AMP/ATP ratio and AMPK kinase activity (Figure 24, lane 1). This furthermore established the role for TSC2 to mediate the energy response downstream of AMPK.

4.5.3 Inhibition of AMPK by Akt despite TSC2 phosphorylation is also required for mTOR activity

It has been demonstrated that TSC1-TSC2 act to antagonize the insulin-signaling pathway through inhibition of S6K, which is downstream of mTOR (McManus and Alessi 2002) and several groups have shown that Akt directly targets TSC2 by phosphorylation in vitro and in vivo. Identified sites are Serine 939, Serine 1086/1088 and Threonine 1462/1422 rat-short cDNA (Tee et al. 2002). A consistent finding among all studies in mammalian cells is that TSC1 and TSC2 form a complex (van Slegtenhorst et al. 1997; Nellist et al. 2002); however, the consequences of Akt-mediated TSC2 phosphorylation are not clear. There are reports supporting a model that Akt phosphorylation of TSC2 disrupts the TSC1-TSC2 complex (Inoki et al. 2002).

Is TSC2 phosphorylation by Akt sufficient to activate mTOR or is the inhibition of AMPK by Akt, leading to reduced AMP/ATP ratios, also required for mTOR activation?

To address this question, an Akt-phosphomimetic mutant of TSC2 HA-tagged TSC2 (S939D/S1086D/S1088D/T1422E) in pcDNA3 (rat-short cDNA (Tee et al. 2002) was used (obtained from K. Inoki and K-L Guan) (Inoki et al. 2002). In this mutant four residues that are phosphorylated by Akt were substituted by acidic amino acids (Inoki et al. 2002).

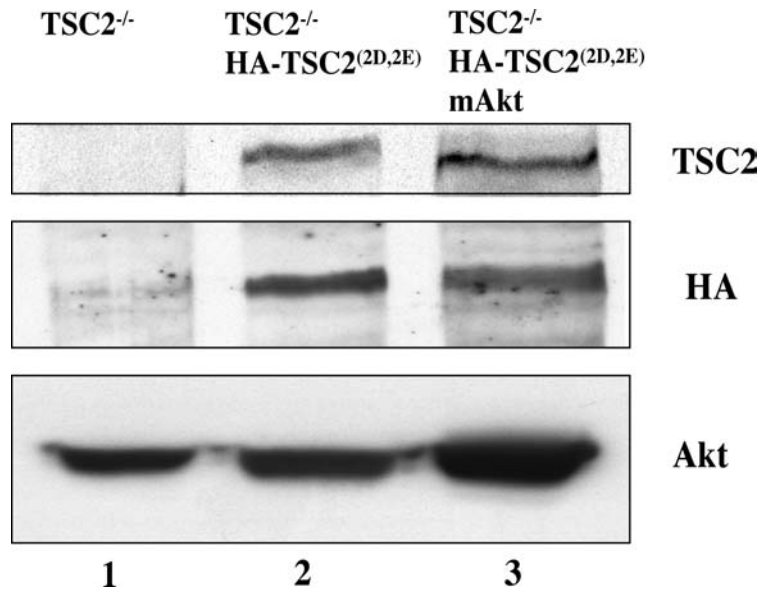


Figure 25: Expression of Akt-phosphomimetic mutant of TSC2 in TSC2^{-/-} cells.

Immunoblot shows the expression of exogenous HA-tagged TSC2 phosphomimetic mutant, TSC2(S939D/S1086D/S1088E/T1422E) (TSC2(2D,2E)), and Akt in control TSC2^{-/-} MEFs, a polyclonal TSC2^{-/-} MEFs cell line expressing HA-TSC2(2D,2E), and a polyclonal TSC2^{-/-} MEFs cell line expressing HA-TSC2(2D,2E), and mAkt.

The retroviral vector pLPCX-HA-TSC2 (S939D/S1086D/S1088D/T1422E) was constructed by inserting TSC2 (S939D/S1086D/S1088D/T1422E) into the Not1 site of pLPCX (retroviral vector). To generate a TSC2^{-/-} polyclonal cell line expressing HA-TSC2 (S939D/S1086D/S1088D/T1422E), TSC2^{-/-} MEFs were infected with high titer pLPCX-HA-TSC2 (S939D/S1086D/S1088D/T1422E) or control pLPCX retrovirus followed by selection with puromycin. To generate polyclonal TSC2 cell lines expressing both HA-TSC2 (S939D/S1086D/S1088D/T1422E) and mAkt, TSC2^{-/-} MEFs expressing HA-TSC2 (S939D/S1086D/S1088D/T1422E) were re-infected with pBabe-eGFP- mAkt retrovirus followed by sorting with FACS.

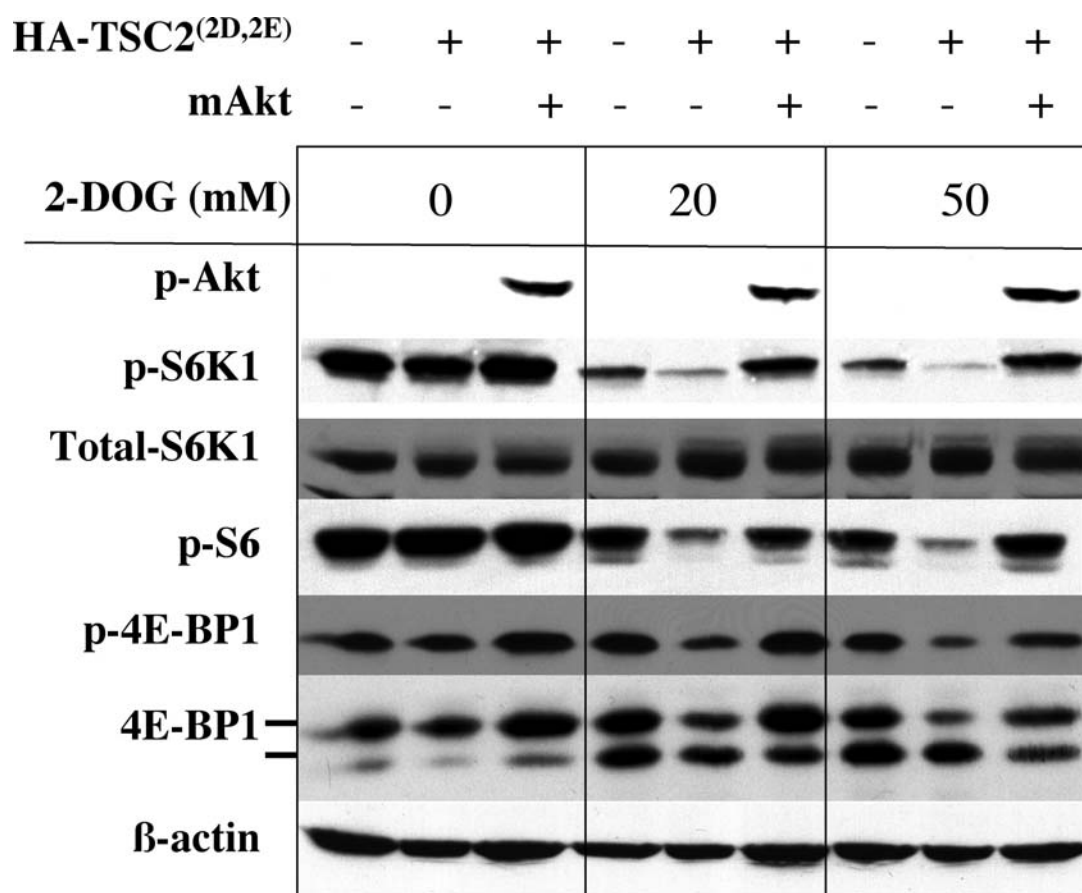


Figure 26: Expression of Akt-phosphomimetic mutant of TSC2 in TSC2^{-/-} cells sensitizes mTOR activity to ATP depletion, which is restored by activated Akt.

Cell lysates from untreated or 2-DOG treated TSC2^{-/-} MEFs (lanes 1, 4, and 7), a polyclonal TSC2^{-/-} MEF cell line expressing HA-TSC2(2D,2E) (lanes 2, 5, and 8), and a polyclonal TSC2^{-/-} MEF cell line expressing HA-TSC2(2D,2E) and mAkt (lanes 3, 6, and 9) were subjected to immunoblotting using anti-p-Akt-S473, anti-p-S6K1-T389, anti-S6K, anti-p-S6-S240/244, anti-p-4E-BP1-S65, anti-4E-BP1 and anti-β-actin a

The expression of the introduced HA-TSC2^(3D,1E) into TSC2^{-/-}/p53^{-/-} cells by retrovirus infection was analysed by immunoblotting with anti-HA and anti-TSC2 antibodies (Figure 25 lanes 1-3) and compared to TSC2^{-/-}/p53^{-/-} cells. 1.0x10⁶ HA-TSC2^(3D,1E)TSC2^{-/-}/p53^{-/-}, mAkt-HA-TSC2^(3D,1E)TSC2^{-/-}/p53^{-/-} and TSC2^{-/-}/p53^{-/-} cells were plated in 10 cm plates in DMEM (5.5mM Glucose). Before treatment with inhibitor for ATP depletion, cells were plated for 24h in DMEM (5.5 mM Glucose) with 10% FBS. ATP was depleted for 30 minutes using 25 and 50 mM 2-Deoxyglucose in DMEM (5.5 mM Glucose).

Figure 26 shows (lanes 2, 5, and 8), that TSC2^(3D,1E) rendered mTOR activity in TSC2^{-/-} cells more sensitive to ATP depletion. The phosphorylation of

TSC2 by Akt was not sufficient to render mTOR activity resistant to ATP depletion. When mAkt was co-expressed, mTOR activity was restored to the level observed in TSC2^{-/-}/p53^{-/-} cells (Figure 26, lanes 3, 6 and 9).

This result finally demonstrated that Akt regulates AMPK activity and supported previous results, which showed that TSC2 is a target for AMPK (Inoki et al. 2003b). Akt leads to the activation of mTOR through both phosphorylation and inactivation of TSC2 and through inhibition of AMPK activity, which has been shown to activate TSC2 (Inoki et al. 2003b). Therefore, the phosphorylation of TSC2 by Akt is not sufficient to fully activate mTOR.

5. Discussion

5.1 Akt can determine the cell mass and is required for mTOR activity

Results in chapter 4.1.1 show the occurrence of severe atrophy and a decrease in cell size of skeletal muscle cells in Akt1/Akt2 DKO mice. In previous studies Akt has been involved in determining skeletal hypertrophy (Bodine et al. 2001; Rommel et al. 2001; Fingar et al. 2002; Pallafacchina et al. 2002). Furthermore, expression of activated Akt has been shown to increase organ cell and organ size (Shioi et al. 2002). This finding is consistent with the studies in *Drosophila* that the loss of Akt reduced cell size (Scanga et al. 2000). These results established for the first time genetic evidence that Akt is required for determining the cell size in mammalian organisms (Peng et al. 2003). Furthermore, this result prompted to investigate the signaling pathways that underlie in these findings.

Akt is required for the phosphorylation and inhibition of 4EBP1 by mTOR (Gingras et al. 1998) and mTOR is responsible for the phosphorylation of p70S6K and activates it, whereas 4EBP1 activity is inhibited by phosphorylation of mTOR. Both 4EBP1 and p70S6K have been implicated in determining the cell size as well (Kozma and Thomas 2002). This study placed mTOR as a central regulator of cell growth (size) and proliferation.

The neonatal lethality of Akt1/Akt2 DKO mice precluded the analysis of the Akt–mTOR pathway in skeletal muscle of Akt1/Akt2 DKO mice. Using Akt1/Akt2 DKO MEFs, intracellular activity of mTOR was determined by the phosphorylation status of 4EBP1 and S6K.

The results in chapter 4.1.2 demonstrate that, upon serum stimulation, there was a significant reduction in 4EBP1 phosphorylation in Akt1/Akt2 DKO cells. In addition, Akt1/Akt2 DKO cells displayed a reduced expression level of 4EBP1, probably as a compensatory mechanism for the inability to efficiently phosphorylate 4EBP1. Under this condition, the S6K1 phosphorylation was not impaired, suggesting there might be another kinase that phosphorylates S6K1, or the threshold of Akt activity for S6K1 phosphorylation is relatively low. It was recently shown that PDK1 and PKC ζ are able to mediate Threonine 389 phosphorylation in an mTOR dependent manner (Romanelli et al. 2002). Genetic

analyses in *Drosophila* have shown that dS6K can function independently of Akt (Radimerski et al. 2002).

However, under steady-state level in proliferating cells, the phosphorylation of both 4EBP1 and S6K1 was markedly reduced in Akt1/Akt2 DKO MEFs; how this occurred needed further examination. This result also established the first genetic evidence that Akt is required for mTOR-mediated phosphorylation.

Akt directly phosphorylates TSC2 (Potter et al. 2001; Inoki et al. 2002; Manning et al. 2002). However, results in chapter 4.1.3 showed there was not always a direct correlation between TSC2 phosphorylation and reduced mTOR activity, as measured by 4EBP1 phosphorylation in Akt1/Akt2 DKO cells. This finding and the observation that over expression of an activated form of mAkt increased the intracellular level of ATP ((Gottlob et al. 2001), and Figure 10) led to further investigation of another potential pathway, by which Akt affects mTOR activity. A previous study showed that the intracellular level of ATP modulated mTOR activity (Dennis et al. 2001).

5.2 Akt is a key regulator for energy metabolism and regulates indirectly AMPK activity

In Rat1a-mAkt ((Gingras et al. 1998), and Fig. 15, 16, 18) and 293-mAkt cells (Fig.16), expressing activated Akt, mTOR was constitutively active even in the absence of growth factors as determined by 4EBP1 phosphorylation and mobility shift. The serine/threonine kinase Akt is a key regulator of energy metabolism induced by growth factors and has been shown to phosphorylate and induce activity of the 6-phosphofructo-2-kinase (PFK-2) in heart, which in turn stimulates glycolysis (Deprez et al. 1997). Also, Akt was shown to regulate glucose metabolism at several levels by enhancing glucose uptake in insulin-responsive tissues. This is mainly due to an effect on the glucose transporters GLUT1, GLUT3 and GLUT4. Akt has been found to increase the expression of the glucose transporters (Mazure et al. 1997; Barthel et al. 1999) and the translocation of GLUT4 to the plasma membrane (Kohn et al. 1996; Cong et al. 1997; Tanti et al. 1997).

Interestingly, it has been shown that Akt localized into the mitochondria, where it was found to reside in the matrix and the inner and outer membranes. Additionally, the level of mitochondrial Akt is regulated very dynamically. Stimulation of a variety of cell types with insulin-like growth factor-1, insulin, or stress (heat shock) induced translocation of Akt to the mitochondria within several minutes of stimulation, causing increases of nearly eight- to 12-fold. Mitochondrial Akt was found to be in its phosphorylated, active state and two mitochondrial proteins were identified to be phosphorylated following stimulation, the β -subunit of ATP synthase and glycogen synthase kinase-3 β (Bijur and Jope 2003).

In Akt1/Akt2 DKO cells the level of intracellular ATP was significantly reduced (2-3 fold) after serum deprivation and following stimulation with insulin or serum (Figure 10, CHAPTER 4.2.1), whereas over expression of activated mAkt in Rat1a cells induced a 2 to 3-fold increase in ATP (Figure 11). The effect of Akt on the generation of ATP is mediated via an increase in glycolysis and oxidative phosphorylation (Gottlob et al. 2001). Although the exact mechanism(s), by which Akt affects these processes, are still unknown, Akt can potentially affect glycolysis through multiple mechanisms including glucose transporter expression and translocation (Kohn et al. 1996; Hajduch et al. 1998; Barthel et al. 1999; Rathmell et al. 2003), and increased activity and expression of glycolytic enzymes (Deprez et al. 1997; Gottlob et al. 2001; Majumder et al. 2004). The ability of Akt to increase glycolytic fluxes could also affect oxidative phosphorylation in the mitochondria by increasing the availability of substrates for oxidative phosphorylation.

AMPK is a heterotrimeric complex comprised of a catalytic (α) subunit and two regulatory (β and γ) subunits. AMP elicits allosteric changes that activate AMPK and promote phosphorylation of Thr172 in the activation loop of the α subunit by AMPK kinase, which was recently identified as LKB1 (reviewed in (Carling 2004)).

Figure 12 (CHAPTER 4.2.1) also shows that the ratio of AMP/ATP is markedly increased in Akt1/Akt2 DKO cells after stimulation when compared to the wildtype, which is mainly due to the insufficient ATP level. Figure 14 (CHAPTER 4.2.3) shows that in the presence and absence of growth factor,

Rat1a exhibited a 3-fold higher AMP/ATP ratio when compared to Rat1a cells expressing activated Akt. The AMP/ATP ratio reflects the status of activation of AMPK, measured by phosphorylation status of AMPK on Thr172 (Figure 15, (Hardie et al. 1998)). Figure 13 (CHAPTER 4.2.2) shows that expression and status of activation of Akt affected AMPK activity and Akt-deficiency induced phosphorylation of Thr172 as well as the *in vivo* activity of AMPK, as measured by the phosphorylation of ACC. The effect of Akt on the ATP level caused a concomitant reduction of the AMP/ATP ratio, and therefore reduced AMPK activity. As a kinase, Akt could potentially affect AMPK activity via phosphorylation of AMPK itself or its upstream regulator LKB1. Indeed, Thr366 of LKB1 lies in a consensus for the optimal phosphorylation motif for Akt. However, it has been reported that Akt couldn't phosphorylate LKB1 *in vitro* (Sapkota et al. 2001; Sapkota et al. 2002).

Rat1a cells expressing activated Akt were subjected to ATP depletion experiments using inhibitors of glycolysis and oxidative phosphorylation (CHAPTER 4.3.1). As discussed above, cells with activated Akt exert constitutively activated mTOR even in the absence of growth factors as determined by 4EBP1 phosphorylation and mobility shift. Figure 16 shows that Akt was constitutively active in the presence of both inhibitors and did not affect TSC2 phosphorylation. However, Akt-mediated mTOR activity was inhibited, when ATP was depleted in a dose-dependent manner. Inhibition of mTOR activity by ATP depletion was less effective in Rat1a-mAkt cells than in Rat1a cells induced by insulin using the same concentration of 5-thioglucoase (compare Figures 16 and 17).

The results strongly suggest that the ability of Akt to mediate mTOR activity is dependent on its ability to increase the intracellular ATP level, which subsequently down regulates AMPK.

To underline the finding that AMPK is down regulated by Akt, experiments were designed to activate endogenous AMPK using AICAR and to over/co-express CA-AMPK (constitutively activated form of AMPK) or DN-AMPK (dominant negative form of AMPK). Kimura et al. have shown that activation of AMPK decreased mTOR activity (Kimura et al. 2003). AICAR, widely used as an AMPK activator, induced AMPK activity and impaired insulin-mediated phosphorylation of S6K. In addition, over expression of dominant negative AMPK

increased S6K phosphorylation, whereas a constitutively active AMPK decreased S6K activity (Kimura et al. 2003).

The treatment of Rat1a-mAkt cells with AICAR, in which mTOR is constitutive active, induced endogenous AMPK activity in a dose-dependent manner with a concomitant decrease in mTOR activity (CHAPTER 4.3.3, Figure 18). Co-expression of constitutively active AMPK and 4EBP1 in 293 cells and in 293-mAkt cells proved the down regulation of AMPK by Akt as a function of different ATP levels and that activated AMPK antagonized this process (CHAPTER 4.3.4, Figure 19).

Characterization of Akt1/Akt2 DKO MEFs compared to wildtype revealed impaired mTOR activity. Using dominant negative AMPK to generate immortalized Akt1/Akt2 DKO MEFs (polyclonal cell line) expressing DN-AMPK clearly demonstrated that Akt's ability to increase mTOR activity is dependent on its function to down regulate AMPK (Figure 20, CHAPTER 4.4.1). These results demonstrate that mTOR activity in Akt1/Akt2 DKO MEFs was impaired as well because of the inability to sufficiently increase the level of intracellular ATP by insulin and growth factor. Over-expression of DN-AMPK in immortalized Akt1/Akt2 DKO MEFs increased mTOR activity in a dose-dependent manner and supported this result (CHAPTER 4.4.2, Figure 21).

Taken together, these results further established a role for Akt as a key regulator for energy metabolism and indirect regulator of AMPK activity.

5.3 Akt-mediated phosphorylation of TSC2 is not sufficient to fully activate mTOR

It was shown that AMPK impairs the induction of mTOR activity by growth factors (Kimura et al. 2003) and that AMPK directly phosphorylates and activates TSC2, thereby inhibiting mTOR activity (Inoki et al. 2003b). In chapter 4.5, it has been shown that in order to fully inhibit TSC2 and to activate mTOR, Akt needs to directly phosphorylate TSC2 and inhibit AMPK to prevent it from activating TSC2.

In cells deficient for Akt1 and Akt2, mTOR activity was impaired without a substantial effect on TSC2 phosphorylation by Akt (CHAPTER 4.1.2 and 4.1.3). However, Figure 13 (CHAPTER 4.2.2) shows that AMPK activity was elevated in

Akt1/Akt2 deficient cells suggesting that the residual Akt activity mediated by Akt3 is sufficient to phosphorylate TSC2 but insufficient to maintain a 'normal' ATP level and thus, leading to the activation of AMPK. Indeed, expression of DN-AMPK in Akt1/Akt2 deficient cells restored mTOR activity (CHAPTER 4.4).

Furthermore, expression of an Akt-phosphomimetic mutant of TSC2 in TSC2 deficient cells, in which mTOR activity is relatively refractive to ATP depletion, restored sensitivity of mTOR to ATP depletion implying that TSC2 phosphorylation by Akt did not prevent the activation of TSC2 by AMPK (CHAPTER 4.5.3, Figure 23). However, expression of activated Akt together with the Akt-phosphomimetic TSC2 mutant reversed the sensitivity of mTOR activity to ATP depletion similar to that observed in TSC2 deficient cells. In TSC2 deficient cells AMPK activity was elevated (Figure 24) and expression of activated Akt inhibits the elevated AMPK activity in these cells (Figures 24 and 26).

Thus, taken together, these results clearly demonstrate that Akt, in addition to inhibiting TSC2 via direct phosphorylation, also inhibits TSC2 and activates mTOR through inhibition of AMPK, establishing a new mechanism for the activation of mTOR by growth factors and Akt.

mRNA translation and ribosomal biogenesis, two processes that are mediated by mTOR, consume high levels of cellular energy. Thus, high consumption of ATP in TSC2-deficient cells together with the reduced Akt activity due to a negative feed back loop (Jaeschke et al. 2002; Zhang et al. 2003a) could contribute to the elevated AMP/ATP ratio and AMPK activity observed in these cells (CHAPTER 4.5.2, Figures 23 and 24).

Although mTOR activity in TSC2 deficient cells was relatively refractive to ATP depletion, it was still reduced to some extent in these cells in response to ATP depletion (CHAPTER 4.5.1, Figures 22 and 26). This suggests that ATP level and AMPK activity can also affect mTOR activity in a TSC2-independent manner. One possibility is that AMPK can directly phosphorylate and inactivate mTOR (Figure 24). It was recently shown that AMPK can phosphorylate Thr2446 of mTOR (Cheng et al. 2004), which resides in the putative negative regulatory domain of mTOR (Sekulic et al. 2000). Phosphorylation of Thr2446 by AMPK inhibited phosphorylation of Thr2448 by Akt and thus, could potentially inhibit mTOR activity (Cheng et al. 2004). However, so far it has not been demonstrated

that Thr2448 phosphorylation by Akt has any impact on mTOR activity (Cheng et al. 2004).

5.4 New mechanism by which growth factors activate mTOR

Both TSC2 and LKB1 appear to act as tumor suppressors and their deficiency leads to the development of benign tumors and hamartomas (Hemminki et al. 1998; Jenne et al. 1998; Cheadle et al. 2000b). It is therefore possible that LKB1 exerts its tumor suppressor activity through activation of AMPK and inhibition of TSC2. Akt is frequently activated in human cancers mainly through the inactivation of the tumor suppressor PTEN; its deficiency can also lead to the development of benign tumors and hamartomas (Parsons and Simpson 2003).

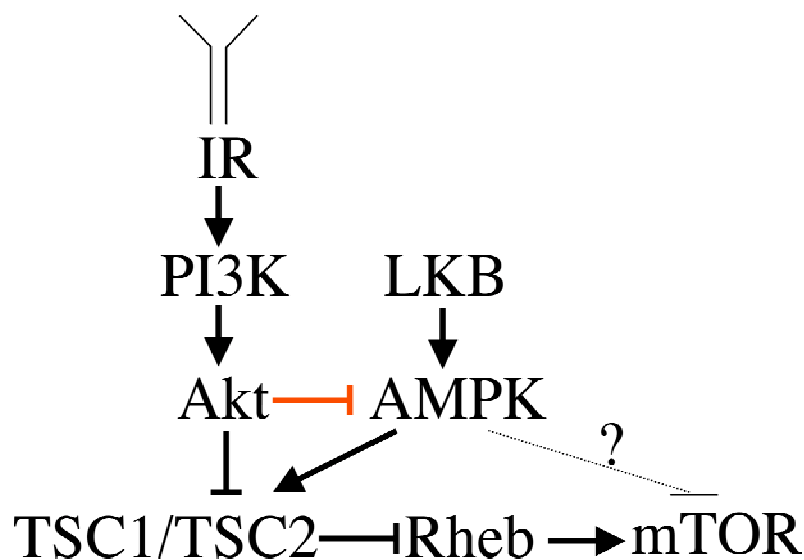


Figure 27: Proposed model for the regulation of mTOR activity by Akt.

Activation of Akt leads to the direct phosphorylation of TSC2. In addition, Akt also regulates mTOR by inhibition of AMPK due to regulation/maintaining energy homeostasis. The downstream target for this regulation is TSC2 (energy response point). AMPK might also act further downstream of TSC2, which should be addressed in further investigations. Abbreviations: IR (Insulin-receptor), (PI3K-phosphatidylinositol-3-kinase), Akt (serine /threonine activated protein kinase), TSC1 (tuberose sclerosis complex1-hamartine), TSC2 (tuberose sclerosis complex2-tuberin), AMPK (AMP-activated kinase), LKB1 (AMPK-kinase), Rheb (Ras homolog enriched in brain), mTOR (mammalian target of rapamycin).

Our results strongly suggest that the phosphorylation of TSC2 by Akt could not be sufficient to overcome the activity of LKB1 as a tumor suppressor. However, the ability of Akt to negate AMPK activity could be sufficient to overcome the tumor suppressor activity of LKB1. Thus, PTEN deficiency should be capable of overcoming the tumor suppressor activities of both TSC2 and LKB1.

5.5 Concluding Remarks

The regulation of mTOR by Akt was shown *in vitro* using primary cells/ cell lines. However, the regulation of mTOR by Akt through inhibition of AMPK could also be determined *in vivo*, e.g., in a mouse model, by obtaining Akt1/Akt 2 DKO mice crossed with transgenic mice for dominant negative AMPK. This model would be suitable to show whether the growth retardation might be reversed in Akt1/Akt2 DKO mice by measuring body weight and skeletal muscle size. In addition, the analysis of the Akt-TSC2-mTOR pathway in MEFs of Akt1/Akt2 DKO mice^{TG-DN-AMPK} would clarify if DN-AMPK activates mTOR in Akt deficient cells *in vivo*. Furthermore, questions about the regulation of the Akt-TSC2-mTOR pathway during the development of Akt1/Akt 2 DKO mice^{TG-DN-AMPK} compared to Akt1/Akt 2 DKO mice could be addressed as well as issues regarding the organ specificity of the pathway regulation.

In vitro studies could further investigate the "differential" regulation of TSC2 by Akt between the two pathways: (1) direct phosphorylation of TSC2 and deactivation of the TSC1/TSC2 complex and (2) inhibition or activation of the phosphorylation of TSC2 by AMPK through AMP/ATP ratios. As shown in Figure 27, both pathways have different effects on TSC2. For example, one may determine mTOR activity after overexpressing Akt-phosphomimetic TSC2 mutant with Serine 1345 and Threonine 1227 converted to Alanine in Akt1/Akt2 DKO cells. These two phosphorylation sites on TSC2 are AMPK-dependent and have been shown to play an important role in the cellular energy response (Inoki et al. 2003b).

Furthermore, it would be interesting to determine if Akt's effect on the intracellular ATP level is due to the global effect on glycolysis and oxidative

phosphorylation, or due to a specific mechanism, for example suggested by Bijur et al., where Akt may locate into the mitochondria and phosphorylate the ATP synthase β -subunit (Bijur and Jope 2003).

6. Summary

The serine/threonine kinase Akt was shown to activate the mammalian target of rapamycin (mTOR) through direct phosphorylation and inhibition of tuberous sclerosis complex 2 (TSC2). Recent reports show that mTOR activity is also dependent on the intracellular level of ATP and reduced AMPK activity, thereby AMPK inhibits mTOR through the phosphorylation and inactivation of TSC2.

Skeletal muscle cells of Akt1/Akt2 DKO mice show severe atrophy and a decrease in cell size. This result established that Akt is required for determining the cell growth or cell mass in mammalian (skeletal muscle) cells. Increasing body of evidence placed mTOR as a central regulator of cell growth (size) and proliferation. The kinase mTOR affects its downstream targets 4EBP1 and S6K1, both are phosphorylated by its kinase activity and increasing protein synthesis.

Biochemical experiments in this thesis show that the activity of mTOR is impaired in Akt1/Akt2 DKO cells, and this provided first genetic evidence that Akt is required for mTOR activity. TSC2 has been shown to be directly phosphorylated by Akt, however, it appears that phosphorylation of TSC2 by Akt is not sufficient to fully activate mTOR.

Genetic and biochemical approaches have been applied to establish that Akt is a regulator of energy homeostasis and is required to maintain a threshold level of ATP in the cell. AMPK activity is dependent on AMP/ATP ratios and not solely on the ATP level. Although it has been demonstrated before that cells over-expressing activated Akt display a higher ATP level, it has never been established that the AMP/ATP level is reduced in those cells, neither their low AMPK activity. This thesis provided for the first time genetic evidence that Akt is required to maintain the intracellular level of ATP, a low AMP/ATP ratio and low AMPK activity. This function of Akt is required in order to fully activate mTOR. Expression of DN-AMPK in Akt deficient cells that display a high AMPK activity restored mTOR activity in those cells.

Additionally, it has been observed for the first time that the ATP level is low and AMPK activity is up-regulated due to a low Akt activity in TSC2-null cells. Finally, the results have proven that direct phosphorylation of TSC2 by Akt is not sufficient to fully activate mTOR and that Akt activates mTOR through an

additional pathway that inhibits AMPK. Using expression of an Akt-phosphomimetic mutant of TSC2 in TSC2-null cells showed that this mutant is not inert to ATP depletion and still inhibits mTOR activity. However, ectopically expression of activated Akt inhibits the activity of the phosphomimetic mutant of TSC2 via downregulation of AMPK.

In summary, this work revealed a linear pathway downstream of Akt that inhibits AMPK, which otherwise activated the TSC2-mTOR pathway. Currently, the activation of mTOR via inhibition of AMPK and through phosphorylation of TSC2 by Akt are viewed as two separate pathways leading to the activation of mTOR.

The findings establish a new pathway from Akt via AMPK to mTOR and challenged the current knowledge by showing that Akt is activating mTOR through both AMPK and through direct phosphorylation of TSC2. The regulation of the Akt-TSC2-mTOR pathway is demonstrated in the scheme in Figure 27 CHAPTER 6.4.

7. Zusammenfassung

Es wurde gezeigt, dass die Serine/Threonine-Kinase Akt, oder auch PKB genannt, mTOR (mammalian target of rapamycin) durch direkte Phosphorylierung aktiviert. Kuerzlich erschienene Reporte zeigten, das mTOR Aktivitaet vom intrazellulaeren ATP-Level und von der AMPK-Aktivitaet abhaengt. AMPK- Aktivitaet inhibiert dabei mTOR durch Phosphorylierung von TSC2.

In Skelettmuskelzellen von Akt1/Akt2 DKO Maeusen konnte starke Muskelatrophie und eine Reduzierung der Zellgroesse festgestellt werden. Dieses Ergebnis etabliert, dass die Kinase Akt notwendig fuer das Zellwachstum und die Zellmasse in Saeugetierzellen (Skelettmuskelzellen) ist.

mTOR ist ein zentraler Regulator von Zellwachstum und Proliferation, das haben zunehmende Beweise in letzter Zeit deutlich gezeigt. Die Kinase mTOR phosphoryliert die beiden "downstream" gelegenen Proteine 4EBP und S6K, deren Phosphorylierung zur erhoehten Proteinsynthese fuehrt.

Unter Verwendung von biochemischen Experimenten konnte gezeigt werden, dass mTOR-Aktivitaet in Akt1/Akt2 DKO MEFs sehr stark reduziert ist, und das liefert den ersten genetischen Beweis, dass Akt notwendig ist fuer mTOR-Aktivierung. Es hat sich auch gezeigt, dass die Phosphorylierung von TSC2 durch Akt nicht ausreicht, um mTOR vollendaendig zu aktivieren.

Genetische und biochemische Methoden wurden verwendet, um Akt als einen Regulator des Energiegleichgewichtes zu etablieren. Zusaetzlich konnte in dieser Arbeit gezeigt werden, dass Akt unbedingt notwendig fuer die Beibehaltung eines basalen Levels von intrazellulaerem ATP ist. AMPK-Aktivitaet ist abhaengig vom AMP/ATP-Verhaeltnis und nicht ausschliesslich vom ATP-Level. Obwohl bereits demonstriert worden ist, dass Ueberexprimieren von aktiviertem Akt zu einem erhoehten intrazellularen ATP-Level fuehrt, wurde nicht gezeigt, welche Auswirkungen dieses auf das AMP/ATP-Verhaeltnis und die AMPK-Aktivitaet hat. In dieser Promotion wurde der erste genetische Beweiss erbracht, dass Akt fuer die Erhaltung des intrazellulaeren ATP-Levels, zur Herunterregulierung des AMP/ATP-Verhaeltnisses und zur Deaktivierung von AMPK notwendig ist. Die Funktion von Akt ist notwendig fuer die vollstaendige

Aktivierung von mTOR. Expression von dominant negativer AMPK fuehrte zur fast vollstaendigen Wiederherstellung der mTOR-Aktivitaet in Akt1/Akt2 DKO Zellen.

Zusaetzlich wurden wichtige Beobachtungen in TSC2-KO Zellen gemacht, denn es zeigte sich, dass in diesen Zellen auf Grund stark reduzierter Akt-Aktivitaet der intrazellulaere ATP-Level reduziert und die AMPK-Aktivitaet dadurch stark erhoeht ist.

Weiterhin ist festzustellen, dass TSC2 Phosphorylierung durch Akt nicht ausreicht, um mTOR vollstaendig zu aktivieren; ein zusaetzlicher Pathway, der AMPK-Aktivitaet inhibiert, wurde notwendig. Um diesen Mechanismus zu untermauern, wurde ein fuer Akt konstitutiv aktiviertes TSC2 Protein in TSC2-KO Zellen ueberexprimiert. Diese Zelllinie war nicht inert gegenueber ATP Reduzierung hervorgerufen durch Inhibitoren im Vergleich zur TSC2-KO Zelllinie. Interessanterweise konnte ein zusaetzliches Ueberexpremieren von aktiviertem Akt in dieser Zelllinie, durch Deaktivierung der AMPK, diesen Effekt umkehren.

Die in dieser Forschungsarbeit herausgestellten Informationen haben zur Entdeckung einer neuen Verbindung im Pathway Akt-TSC2-mTOR gefuehrt, der linear von Akt zur Inhibierung von AMPK fuehrt. In der Literatur wird die Aktivierung von mTOR durch die Inhibierung von AMPK und durch die direkte Phosphorylierung von TSC2 als zwei separate Pathways dargestellt. Es wurde gezeigt, dass Akt mTOR durch AMPK und direkte Phosphorylierung von TSC2 aktiviert. Ein Schema des etablierten Akt-TSC2-mTOR Pathways ist in Abbildung 27, Kapitel 6.4., dargestellt.

III. References

- Alessi, D.R., M. Andjelkovic, B. Caudwell, P. Cron, N. Morrice, P. Cohen, and B.A. Hemmings. 1996. Mechanism of activation of protein kinase B by insulin and IGF-1. *Embo J* **15**: 6541-51.
- Altomare, D.A., K. Guo, J.Q. Cheng, G. Sonoda, K. Walsh, and J.R. Testa. 1995. Cloning, chromosomal localization and expression analysis of the mouse Akt2 oncogene. *Oncogene* **11**: 1055-60.
- Altomare, D.A., G.E. Lyons, Y. Mitsuchi, J.Q. Cheng, and J.R. Testa. 1998. Akt2 mRNA is highly expressed in embryonic brown fat and the AKT2 kinase is activated by insulin. *Oncogene* **16**: 2407-11.
- Anderson, K.E., J. Coadwell, L.R. Stephens, and P.T. Hawkins. 1998. Translocation of PDK-1 to the plasma membrane is important in allowing PDK-1 to activate protein kinase B. *Curr Biol* **8**: 684-91.
- Andjelkovic, M., D.R. Alessi, R. Meier, A. Fernandez, N.J. Lamb, M. Frech, P. Cron, P. Cohen, J.M. Lucocq, and B.A. Hemmings. 1997. Role of translocation in the activation and function of protein kinase B. *J Biol Chem* **272**: 31515-24.
- Andrade, M.A. and P. Bork. 1995. HEAT repeats in the Huntington's disease protein. *Nat Genet* **11**: 115-6.
- Barbet, N.C., U. Schneider, S.B. Helliwell, I. Stansfield, M.F. Tuite, and M.N. Hall. 1996. TOR controls translation initiation and early G1 progression in yeast. *Mol Biol Cell* **7**: 25-42.
- Barthel, A., S.T. Okino, J. Liao, K. Nakatani, J. Li, J.P. Whitlock, Jr., and R.A. Roth. 1999. Regulation of GLUT1 gene transcription by the serine/threonine kinase Akt1. *J Biol Chem* **274**: 20281-6.
- Bellacosa, A., J.R. Testa, S.P. Staal, and P.N. Tsichlis. 1991. A retroviral oncogene, akt, encoding a serine-threonine kinase containing an SH2-like region. *Science* **254**: 274-7.
- Bijur, G.N. and R.S. Jope. 2003. Rapid accumulation of Akt in mitochondria following phosphatidylinositol 3-kinase activation. *J Neurochem* **87**: 1427-35.
- Bodine, S.C., T.N. Stitt, M. Gonzalez, W.O. Kline, G.L. Stover, R. Bauerlein, E. Zlotchenko, A. Scrimgeour, J.C. Lawrence, D.J. Glass, and G.D. Yancopoulos. 2001. Akt/mTOR pathway is a crucial regulator of skeletal muscle hypertrophy and can prevent muscle atrophy in vivo. *Nat Cell Biol* **3**: 1014-9.
- Bolster, D.R., S.J. Crozier, S.R. Kimball, and L.S. Jefferson. 2002. AMP-activated protein kinase suppresses protein synthesis in rat skeletal muscle through down-regulated mammalian target of rapamycin (mTOR) signaling. *J Biol Chem* **277**: 23977-80.
- Boudeau, J., A. Kieloch, D.R. Alessi, A. Stella, G. Guanti, and N. Resta. 2003a. Functional analysis of LKB1/STK11 mutants and two aberrant isoforms found in Peutz-Jeghers Syndrome patients. *Hum Mutat* **21**: 172.
- Boudeau, J., G. Sapkota, and D.R. Alessi. 2003b. LKB1, a protein kinase regulating cell proliferation and polarity. *FEBS Lett* **546**: 159-65.
- Brazil, D.P., J. Park, and B.A. Hemmings. 2002. PKB binding proteins. Getting in on the Akt. *Cell* **111**: 293-303.

- Brodbeck, D., P. Cron, and B.A. Hemmings. 1999. A human protein kinase Bgamma with regulatory phosphorylation sites in the activation loop and in the C-terminal hydrophobic domain. *J Biol Chem* **274**: 9133-6.
- Brown, E.J., M.W. Albers, T.B. Shin, K. Ichikawa, C.T. Keith, W.S. Lane, and S.L. Schreiber. 1994. A mammalian protein targeted by G1-arresting rapamycin-receptor complex. *Nature* **369**: 756-8.
- Brown, E.J., P.A. Beal, C.T. Keith, J. Chen, T.B. Shin, and S.L. Schreiber. 1995. Control of p70 s6 kinase by kinase activity of FRAP in vivo. *Nature* **377**: 441-6.
- Burgering, B.M. and P.J. Coffey. 1995. Protein kinase B (c-Akt) in phosphatidylinositol-3-OH kinase signal transduction. *Nature* **376**: 599-602.
- Cafferkey, R., M.M. McLaughlin, P.R. Young, R.K. Johnson, and G.P. Livi. 1994. Yeast TOR (DRR) proteins: amino-acid sequence alignment and identification of structural motifs. *Gene* **141**: 133-6.
- Cardone, M.H., N. Roy, H.R. Stennicke, G.S. Salvesen, T.F. Franke, E. Stanbridge, S. Frisch, and J.C. Reed. 1998. Regulation of cell death protease caspase-9 by phosphorylation. *Science* **282**: 1318-21.
- Carling, D. 2004. Ampk. *Curr Biol* **14**: R220.
- Castro, A.F., J.F. Rebhun, G.J. Clark, and L.A. Quilliam. 2003. Rheb binds tuberous sclerosis complex 2 (TSC2) and promotes S6 kinase activation in a rapamycin- and farnesylation-dependent manner. *J Biol Chem* **278**: 32493-6.
- Chan, T.O., S.E. Rittenhouse, and P.N. Tsichlis. 1999. AKT/PKB and other D3 phosphoinositide-regulated kinases: kinase activation by phosphoinositide-dependent phosphorylation. *Annu Rev Biochem* **68**: 965-1014.
- Cheadle, J.P., L. Dobbie, S. Idziaszczyk, A.K. Hodges, A.J. Smith, J.R. Sampson, and J. Young. 2000a. Genomic organization and comparative analysis of the mouse tuberous sclerosis 1 (Tsc1) locus. *Mamm Genome* **11**: 1135-8.
- Cheadle, J.P., M.P. Reeve, J.R. Sampson, and D.J. Kwiatkowski. 2000b. Molecular genetic advances in tuberous sclerosis. *Hum Genet* **107**: 97-114.
- Chen, C., J. Jack, and R.S. Garofalo. 1996. The Drosophila insulin receptor is required for normal growth. *Endocrinology* **137**: 846-56.
- Chen, J., X.F. Zheng, E.J. Brown, and S.L. Schreiber. 1995. Identification of an 11-kDa FKBP12-rapamycin-binding domain within the 289-kDa FKBP12-rapamycin-associated protein and characterization of a critical serine residue. *Proc Natl Acad Sci U S A* **92**: 4947-51.
- Chen, W.S., P.Z. Xu, K. Gottlob, M.L. Chen, K. Sokol, T. Shiyanova, I. Roninson, W. Weng, R. Suzuki, K. Tobe, T. Kadowaki, and N. Hay. 2001. Growth retardation and increased apoptosis in mice with homozygous disruption of the Akt1 gene. *Genes Dev* **15**: 2203-8.
- Cheng, J.Q., A.K. Godwin, A. Bellacosa, T. Taguchi, T.F. Franke, T.C. Hamilton, P.N. Tsichlis, and J.R. Testa. 1992. AKT2, a putative oncogene encoding a member of a subfamily of protein-serine/threonine kinases, is amplified in human ovarian carcinomas. *Proc Natl Acad Sci U S A* **89**: 9267-71.

- Cheng, S.W., L.G. Fryer, D. Carling, and P.R. Shepherd. 2004. Thr2446 is a novel mammalian target of rapamycin (mTOR) phosphorylation site regulated by nutrient status. *J Biol Chem* **279**: 15719-22.
- Chiu, M.I., H. Katz, and V. Berlin. 1994. RAPT1, a mammalian homolog of yeast Tor, interacts with the FKBP12/rapamycin complex. *Proc Natl Acad Sci U S A* **91**: 12574-8.
- Choi, J., J. Chen, S.L. Schreiber, and J. Clardy. 1996. Structure of the FKBP12-rapamycin complex interacting with the binding domain of human FRAP. *Science* **273**: 239-42.
- Coffer, P.J. and J.R. Woodgett. 1991. Molecular cloning and characterisation of a novel putative protein-serine kinase related to the cAMP-dependent and protein kinase C families. *Eur J Biochem* **201**: 475-81.
- Cong, L.N., H. Chen, Y. Li, L. Zhou, M.A. McGibbon, S.I. Taylor, and M.J. Quon. 1997. Physiological role of Akt in insulin-stimulated translocation of GLUT4 in transfected rat adipose cells. *Mol Endocrinol* **11**: 1881-90.
- Corradetti, M.N., K. Inoki, N. Bardeesy, R.A. DePinho, and K.L. Guan. 2004. Regulation of the TSC pathway by LKB1: evidence of a molecular link between tuberous sclerosis complex and Peutz-Jeghers syndrome. *Genes Dev* **18**: 1533-8.
- Cross, D.A., D.R. Alessi, P. Cohen, M. Andjelkovich, and B.A. Hemmings. 1995. Inhibition of glycogen synthase kinase-3 by insulin mediated by protein kinase B. *Nature* **378**: 785-9.
- Dan, H.C., M. Sun, L. Yang, R.I. Feldman, X.M. Sui, C.C. Ou, M. Nellist, R.S. Yeung, D.J. Halley, S.V. Nicosia, W.J. Pledger, and J.Q. Cheng. 2002. Phosphatidylinositol 3-kinase/Akt pathway regulates tuberous sclerosis tumor suppressor complex by phosphorylation of tuberin. *J Biol Chem* **277**: 35364-70.
- Datta, S.R., H. Dudek, X. Tao, S. Masters, H. Fu, Y. Gotoh, and M.E. Greenberg. 1997. Akt phosphorylation of BAD couples survival signals to the cell-intrinsic death machinery. *Cell* **91**: 231-41.
- Day, S.J. and P.A. Lawrence. 2000. Measuring dimensions: the regulation of size and shape. *Development* **127**: 2977-87.
- del Peso, L., M. Gonzalez-Garcia, C. Page, R. Herrera, and G. Nunez. 1997. Interleukin-3-induced phosphorylation of BAD through the protein kinase Akt. *Science* **278**: 687-9.
- Dennis, P.B., A. Jaeschke, M. Saitoh, B. Fowler, S.C. Kozma, and G. Thomas. 2001. Mammalian TOR: a homeostatic ATP sensor. *Science* **294**: 1102-5.
- Deprez, J., D. Vertommen, D.R. Alessi, L. Hue, and M.H. Rider. 1997. Phosphorylation and activation of heart 6-phosphofructo-2-kinase by protein kinase B and other protein kinases of the insulin signaling cascades. *J Biol Chem* **272**: 17269-75.
- Downward, J. 1999. How BAD phosphorylation is good for survival. *Nat Cell Biol* **1**: E33-5.
- Dufner, A. and G. Thomas. 1999. Ribosomal S6 kinase signaling and the control of translation. *Exp Cell Res* **253**: 100-9.
- Efstratiadis, A. 1998. Genetics of mouse growth. *Int J Dev Biol* **42**: 955-76.
- Eves, E.M., W. Xiong, A. Bellacosa, S.G. Kennedy, P.N. Tsichlis, M.R. Rosner, and N. Hay. 1998. Akt, a target of phosphatidylinositol 3-kinase, inhibits apoptosis in a differentiating neuronal cell line. *Mol Cell Biol* **18**: 2143-52.

- Fingar, D.C., S. Salama, C. Tsou, E. Harlow, and J. Blenis. 2002. Mammalian cell size is controlled by mTOR and its downstream targets S6K1 and 4EBP1/eIF4E. *Genes Dev* **16**: 1472-87.
- Franke, T.F., S.I. Yang, T.O. Chan, K. Datta, A. Kazlauskas, D.K. Morrison, D.R. Kaplan, and P.N. Tsichlis. 1995. The protein kinase encoded by the Akt proto-oncogene is a target of the PDGF-activated phosphatidylinositol 3-kinase. *Cell* **81**: 727-36.
- Frech, M., M. Andjelkovic, E. Ingley, K.K. Reddy, J.R. Falck, and B.A. Hemmings. 1997. High affinity binding of inositol phosphates and phosphoinositides to the pleckstrin homology domain of RAC/protein kinase B and their influence on kinase activity. *J Biol Chem* **272**: 8474-81.
- Fujio, Y., K. Guo, T. Mano, Y. Mitsuuchi, J.R. Testa, and K. Walsh. 1999. Cell cycle withdrawal promotes myogenic induction of Akt, a positive modulator of myocyte survival. *Mol Cell Biol* **19**: 5073-82.
- Garami, A., F.J. Zwartkruis, T. Nobukuni, M. Joaquin, M. Rocco, H. Stocker, S.C. Kozma, E. Hafen, J.L. Bos, and G. Thomas. 2003. Insulin activation of Rheb, a mediator of mTOR/S6K/4E-BP signaling, is inhibited by TSC1 and 2. *Mol Cell* **11**: 1457-66.
- Gingras, A.C., S.G. Kennedy, M.A. O'Leary, N. Sonenberg, and N. Hay. 1998. 4E-BP1, a repressor of mRNA translation, is phosphorylated and inactivated by the Akt(PKB) signaling pathway. *Genes Dev* **12**: 502-13.
- Gingras, A.C., B. Raught, and N. Sonenberg. 2001. Regulation of translation initiation by FRAP/mTOR. *Genes Dev* **15**: 807-26.
- Goncharova, E.A., D.A. Goncharov, A. Eszterhas, D.S. Hunter, M.K. Glassberg, R.S. Yeung, C.L. Walker, D. Noonan, D.J. Kwiatkowski, M.M. Chou, R.A. Panettieri, Jr., and V.P. Krymskaya. 2002. Tuberin regulates p70 S6 kinase activation and ribosomal protein S6 phosphorylation. A role for the TSC2 tumor suppressor gene in pulmonary lymphangioleiomyomatosis (LAM). *J Biol Chem* **277**: 30958-67.
- Gottlob, K., N. Majewski, S. Kennedy, E. Kandel, R.B. Robey, and N. Hay. 2001. Inhibition of early apoptotic events by Akt/PKB is dependent on the first committed step of glycolysis and mitochondrial hexokinase. *Genes Dev* **15**: 1406-18.
- Gregory, C.R., X. Huang, R.E. Pratt, V.J. Dzau, R. Shorthouse, M.E. Billingham, and R.E. Morris. 1995. Treatment with rapamycin and mycophenolic acid reduces arterial intimal thickening produced by mechanical injury and allows endothelial replacement. *Transplantation* **59**: 655-61.
- Ha, J., S. Daniel, S.S. Broyles, and K.H. Kim. 1994. Critical phosphorylation sites for acetyl-CoA carboxylase activity. *J Biol Chem* **269**: 22162-8.
- Hajdуч, E., D.R. Alessi, B.A. Hemmings, and H.S. Hundal. 1998. Constitutive activation of protein kinase B alpha by membrane targeting promotes glucose and system A amino acid transport, protein synthesis, and inactivation of glycogen synthase kinase 3 in L6 muscle cells. *Diabetes* **47**: 1006-13.
- Hanada, M., J. Feng, and B.A. Hemmings. 2004. Structure, regulation and function of PKB/AKT--a major therapeutic target. *Biochim Biophys Acta* **1697**: 3-16.
- Hara, K., Y. Maruki, X. Long, K. Yoshino, N. Oshiro, S. Hidayat, C. Tokunaga, J. Avruch, and K. Yonezawa. 2002. Raptor, a binding partner of target of rapamycin (TOR), mediates TOR action. *Cell* **110**: 177-89.

- Hara, K., K. Yonezawa, Q.P. Weng, M.T. Kozlowski, C. Belham, and J. Avruch. 1998. Amino acid sufficiency and mTOR regulate p70 S6 kinase and eIF-4E BP1 through a common effector mechanism. *J Biol Chem* **273**: 14484-94.
- Hardie, D.G., D. Carling, and M. Carlson. 1998. The AMP-activated/SNF1 protein kinase subfamily: metabolic sensors of the eukaryotic cell? *Annu Rev Biochem* **67**: 821-55.
- Hawley, S.A., M.A. Selbert, E.G. Goldstein, A.M. Edelman, D. Carling, and D.G. Hardie. 1995. 5'-AMP activates the AMP-activated protein kinase cascade, and Ca²⁺/calmodulin activates the calmodulin-dependent protein kinase I cascade, via three independent mechanisms. *J Biol Chem* **270**: 27186-91.
- Hay, N. and N. Sonenberg. 2004. Upstream and downstream of mTOR. *Genes Dev* **18**: 1926-45.
- Hemminki, A., D. Markie, I. Tomlinson, E. Avizienyte, S. Roth, A. Loukola, G. Bignell, W. Warren, M. Aminoff, P. Hoglund, H. Jarvinen, P. Kristo, K. Pelin, M. Ridanpaa, R. Salovaara, T. Toro, W. Bodmer, S. Olschwang, A.S. Olsen, M.R. Stratton, A. de la Chapelle, and L.A. Aaltonen. 1998. A serine/threonine kinase gene defective in Peutz-Jeghers syndrome. *Nature* **391**: 184-7.
- Inoki, K., Y. Li, T. Xu, and K.L. Guan. 2003a. Rheb GTPase is a direct target of TSC2 GAP activity and regulates mTOR signaling. *Genes Dev* **17**: 1829-34.
- Inoki, K., Y. Li, T. Zhu, J. Wu, and K.L. Guan. 2002. TSC2 is phosphorylated and inhibited by Akt and suppresses mTOR signalling. *Nat Cell Biol* **4**: 648-57.
- Inoki, K., T. Zhu, and K.L. Guan. 2003b. TSC2 mediates cellular energy response to control cell growth and survival. *Cell* **115**: 577-90.
- Jaeschke, A., J. Hartkamp, M. Saitoh, W. Roworth, T. Nobukuni, A. Hodges, J. Sampson, G. Thomas, and R. Lamb. 2002. Tuberous sclerosis complex tumor suppressor-mediated S6 kinase inhibition by phosphatidylinositol-3-OH kinase is mTOR independent. *J Cell Biol* **159**: 217-24.
- James, S.R., C.P. Downes, R. Gigg, S.J. Grove, A.B. Holmes, and D.R. Alessi. 1996. Specific binding of the Akt-1 protein kinase to phosphatidylinositol 3,4,5-trisphosphate without subsequent activation. *Biochem J* **315** (Pt 3): 709-13.
- Jenne, D.E., H. Reimann, J. Nezu, W. Friedel, S. Loff, R. Jeschke, O. Muller, W. Back, and M. Zimmer. 1998. Peutz-Jeghers syndrome is caused by mutations in a novel serine threonine kinase. *Nat Genet* **18**: 38-43.
- Jones, P.F., T. Jakubowicz, F.J. Pitossi, F. Maurer, and B.A. Hemmings. 1991. Molecular cloning and identification of a serine/threonine protein kinase of the second-messenger subfamily. *Proc Natl Acad Sci U S A* **88**: 4171-5.
- Kandel, E.S. and N. Hay. 1999. The regulation and activities of the multifunctional serine/threonine kinase Akt/PKB. *Exp Cell Res* **253**: 210-29.
- Kemp, B.E., K.I. Mitchelhill, D. Stapleton, B.J. Michell, Z.P. Chen, and L.A. Witters. 1999. Dealing with energy demand: the AMP-activated protein kinase. *Trends Biochem Sci* **24**: 22-5.
- Kennedy, S.G., E.S. Kandel, T.K. Cross, and N. Hay. 1999. Akt/Protein kinase B inhibits cell death by preventing the release of cytochrome c from mitochondria. *Mol Cell Biol* **19**: 5800-10.

- Kennedy, S.G., A.J. Wagner, S.D. Conzen, J. Jordan, A. Bellacosa, P.N. Tsichlis, and N. Hay. 1997. The PI 3-kinase/Akt signaling pathway delivers an anti-apoptotic signal. *Genes Dev* **11**: 701-13.
- Kim, D.H., D.D. Sarbassov, S.M. Ali, J.E. King, R.R. Latek, H. Erdjument-Bromage, P. Tempst, and D.M. Sabatini. 2002. mTOR interacts with raptor to form a nutrient-sensitive complex that signals to the cell growth machinery. *Cell* **110**: 163-75.
- Kim, D.H., D. Sarbassov dos, S.M. Ali, R.R. Latek, K.V. Guntur, H. Erdjument-Bromage, P. Tempst, and D.M. Sabatini. 2003. GbetaL, a positive regulator of the rapamycin-sensitive pathway required for the nutrient-sensitive interaction between raptor and mTOR. *Mol Cell* **11**: 895-904.
- Kimura, N., C. Tokunaga, S. Dalal, C. Richardson, K. Yoshino, K. Hara, B.E. Kemp, L.A. Witters, O. Mimura, and K. Yonezawa. 2003. A possible linkage between AMP-activated protein kinase (AMPK) and mammalian target of rapamycin (mTOR) signalling pathway. *Genes Cells* **8**: 65-79.
- Kitamura, T., Y. Kitamura, S. Kuroda, Y. Hino, M. Ando, K. Kotani, H. Konishi, H. Matsuzaki, U. Kikkawa, W. Ogawa, and M. Kasuga. 1999. Insulin-induced phosphorylation and activation of cyclic nucleotide phosphodiesterase 3B by the serine-threonine kinase Akt. *Mol Cell Biol* **19**: 6286-96.
- Kohn, A.D., K.S. Kovacina, and R.A. Roth. 1995. Insulin stimulates the kinase activity of RAC-PK, a pleckstrin homology domain containing ser/thr kinase. *Embo J* **14**: 4288-95.
- Kohn, A.D., S.A. Summers, M.J. Birnbaum, and R.A. Roth. 1996. Expression of a constitutively active Akt Ser/Thr kinase in 3T3-L1 adipocytes stimulates glucose uptake and glucose transporter 4 translocation. *J Biol Chem* **271**: 31372-8.
- Kozma, S.C. and G. Thomas. 2002. Regulation of cell size in growth, development and human disease: PI3K, PKB and S6K. *Bioessays* **24**: 65-71.
- Krymskaya, V.P. 2003. Tumour suppressors hamartin and tuberlin: intracellular signalling. *Cell Signal* **15**: 729-39.
- Kwiatkowski, D.J., H. Zhang, J.L. Bandura, K.M. Heiberger, M. Glogauer, N. el-Hashemite, and H. Onda. 2002. A mouse model of TSC1 reveals sex-dependent lethality from liver hemangiomas, and up-regulation of p70S6 kinase activity in Tsc1 null cells. *Hum Mol Genet* **11**: 525-34.
- Li, D.M. and H. Sun. 1998. PTEN/MMAC1/TEP1 suppresses the tumorigenicity and induces G1 cell cycle arrest in human glioblastoma cells. *Proc Natl Acad Sci U S A* **95**: 15406-11.
- Li, Y., M.N. Corradetti, K. Inoki, and K.L. Guan. 2004. TSC2: filling the GAP in the mTOR signaling pathway. *Trends Biochem Sci* **29**: 32-8.
- Liang, J., J. Zubovitz, T. Petrocelli, R. Kotchetkov, M.K. Connor, K. Han, J.H. Lee, S. Ciarallo, C. Catzavelos, R. Beniston, E. Franssen, and J.M. Slingerland. 2002. PKB/Akt phosphorylates p27, impairs nuclear import of p27 and opposes p27-mediated G1 arrest. *Nat Med* **8**: 1153-60.
- Loewith, R., E. Jacinto, S. Wulschleger, A. Lorberg, J.L. Crespo, D. Bonenfant, W. Oppliger, P. Jenoe, and M.N. Hall. 2002. Two TOR complexes, only one of which is rapamycin sensitive, have distinct roles in cell growth control. *Mol Cell* **10**: 457-68.

- Maehama, T. and J.E. Dixon. 1998. The tumor suppressor, PTEN/MMAC1, dephosphorylates the lipid second messenger, phosphatidylinositol 3,4,5-trisphosphate. *J Biol Chem* **273**: 13375-8.
- Majewski, N., V. Nogueira, R.B. Robey, and N. Hay. 2004. Akt inhibits apoptosis downstream of BID cleavage via a glucose-dependent mechanism involving mitochondrial hexokinases. *Mol Cell Biol* **24**: 730-40.
- Majumder, P.K., P.G. Febbo, R. Bikoff, R. Berger, Q. Xue, L.M. McMahon, J. Manola, J. Brugarolas, T.J. McDonnell, T.R. Golub, M. Loda, H.A. Lane, and W.R. Sellers. 2004. mTOR inhibition reverses Akt-dependent prostate intraepithelial neoplasia through regulation of apoptotic and HIF-1-dependent pathways. *Nat Med* **10**: 594-601.
- Manning, B.D., A.R. Tee, M.N. Logsdon, J. Blenis, and L.C. Cantley. 2002. Identification of the tuberous sclerosis complex-2 tumor suppressor gene product tuberin as a target of the phosphoinositide 3-kinase/akt pathway. *Mol Cell* **10**: 151-62.
- Mayo, L.D. and D.B. Donner. 2001. A phosphatidylinositol 3-kinase/Akt pathway promotes translocation of Mdm2 from the cytoplasm to the nucleus. *Proc Natl Acad Sci U S A* **98**: 11598-603.
- Mazure, N.M., E.Y. Chen, K.R. Laderoute, and A.J. Giaccia. 1997. Induction of vascular endothelial growth factor by hypoxia is modulated by a phosphatidylinositol 3-kinase/Akt signaling pathway in Ha-ras-transformed cells through a hypoxia inducible factor-1 transcriptional element. *Blood* **90**: 3322-31.
- McManus, E.J. and D.R. Alessi. 2002. TSC1-TSC2: a complex tale of PKB-mediated S6K regulation. *Nat Cell Biol* **4**: E214-6.
- Meisse, D., M. Van de Casteele, C. Beauloye, I. Hainault, B.A. Kefas, M.H. Rider, F. Foufelle, and L. Hue. 2002. Sustained activation of AMP-activated protein kinase induces c-Jun N-terminal kinase activation and apoptosis in liver cells. *FEBS Lett* **526**: 38-42.
- Morgenstern, J.P. and H. Land. 1990. Advanced mammalian gene transfer: high titre retroviral vectors with multiple drug selection markers and a complementary helper-free packaging cell line. *Nucleic Acids Res* **18**: 3587-96.
- Mu, J., J.T. Brozinick, Jr., O. Valladares, M. Bucan, and M.J. Birnbaum. 2001. A role for AMP-activated protein kinase in contraction- and hypoxia-regulated glucose transport in skeletal muscle. *Mol Cell* **7**: 1085-94.
- Myers, M.P., I. Pass, I.H. Batty, J. Van der Kaay, J.P. Stolarov, B.A. Hemmings, M.H. Wigler, C.P. Downes, and N.K. Tonks. 1998. The lipid phosphatase activity of PTEN is critical for its tumor suppressor function. *Proc Natl Acad Sci U S A* **95**: 13513-8.
- Nave, B.T., M. Ouwers, D.J. Withers, D.R. Alessi, and P.R. Shepherd. 1999. Mammalian target of rapamycin is a direct target for protein kinase B: identification of a convergence point for opposing effects of insulin and amino-acid deficiency on protein translation. *Biochem J* **344 Pt 2**: 427-31.
- Nellist, M., M.A. Goedbloed, C. de Winter, B. Verhaaf, A. Jankie, A.J. Reuser, A.M. van den Ouweland, P. van der Sluijs, and D.J. Halley. 2002. Identification and characterization of the interaction between tuberin and 14-3-3zeta. *J Biol Chem* **277**: 39417-24.
- Ossovskaya, V.S., I.A. Mazo, M.V. Chernov, O.B. Chernova, Z. Strezoska, R. Kondratov, G.R. Stark, P.M. Chumakov, and A.V. Gudkov. 1996. Use of

- genetic suppressor elements to dissect distinct biological effects of separate p53 domains. *Proc Natl Acad Sci U S A* **93**: 10309-14.
- Paduch, M., F. Jelen, and J. Otlewski. 2001. Structure of small G proteins and their regulators. *Acta Biochim Pol* **48**: 829-50.
- Pallafacchina, G., E. Calabria, A.L. Serrano, J.M. Kalhovde, and S. Schiaffino. 2002. A protein kinase B-dependent and rapamycin-sensitive pathway controls skeletal muscle growth but not fiber type specification. *Proc Natl Acad Sci U S A* **99**: 9213-8.
- Pan, D., J. Dong, Y. Zhang, and X. Gao. 2004. Tuberous sclerosis complex: from *Drosophila* to human disease. *Trends Cell Biol* **14**: 78-85.
- Parsons, R. and L. Simpson. 2003. PTEN and cancer. *Methods Mol Biol* **222**: 147-66.
- Peng, X.D., P.Z. Xu, M.L. Chen, A. Hahn-Windgassen, J. Skeen, J. Jacobs, D. Sundararajan, W.S. Chen, S.E. Crawford, K.G. Coleman, and N. Hay. 2003. Dwarfism, impaired skin development, skeletal muscle atrophy, delayed bone development, and impeded adipogenesis in mice lacking Akt1 and Akt2. *Genes Dev* **17**: 1352-65.
- Peterson, R.T. and S.L. Schreiber. 1999. Kinase phosphorylation: Keeping it all in the family. *Curr Biol* **9**: R521-4.
- Podsypanina, K., R.T. Lee, C. Politis, I. Hennessy, A. Crane, J. Puc, M. Neshat, H. Wang, L. Yang, J. Gibbons, P. Frost, V. Dreisbach, J. Blenis, Z. Gaciong, P. Fisher, C. Sawyers, L. Hedrick-Ellenson, and R. Parsons. 2001. An inhibitor of mTOR reduces neoplasia and normalizes p70/S6 kinase activity in Pten^{+/-} mice. *Proc Natl Acad Sci U S A* **98**: 10320-5.
- Potter, C.J., H. Huang, and T. Xu. 2001. *Drosophila* Tsc1 functions with Tsc2 to antagonize insulin signaling in regulating cell growth, cell proliferation, and organ size. *Cell* **105**: 357-68.
- Potter, C.J., L.G. Pedraza, and T. Xu. 2002. Akt regulates growth by directly phosphorylating Tsc2. *Nat Cell Biol* **4**: 658-65.
- Proud, C.G. 2002. Regulation of mammalian translation factors by nutrients. *Eur J Biochem* **269**: 5338-49.
- Radimerski, T., J. Montagne, M. Hemmings-Mieszczak, and G. Thomas. 2002. Lethality of *Drosophila* lacking TSC tumor suppressor function rescued by reducing dS6K signaling. *Genes Dev* **16**: 2627-32.
- Rathmell, J.C., C.J. Fox, D.R. Plas, P.S. Hammerman, R.M. Cinalli, and C.B. Thompson. 2003. Akt-directed glucose metabolism can prevent Bax conformation change and promote growth factor-independent survival. *Mol Cell Biol* **23**: 7315-28.
- Ravichandran, L.V., H. Chen, Y. Li, and M.J. Quon. 2001. Phosphorylation of PTP1B at Ser(50) by Akt impairs its ability to dephosphorylate the insulin receptor. *Mol Endocrinol* **15**: 1768-80.
- Reynolds, T.H.t., S.C. Bodine, and J.C. Lawrence, Jr. 2002. Control of Ser2448 phosphorylation in the mammalian target of rapamycin by insulin and skeletal muscle load. *J Biol Chem* **277**: 17657-62.
- Roach, E.S., M.R. Gomez, and H. Northrup. 1998. Tuberous sclerosis complex consensus conference: revised clinical diagnostic criteria. *J Child Neurol* **13**: 624-8.
- Romanelli, A., V.C. Dreisbach, and J. Blenis. 2002. Characterization of phosphatidylinositol 3-kinase-dependent phosphorylation of the

- hydrophobic motif site Thr(389) in p70 S6 kinase 1. *J Biol Chem* **277**: 40281-9.
- Rommel, C., S.C. Bodine, B.A. Clarke, R. Rossman, L. Nunez, T.N. Stitt, G.D. Yancopoulos, and D.J. Glass. 2001. Mediation of IGF-1-induced skeletal myotube hypertrophy by PI(3)K/Akt/mTOR and PI(3)K/Akt/GSK3 pathways. *Nat Cell Biol* **3**: 1009-13.
- Rossi, D.J., A. Ylikorkala, N. Korsisaari, R. Salovaara, K. Luukko, V. Launonen, M. Henkemeyer, A. Ristimäki, L.A. Aaltonen, and T.P. Mäkelä. 2002. Induction of cyclooxygenase-2 in a mouse model of Peutz-Jeghers polyposis. *Proc Natl Acad Sci U S A* **99**: 12327-32.
- Ryazanov, A.G., M.D. Ward, C.E. Mendola, K.S. Pavur, M.V. Dorovkov, M. Wiedmann, H. Erdjument-Bromage, P. Tempst, T.G. Parmer, C.R. Prostko, F.J. Germino, and W.N. Hait. 1997. Identification of a new class of protein kinases represented by eukaryotic elongation factor-2 kinase. *Proc Natl Acad Sci U S A* **94**: 4884-9.
- Sabatini, D.M., H. Erdjument-Bromage, M. Lui, P. Tempst, and S.H. Snyder. 1994. RAFT1: a mammalian protein that binds to FKBP12 in a rapamycin-dependent fashion and is homologous to yeast TORs. *Cell* **78**: 35-43.
- Sabers, C.J., M.M. Martin, G.J. Brunn, J.M. Williams, F.J. Dumont, G. Wiederrecht, and R.T. Abraham. 1995. Isolation of a protein target of the FKBP12-rapamycin complex in mammalian cells. *J Biol Chem* **270**: 815-22.
- Sambrook, J., Fritsch, E.F., Maniatis, T. 1998. Molecular Cloning: A Laboratory Manual. 2nd ed., Cold Spring Harbor Laboratory Press.
- Sanchez-Cespedes, M., P. Parrella, M. Esteller, S. Nomoto, B. Trink, J.M. Engles, W.H. Westra, J.G. Herman, and D. Sidransky. 2002. Inactivation of LKB1/STK11 is a common event in adenocarcinomas of the lung. *Cancer Res* **62**: 3659-62.
- Sapkota, G.P., J. Boudeau, M. Deak, A. Kieloch, N. Morrice, and D.R. Alessi. 2002. Identification and characterization of four novel phosphorylation sites (Ser31, Ser325, Thr336 and Thr366) on LKB1/STK11, the protein kinase mutated in Peutz-Jeghers cancer syndrome. *Biochem J* **362**: 481-90.
- Sapkota, G.P., A. Kieloch, J.M. Lizcano, S. Lain, J.S. Arthur, M.R. Williams, N. Morrice, M. Deak, and D.R. Alessi. 2001. Phosphorylation of the protein kinase mutated in Peutz-Jeghers cancer syndrome, LKB1/STK11, at Ser431 by p90(RSK) and cAMP-dependent protein kinase, but not its farnesylation at Cys(433), is essential for LKB1 to suppress cell growth. *J Biol Chem* **276**: 19469-82.
- Saucedo, L.J. and B.A. Edgar. 2002. Why size matters: altering cell size. *Curr Opin Genet Dev* **12**: 565-71.
- Saucedo, L.J., X. Gao, D.A. Chiarelli, L. Li, D. Pan, and B.A. Edgar. 2003. Rheb promotes cell growth as a component of the insulin/TOR signalling network. *Nat Cell Biol* **5**: 566-71.
- Scanga, S.E., L. Ruel, R.C. Binari, B. Snow, V. Stambolic, D. Bouchard, M. Peters, B. Calvieri, T.W. Mak, J.R. Woodgett, and A.S. Manoukian. 2000. The conserved PI3K/PTEN/Akt signaling pathway regulates both cell size and survival in Drosophila. *Oncogene* **19**: 3971-7.
- Schalm, S.S. and J. Blenis. 2002. Identification of a conserved motif required for mTOR signaling. *Curr Biol* **12**: 632-9.

- Scott, P.H. and J.C. Lawrence, Jr. 1998. Attenuation of mammalian target of rapamycin activity by increased cAMP in 3T3-L1 adipocytes. *J Biol Chem* **273**: 34496-501.
- Sekulic, A., C.C. Hudson, J.L. Homme, P. Yin, D.M. Otterness, L.M. Karnitz, and R.T. Abraham. 2000. A direct linkage between the phosphoinositide 3-kinase-AKT signaling pathway and the mammalian target of rapamycin in mitogen-stimulated and transformed cells. *Cancer Res* **60**: 3504-13.
- Shaw, R.J., N. Bardeesy, B.D. Manning, L. Lopez, M. Kosmatka, R.A. DePinho, and L.C. Cantley. 2004. The LKB1 tumor suppressor negatively regulates mTOR signaling. *Cancer Cell* **6**: 91-9.
- Shin, I., F.M. Yakes, F. Rojo, N.Y. Shin, A.V. Bakin, J. Baselga, and C.L. Arteaga. 2002. PKB/Akt mediates cell-cycle progression by phosphorylation of p27(Kip1) at threonine 157 and modulation of its cellular localization. *Nat Med* **8**: 1145-52.
- Shioi, T., J.R. McMullen, P.M. Kang, P.S. Douglas, T. Obata, T.F. Franke, L.C. Cantley, and S. Izumo. 2002. Akt/protein kinase B promotes organ growth in transgenic mice. *Mol Cell Biol* **22**: 2799-809.
- Stambolic, V., A. Suzuki, J.L. de la Pompa, G.M. Brothers, C. Mirtsos, T. Sasaki, J. Ruland, J.M. Penninger, D.P. Siderovski, and T.W. Mak. 1998. Negative regulation of PKB/Akt-dependent cell survival by the tumor suppressor PTEN. *Cell* **95**: 29-39.
- Stephens, L., K. Anderson, D. Stokoe, H. Erdjument-Bromage, G.F. Painter, A.B. Holmes, P.R. Gaffney, C.B. Reese, F. McCormick, P. Tempst, J. Coadwell, and P.T. Hawkins. 1998. Protein kinase B kinases that mediate phosphatidylinositol 3,4,5-trisphosphate-dependent activation of protein kinase B. *Science* **279**: 710-4.
- Stocker, H., T. Radimerski, B. Schindelholtz, F. Wittwer, P. Belawat, P. Daram, S. Breuer, G. Thomas, and E. Hafen. 2003. Rheb is an essential regulator of S6K in controlling cell growth in Drosophila. *Nat Cell Biol* **5**: 559-65.
- Tanti, J.F., S. Grillo, T. Gremeaux, P.J. Coffey, E. Van Obberghen, and Y. Le Marchand-Brustel. 1997. Potential role of protein kinase B in glucose transporter 4 translocation in adipocytes. *Endocrinology* **138**: 2005-10.
- Tee, A.R., D.C. Fingar, B.D. Manning, D.J. Kwiatkowski, L.C. Cantley, and J. Blenis. 2002. Tuberous sclerosis complex-1 and -2 gene products function together to inhibit mammalian target of rapamycin (mTOR)-mediated downstream signaling. *Proc Natl Acad Sci U S A* **99**: 13571-6.
- Tokunaga, C., K. Yoshino, and K. Yonezawa. 2004. mTOR integrates amino acid- and energy-sensing pathways. *Biochem Biophys Res Commun* **313**: 443-6.
- van Slegtenhorst, M., R. de Hoogt, C. Hermans, M. Nellist, B. Janssen, S. Verhoef, D. Lindhout, A. van den Ouweland, D. Halley, J. Young, M. Burley, S. Jeremiah, K. Woodward, J. Nahmias, M. Fox, R. Ekong, J. Osborne, J. Wolfe, S. Povey, R.G. Snell, J.P. Cheadle, A.C. Jones, M. Tachataki, D. Ravine, D.J. Kwiatkowski, and et al. 1997. Identification of the tuberous sclerosis gene TSC1 on chromosome 9q34. *Science* **277**: 805-8.
- Vanhaesebroeck, B. and M.D. Waterfield. 1999. Signaling by distinct classes of phosphoinositide 3-kinases. *Exp Cell Res* **253**: 239-54.
- Viglietto, G., M.L. Motti, P. Bruni, R.M. Melillo, A. D'Alessio, D. Califano, F. Vinci, G. Chiappetta, P. Tsichlis, A. Bellacosa, A. Fusco, and M. Santoro. 2002.

- Cytoplasmic relocation and inhibition of the cyclin-dependent kinase inhibitor p27(Kip1) by PKB/Akt-mediated phosphorylation in breast cancer. *Nat Med* **8**: 1136-44.
- Vousden, K.H. and X. Lu. 2002. Live or let die: the cell's response to p53. *Nat Rev Cancer* **2**: 594-604.
- Walker, K.S., M. Deak, A. Paterson, K. Hudson, P. Cohen, and D.R. Alessi. 1998. Activation of protein kinase B beta and gamma isoforms by insulin in vivo and by 3-phosphoinositide-dependent protein kinase-1 in vitro: comparison with protein kinase B alpha. *Biochem J* **331** (Pt 1): 299-308.
- Williams, M.R., J.S. Arthur, A. Balendran, J. van der Kaay, V. Poli, P. Cohen, and D.R. Alessi. 2000. The role of 3-phosphoinositide-dependent protein kinase 1 in activating AGC kinases defined in embryonic stem cells. *Curr Biol* **10**: 439-48.
- Woods, A., D. Azzout-Marniche, M. Foretz, S.C. Stein, P. Lemarchand, P. Ferre, F. Foufelle, and D. Carling. 2000. Characterization of the role of AMP-activated protein kinase in the regulation of glucose-activated gene expression using constitutively active and dominant negative forms of the kinase. *Mol Cell Biol* **20**: 6704-11.
- Xu, G., G. Kwon, W.S. Cruz, C.A. Marshall, and M.L. McDaniel. 2001. Metabolic regulation by leucine of translation initiation through the mTOR-signaling pathway by pancreatic beta-cells. *Diabetes* **50**: 353-60.
- Zhang, H., G. Cicchetti, H. Onda, H.B. Koon, K. Asrican, N. Bajraszewski, F. Vazquez, C.L. Carpenter, and D.J. Kwiatkowski. 2003a. Loss of Tsc1/Tsc2 activates mTOR and disrupts PI3K-Akt signaling through downregulation of PDGFR. *J Clin Invest* **112**: 1223-33.
- Zhang, Y., X. Gao, L.J. Saucedo, B. Ru, B.A. Edgar, and D. Pan. 2003b. Rheb is a direct target of the tuberous sclerosis tumour suppressor proteins. *Nat Cell Biol* **5**: 578-81.
- Zhou, B.P., Y. Liao, W. Xia, Y. Zou, B. Spohn, and M.C. Hung. 2001. HER-2/neu induces p53 ubiquitination via Akt-mediated MDM2 phosphorylation. *Nat Cell Biol* **3**: 973-82.

Lebenslauf

05.12.1968	geboren in Burg Vater: Dieter Hahn, Landwirt Mutter: Renate Hahn, Versicherungskauffrau
1975-1985	Allgemeinbildene Oberschule in Tucheim
1985-1987	Ausbildung zum Facharbeiter Anlagen-und Prozess technik bei der Henkel AG in Genthin
1987-1988	Erziehungsurlaub fuer meinen Sohn Sebastian
1988-1991	Fachschulausbildung in Gerwisch (Hochschulzugangsberechtigung)
1991-1996	Mitarbeiter bei der Firma Herbstreith & Fox in Werder und Wyeth Pharmaceutical in Leipzig
1996-2001	Studium der Biotechnology an der Technischen Universitaet Berlin Abschluss als Diplom-Ingenieurin Diplomarbeit am Max-Delbrueck-Institut in Berlin
2001-laufend	Wissenschaftlicher Mitarbeiter (Research Specialist) Im Fachbereich Biochemie und molekulare Genetik an der University of Illinois in Chicago in der Arbeitsgruppe von Prof. Dr. Nissim Hay. Betreuung der Dissertation durch Prof. Dr. Ulf Stahl an der Technischen Universitaet Berlin.

Chicago, 10.Oktober 2004

Annett Hahn-Windgassen